JYU DISSERTATIONS 146

Mira Laajala

Cellular and Viral Factors Promoting Efficient Enterovirus Uncoating and Replication

UNIVERSITY OF JYVÄSKYLÄ
FACULTY OF MATHEMATICS
AND SCIENCE

JYU DISSERTATIONS 146

Mira Laajala

Cellular and Viral Factors Promoting Efficient Enterovirus Uncoating and Replication

Esitetään Jyväskylän yliopiston matemaattis-luonnontieteellisen tiedekunnan suostumuksella
julkisesti tarkastettavaksi yliopiston Ambiotica-rakennuksen luentosalissa YAA303
marraskuun 22. päivänä 2019 kello 12.

Academic dissertation to be publicly discussed, by permission of
the Faculty of Mathematics and Science of the University of Jyväskylä,
in building Ambiotica, hall YAA303, on November 22, 2019 at 12 o'clock noon.

JYVÄSKYLÄN YLIOPISTO
UNIVERSITY OF JYVÄSKYLÄ

JYVÄSKYLÄ 2019

Editors
Varpu Marjomäki
Department of Biological and Environmental Science, University of Jyväskylä
Ville Korkiakangas
Open Science Centre, University of Jyväskylä

Permanent link to this publication: http://urn.fi/URN:ISBN:978-951-39-7896-9

ISBN 978-951-39-7896-9 (PDF)
URN:ISBN:978-951-39-7896-9
ISSN 2489-9003

ABSTRACT

Laajala, Mira
Cellular and viral factors promoting efficient enterovirus uncoating and replication
Jyväskylä: University of Jyväskylä, 2019, 85 p.
(JYU Dissertations
ISSN 2489-9003; 146)
ISBN 978-951-39-7896-9 (PDF)
Yhteenveto: Enterovirusten tehokasta avautumista ja replikaatiota edistävät solu- ja virustekijät
Diss.

Enteroviruses are small non-enveloped RNA viruses, which belong to the family of picornaviruses. Although most of the diseases that enteroviruses cause are symptomless or mild, enteroviruses are the most common viruses infecting humans. In addition, enteroviruses can cause more severe diseases such as encephalitis or myocarditis. Despite their prevalence, there are no antivirals on the market against these viruses, and vaccines have been developed only against couple of serotypes. For antiviral development, it is crucial to obtain detailed information about factors that contribute to efficient infection. Thus, this thesis focuses on viral and host cell factors that promote the infection of enterovirus B species after cell entry. In the first study, we characterized a new echovirus 1 particle during infection, likely a novel form of an uncoating intermediate. This particle was more open compared to the native virus, but still contained VP4 protein, and was able to bind to a receptor and cause infection. The second part of the thesis focused on steps after RNA release, namely translation and replication. First, we showed that in addition to viral proteases, cellular calpain proteases can cleave structural proteins from the enteroviral polyprotein, suggesting that calpains might contribute to proteolytic processing during infection. This was shown in an in-vitro study, where calpains released capsid proteins from the P1 precursor. Second, we showed that translation of enteroviral proteins induced the rearrangement of cellular intermediate filament, vimentin. Vimentin cages associated with components of endoplasmic reticulum and Golgi, as well as with replicating viral RNA and non-structural, but not structural proteins. Furthermore, inhibition of vimentin dynamics resulted in lower production of the non-structural compared to structural proteins, indicating that enteroviral proteins can be produced differently, depending on their association with vimentin cages.

Keywords: Calpain; enterovirus; polyprotein processing; replication; translation; uncoating; vimentin.

Mira Laajala, University of Jyväskylä, Department of Biological and Environmental Science, P.O. Box 35, FI-40014 University of Jyväskylä, Finland

TIIVISTELMÄ

Laajala, Mira
Enterovirusten tehokasta avautumista ja replikaatiota edistävät solu- ja virustekijät
Jyväskylä: Jyväskylän yliopisto, 2019, 85 p.
(JYU Dissertations
ISSN 2489-9003; 146)
ISBN 978-951-39-7896-9 (PDF)
Yhteenveto: Cellular and viral factors promoting efficient enterovirus uncoating and replication
Diss.

Enterovirukset ovat pieniä vaipattomia RNA viruksia, jotka kuuluvat pikornaviruksiin. Vaikka enterovirukset useimmiten aiheuttavat oireettomia tai lieviä tauteja, ne ovat myös yleisin ihmisiä infektoiva virusryhmä. Lisäksi joissakin tapauksissa enterovirukset voivat aiheuttaa myös vakavampia tauteja kuten enkefaliittia tai myokardiittia. Vaikka enterovirusinfektiot ovat yleisiä, näitä viruksia vastaan ei ole lääkitystä ja rokote on kehitetty ainoastaan muutamalle serotyypille. Viruslääkkeiden kehittelyn tärkein lähtökohta on ymmärtää tehokkaaseen infektioon vaikuttavat tekijät yksityiskohtaisesti. Niinpä tässä väitöskirjassa keskityttiin tutkimaan virus- ja solutekijöitä, jotka edistävät tehokasta enterovirus B -lajin infektiota sisäänmenovaiheen jälkeen. Ensimmäisessä osatyössä kuvailimme uuden echovirus 1 partikkelin, joka todennäköisesti on välimuotopartikkeli, joka syntyy infektion aikana viruksen avautuessa. Tämä partikkeli oli rakenteeltaan avonaisempi verrattuna natiiviin virukseen, mutta sisälsi kuitenkin VP4 proteiinin, pystyi sitoutumaan reseptoriin ja aiheutti infektion soluissa. Seuraavissa osatöissä keskityimme infektiovaiheisiin RNA:n vapautumisen jälkeen, translaatioon ja replikaatioon. Ensiksi osoitimme in-vitro kokeilla, että viruksen omien proteaasien lisäksi myös solun kalpaiinit pystyivät prosessoimaan enteroviruksen polyproteiinia alueelta, joka sisälsi viruksen rakenneproteiinit. Seuraavaksi osoitimme, että virusproteiinien translaatio sai aikaan muutoksia solun välimuotoisia säikeitä muodostavassa vimentiiniproteiinissa. Syntyneeseen vimentiinihäkkiin kertyi solun endoplasmakalvoston ja Golgin laitteen rakenteita, sekä viruksen RNA ja ei-rakenteelliset proteiinit, mutta ei rakenneproteiineja. Lisäksi vimentiinihäkin muodostumisen estäminen johti ei-rakenteellisten proteiinien heikompaan tuottoon verrattuna rakenneproteiineihin, mikä osoitti, että vimentiinirakenne on tärkeä tiettyjen enteroviruksen proteiinien tuotossa.

Avainsanat: Enterovirus; kalpaiini; polyproteiinin prosessointi; replikaatio; translaatio, vimentiini, viruksen avautuminen.

Mira Laajala, Jyväskylän yliopisto, bio- ja ympäristötieteiden laitos
PL 35, 40014 Jyväskylän yliopisto

Author's address Mira Laajala
Department of Biological and Environmental Science
P.O. Box 35
FI-40014 University of Jyväskylä
Finland
mira.a.laajala@jyu.fi

Supervisor Docent Varpu Marjomäki
Department of Biological and Environmental Science
P.O. Box 35
FI-40014 University of Jyväskylä
Finland

Reviewers Professor Kalle Saksela
Haartman Institute
Department of Virology
PO box 21 (Haartmanin katu 3)
00014 University of Helsinki
Finland

Docent Tero Ahola
Department of Microbiology
Faculty of Agriculture and Forestry
PL 56 (Viikinkaari 9)
00014 University of Helsinki
Finland

Opponent Dr. Marco Vignuzzi
Viral Populations and Pathogenesis Unit (PVP)
CNRS UMR 3569
Institut Pasteur
28 rue du Dr Roux
75724 Paris cedex 15
France

CONTENTS

LIST OF ORIGINAL PUBLICATIONS

The thesis is based on the following original papers, which will be referred to in the text by their Roman numerals I-III.

I Myllynen M., Kazmertsuk A. & Marjomäki V. 2016. A Novel Open and Infectious Form of Echovirus 1. Journal of Virology 90: 6759-6770. (Chosen for spotlight in the Journal of Virology 23.5.2016).

II Laajala M., Hankaniemi M.M., Määttä J., Hytönen V.P., Laitinen O.H., Marjomäki V. 2019. Host Cell Calpains Can Cleave Structural Proteins from the Enterovirus Polyprotein. Submitted manuscript.

III Turkki P., Laajala M., Flodström-Tullberg M., Marjomäki V., 2019. Human Enterovirus Group B Viruses Rely on Vimentin Dynamics for Efficient Processing of Viral Non-structural Proteins. Journal of Virology, in press.

RESPONSIBILITIES

Article I: The original discovery of the dense particle and initial planning of the experiments were done by Artur Kazmertsuk and Varpu Marjomäki. I participated in the planning of the experiments at later stages of the research. The experiments were performed by me and Artur Kazmertsuk. I contributed to all the experiments except thermal stability assays. Analysis of the data was performed by me, Artur Kazmertsuk and Varpu Marjomäki. All authors participated in the writing process.

Article II: The original idea and planning of the experiments were done by Varpu Marjomäki and me. All the experiments were carried out by me, except the design of baculoviral vectors, the production of the baculoviruses and mass spectrometry. I wrote the paper together with Varpu Marjomäki.

Article III: The original discovery of vimentin cage and initial planning of the experiments were done by Paula Turkki and Varpu Marjomäki. I participated in the planning of the experiments at later stages of the research. The experiments were performed by Paula Turkki, me and Varpu Marjomäki. I performed the virus infections, immunolabelings, confocal microscopy and Western blotting related to comparison of structural and non-structural proteins. I also performed the qPCR and metabolic labeling experiments. Data analysis was done by Paula Turkki, Varpu Marjomäki and me. Writing of the paper was performed by Paula Turkki, Varpu Marjomäki and me.

ABBREVIATIONS

A549	adenocarcinomic human alveolar basal epithelial
CAR	coxsackievirus-adenovirus receptor
CPE	cytopathic effect
CRE	cis-acting RNA element
CsCl	caesium chloride
CVA	coxsackie virus A
CVB	coxsackie virus B
DAF	decay-accelerating factor
dsRNA	double-stranded RNA
EGTA	egtazic acid
EM	electron microscopy
ER	endoplasmic reticulum
EV1	echovirus 1
EV71	enterovirus 71
FMDV	foot and mouth disease virus
GuHCl	guanidine hydrochloride
G3BP1	ras-GTPase-activating protein-binding protein 1
HSP	heat shock protein
IDPN	β, β'-Iminodipropionitrile
IRES	internal ribosome entry site
ITAF	IRES trans-acting factor
NR	neutral red

PCBP2	poly(rC) binding protein 2
p.i.	post infection
PI4P	phosphatidylinositol 4-phosphate
PABP	poly A binding protein
PTB	polypyrimidine track binding protein
S	svedberg unit
SG II	sybr green II
siRNA	small interfering RNA
VPg	viral protein genome linked

1 INTRODUCTION

Enteroviruses are important pathogens that have been associated with several diseases among humans and other mammals with a wide range of severity. Despite the prevalence of enterovirus infections, the treatment of these infections is mostly supportive as no approved antivirals exist on the market. In addition, vaccines have only been developed against a couple of enteroviruses. After its identification in 1908, the best known enterovirus, poliovirus, has been extensively investigated in order to understand the life cycle of the virus. Over the years, many aspects of poliovirus infection have been covered, many of which are also common to all enteroviruses. The infection cycle begins when the virus first binds to a receptor on host cell surface, after which the virus is internalized via endocytosis. Next, viral RNA is released out from the virus particle during uncoating and is also released into the cell cytoplasm through the endosomal membrane. In the cytoplasm, viral RNA is translated, processed and replicated in order to produce new virions, which finally are released from the cell. Despite years of poliovirus and other enterovirus research, some of the infection steps are still poorly understood and it has also become evident that differences between enterovirus species occur. Thus, the research on fundamental details of enterovirus infection is still of great importance in order to find potential and common targets for antiviral therapy.

This thesis concentrates on the infection steps of enterovirus B species after the viral entry into the host cell, more specifically on factors that promote uncoating and replication. A new uncoating intermediate of EV1 was characterized and in addition, cellular factors that affect efficient replication of enteroviruses were investigated. It was found that, in addition to the proteases of enteroviruses themselves, cellular calpains can cleave the viral polyprotein in-vitro, and may contribute to polyprotein processing during infection. In addition, it was shown that during infection, host cell intermediate filament, vimentin, affects infection by promoting the efficient production of viral non-structural proteins, such as proteases, by helping to organize the replication compartment in the perinuclear region.

2 REVIEW OF THE LITERATURE

2.1 Enteroviruses

The genus enterovirus is part of the *picornaviridae* family. Inside enterovirus genus, the species which infect humans are divided into four enterovirus species A-D and three rhinovirus species A-C that contain over 100 different virus serotypes. The enterovirus B species contains 63 serotypes of coxsackieviruses and echoviruses including coxsackie virus B (CVB) serotypes 1-6, coxsackie virus A 9 (CVA9) and echovirus 1 (EV1). Enteroviruses are one of the most common human viruses and can cause variety of different diseases whose severity can vary from mild flu like symptoms or rashes to encephalitis or myocarditis (Tapparel *et al.* 2013, Pons-Salort *et al.* 2015). Severe enterovirus diseases occur especially in neonates and immuno-compromised individuals (Muehlenbachs *et al.* 2015). Enterovirus species infect via fecal-oral route and rhinovirus species via respiratory track where the primary infection takes place. From primary infection sites, enteroviruses can spread into secondary tissues and cause infection in other organs such as heart, liver and brain. In addition to acute infection, enterovirus and rhinovirus species have also been associated with chronic diseases such as chronic obstructive pulmonary disease, atherosclerosis and type 1 diabetes (Roivainen *et al.* 1998, Hober and Sauter 2010, Thibaut *et al.* 2016), which increases their clinical importance.

Despite the great clinical and economic impact of enteroviruses, vaccines have only been developed against poliovirus and enterovirus 71 (EV71) from the enterovirus C and A species, respectively. Moreover, the development of vaccines against all enterovirus serotypes is not feasible. In addition, although several enterovirus inhibitors have been identified and entered clinical trials, none of them have passed through for use in general population. Thus, a broad-range enterovirus antiviral is needed, which requires identification and high-level understanding of the function of viral and cellular components in enterovirus infection.

2.1.1 Overview of enterovirus structure and infection cycle

Enteroviruses are small non-enveloped viruses, which have positive sense RNA as their genome. The genome is encapsidated by an icosahedral capsid, which is composed of four different proteins VP1-VP4. The capsid is composed of 60 copies of each protein of which VP1-VP3 are located on the capsid surface, whereas VP4 is an internal protein (Fig. 1).

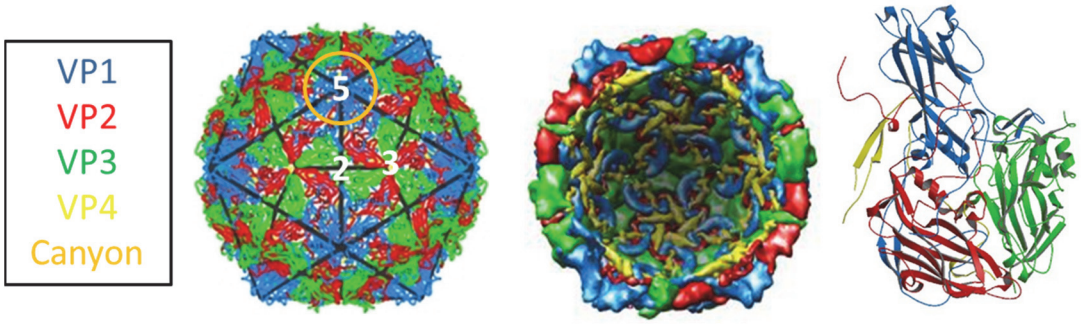

FIGURE 1 Schematic representation of an enterovirus particle. The capsid is an icosahedron structure with 2- 3- and 5-fold symmetry axes (marked on the left) and is formed from 60 protomers of VP1-VP4 proteins (ribbon structure on the right). Proteins VP1-VP3 are situated on the surface, while VP4 is an internal protein (inside view, in the middle). In the left figure, also a depression around the 5-fold symmetry axis, the canyon, is marked in orange. The figures were obtained from ViperDB (http://viperdb.scripps.edu), using the PDB ID for echovirus 1 (1ev1) (Carrillo-Tripp *et al.* 2009).

Although there are many different enteroviruses, they all share several common properties related to their infection, and in general the life cycle is well known (Fig. 2, reviewed in Baggen, Thibaut *et al.* 2018). Enteroviruses enter the cell by binding to a specific receptor on the cell surface. Several of these attachment receptors have been identified: PVR for poliovirus, integrins for EV1 and CVA9, decay-accelerating factor (DAF) and coxsackievirus-adenovirus receptor (CAR) for CVBs, DAF for several echoviruses and, the most recent finding, a neonatal Fc receptor for several echoviruses, to mention a few (listed in Baggen, Thibaut *et al.* 2018, Laajala and Marjomaki 2019), and Table 1). Receptor binding results in receptor mediated endocytosis, which can vary depending on the virus serotype and, also, the cell type. In the endosomes, uncoating of the viral genome occurs and the RNA is released into the cytoplasm. Next, the single large open reading frame is translated resulting in a single polyprotein. Subsequently, the polyprotein is proteolytically processed by viral proteases in order to release individual proteins needed for viral replication and capsid assembly. Synthesis of the RNA is carried out by viral RNA dependent RNA polymerase (3D polymerase), which first produces a negative strand copy of the incoming positive strand. The negative strand then serves as a template for the synthesis of positive strand RNA, which can either be translated to produce more viral proteins or packed into new virions. The assembly of viral particles takes place in the cytoplasm when capsid proteins VP0, VP1 and VP3 assemble into

protomers and further pentamers. Pentamers condense around the replicated RNA to produce a provirion, which finally maturates into infectious virion when VP0 is cleaved into VP2 and VP4 (Basavappa *et al.* 1994). In addition, it has been shown with other picornavirus, namely parechovirus, that RNA folding has an important role in the assembly (Shakeel *et al.* 2017). In the last step of the infection cycle, the mature virions are released out from the cell by lysis (reviewed in Harris, K. G. and Coyne 2014) or as more recent and increasing evidence shows, non-lytically via extracellular vesicles (reviewed in Lai *et al.* 2016).

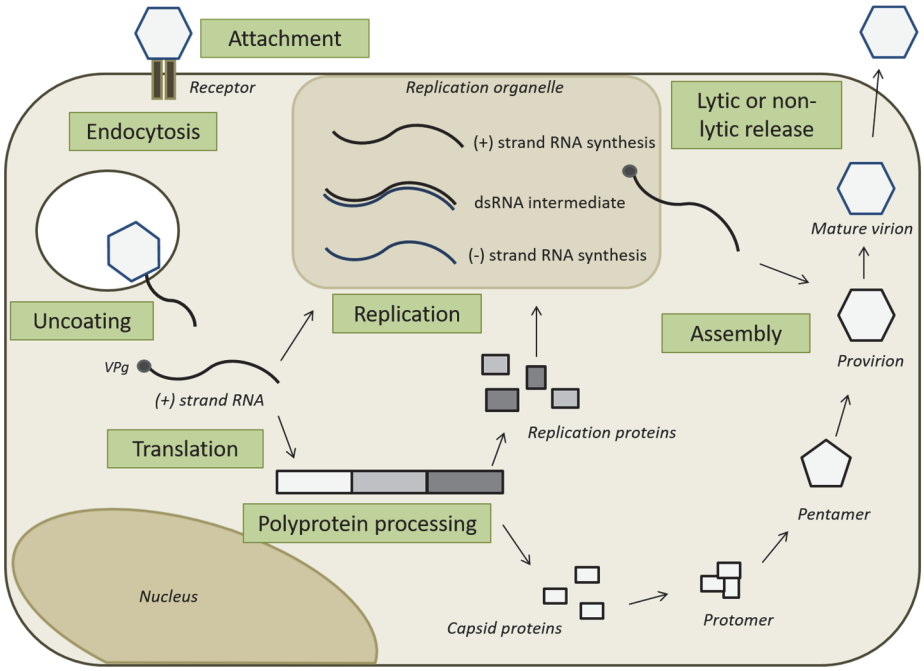

FIGURE 2 Overview of the enterovirus lifecycle. The image was modified from a review by Baggen, Thibaut *et al.* 2018. The lifecycle of enteroviruses starts when the virus binds to a specific receptor on the cell surface. This triggers a receptor mediated endocytosis and the virus is internalized into the host cell. In the endosome, uncoating occurs and viral RNA is subsequently released into the cytoplasm of the host cell. The viral positive sense RNA is next translated in the cytoplasm as one unit, following processing of the formed polyprotein. The proteins needed for capsid assembly and replication are released from the polyprotein during processing. In addition to translation, the viral RNA is also replicated. The RNA contains a viral VPg (3B) protein, which is needed for replication carried out by viral RNA-dependent RNA polymerase, 3D polymerase. The replication takes place on host cell-derived membranous replication organelles, when the polymerase synthesizes first negative sense RNA and, through a dsRNA intermediate, also new copies of positive sense RNA. Next, the positive sense RNA can go through another round of translation or replication or be packed into new virions. The assembly occurs in the cytoplasm when the capsid proteins first assemble into protomers and subsequently pentamers, which finally condense around the viral RNA, forming a provirion. After maturation of the provirion, new infectious virions are released out from the cell via lysis or non-lytically in extracellular vesicles. Abbreviations: VPg, viral protein genome linked; dsRNA, double-stranded RNA.

2.1.2 Uncoating

Once the virus has entered the host cell by endocytosis, it is still in a different compartment from the cellular translation and replication machinery, and thus, the virus still needs to translocate the RNA into the cytoplasm. This phase includes two steps. First, during uncoating, the RNA comes out of the viral capsid, which needs to be metastable in order to protect the RNA outside the cell, but on the other hand, to be able to open and release the genome inside the host cell. Second, during RNA release, the RNA is translocated through the endosomal membrane into the cytoplasm, where translation and replication take place (reviewed in Baggen, Thibaut *et al.* 2018).

TABLE 1 Enterovirus receptors. The table was modified from a review by Baggen, Thibaut *et al.* 2018. Abbreviations: CAR, coxsackievirus–adenovirus receptor; CDHR3, cadherin-related family member 3; CV, coxsackievirus; CV-A24v, coxsackievirus A24 variant; DAF, complement decay-accelerating factor; DC-SIGN, dendritic cell-specific ICAM-grabbing non-integrin; E, echovirus; EV, enterovirus; EV-A71-PB, EV-A71-PSGL1-binder; FcRn, neonatal Fc receptor; ICAM, intercellular adhesion molecule; LDLR, low-density lipoprotein receptor; LRP, LDLR-related protein; PSGL, P-selectin glycoprotein ligand 1; PVR, poliovirus receptor; SCARB2, scavenger receptor class B member 2; VLA2, very-late antigen 2; VLDLR, very-low-density lipoprotein receptor.

Receptor	**Virus**	**Reference**
PVR	Poliovirus (serotypes 1-3)	Mendelsohn *et al.* 1989
SCARB2	EV-A71 CV-A (serotypes 7, 14, 16)	Yamayoshi *et al.* 2009, Yamayoshi *et al.* 2012
PSGL1	EV-A71-PB CV-A (serotypes 2, 7, 10, 14, 16)	Nishimura *et al.* 2009, Nishimura and Shimizu 2012
Annexin II, DC-SIGN, nucleolin and vimentin	EV-A71	Reviewed in Yamayoshi *et al.* 2014
Heparan sulfate	EV-A71 E-5	Reviewed in Yamayoshi *et al.* 2014, Royston and Tapparel 2016
Sialic acid	EV-A71, CV-A24v EV-D70, EV-D68	Yamayoshi *et al.* 2014, Baggen *et al.* 2016, Baggen, Hurdiss *et al.* 2018
ICAM5	EV-D68	Wei *et al.* 2016
LDLR, VLDLR and LRP	Rhinovirus (minor)	Hofer *et al.* 1994

ICAM1	Rhinovirus (major) CV-A21, CV-A24	Greve *et al.* 1989, Royston and Tapparel 2016, Baggen, Hurdiss *et al.* 2018
CDHR3	Rhinovirus C	Bochkov *et al.* 2015
DAF	CV-A21 CV-B (serotypes 1, 3, 5) E (10+ serotypes)	Bergelson *et al.* 1994, Royston and Tapparel 2016
CAR	CV-B (serotypes 1-6)	Martino *et al.* 2000
Integrin $\alpha_v\beta_3$	CV-A9, E-9	Roivainen *et al.* 1994, Nelsen-Salz *et al.* 1999
Integrin $\alpha_v\beta_6$	CV-A9	Williams *et al.* 2004
Integrin $\alpha_2\beta_1$ (VLA2)	E-1, E-8	Bergelson *et al.* 1992
FcRn	E (serotypes 1, 3, 5-7, 9, 11, 13, 14, 25, 26, 30) EV-B85, CV-A9	Morosky *et al.* 2019, Zhao *et al.* 2019

Some enteroviruses are acid labile and the uncoating process is triggered by low pH in endosomes (Prchla *et al.* 1994, Liu *et al.* 2018). On the other hand, many enteroviruses are acid stabile and for many of these viruses, receptor binding induces conformational changes that lead to uncoating (Tsang *et al.* 2001, Coyne and Bergelson 2006, Yamayoshi *et al.* 2013, Wei *et al.* 2016). Most of these uncoating receptors bind to a deep surface suppression called canyon, leading to an expulsion of a stabilizing lipid moiety, called a pocket factor, from the canyon floor (Rossmann *et al.* 2002, Butan *et al.* 2014).

However, the uncoating cue for some acid stabile enteroviruses, such as EV1 and CVA9 is still unknown. EV1 and CVA9 receptors, α2β1 and αvβ3 integrins respectively, do not seem to trigger uncoating, and in addition, the viruses are internalized into pH neutral multivesicular bodies (Marjomaki *et al.* 2002, Xing *et al.* 2004, Karjalainen *et al.* 2011, Shakeel *et al.* 2013, Huttunen *et al.* 2014). Furthermore, in some cases, the attachment receptor might be different from the uncoating receptor like with CVBs, which first bind to DAF but subsequently must interact with CAR in order to start the uncoating process (Coyne and Bergelson 2006). Interestingly, it was shown recently that like CAR for CVBs, neonatal Fc receptor could serve as a common uncoating receptor for echoviruses (Zhao *et al.* 2019). In that study, several echoviruses were shown to be dependent on Fc receptor for successful infection, and in addition, the receptor was more specifically shown to induce uncoating of echovirus 6.

Although enteroviruses use many different receptors and entry routes and the cues for uncoating vary, the subsequent uncoating steps are conserved in many ways. It has been shown that three distinct particles exist during uncoating

process (Belnap *et al.* 2000, Tuthill *et al.* 2006) (Fig. 3). First is the RNA containing intact form of the virion, which is able to bind to the receptor. Second is an intermediate particle, also called expanded or A-particle, which still has RNA inside but has gone through structural alterations triggered by either pH, receptor engagement or some other unknown factor. Finally, is the empty particle, which has released the genome and is no longer infective. Usually these different particle forms have been separated in sucrose gradients and according to their different sedimentation coefficient, intact, intermediate and empty particles have also been named as e.g. 160S, 135S and 80S, respectively.

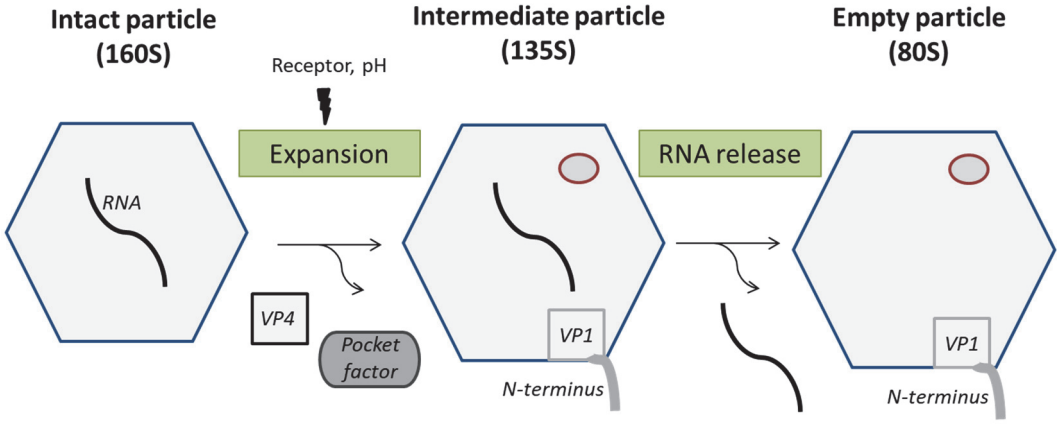

FIGURE 3 Uncoating process of enteroviruses. The image was modified from a review by Baggen, Thibaut *et al.* 2018. Three different particle types have been observed during enterovirus uncoating. First is the native virion, an intact particle, which includes all four capsid proteins VP1-VP4 and RNA. Second, is an intermediate particle, which has expanded and externalized pocket factor, VP4 protein and N-terminus of VP1 protein, which anchors the particle to the endosomal membrane. The uncoating trigger can either be pH, receptor binding or some other unknown cue. Third, is the non-infectious empty particle, which has externalized RNA through an opening near the twofold symmetry axis (indicated by a red circle). The different particle forms have different sedimentation coefficients in sucrose gradient, which are indicated in brackets.

Typically, the uncoating intermediate particle has been studied by either heating the intact particle in elevated temperatures or treating the particle in acidic environment, with or without receptor engagement (Gomez Yafal *et al.* 1993, Xing *et al.* 2000, Nurani *et al.* 2003, Milstone *et al.* 2005, Garriga *et al.* 2012, Harutyunyan *et al.* 2013, Ren *et al.* 2013, Shingler *et al.* 2013, Butan *et al.* 2014). These in vitro studies have revealed that the intermediate particles are 4% larger compared to intact virions (Belnap *et al.* 2000), have lost the pocket factor (Butan *et al.* 2014) and are able to interact with membranes since the hydrophobic N-terminus of VP1 is externalized from the capsid (Fricks and Hogle 1990). In addition, an internal protein VP4 is released from the particle (Crowell and Philipson 1971), and finally the most recent studies suggest that RNA exits from an opening near the two-fold axis (Levy *et al.* 2010, Bostina *et al.* 2011). Despite of numerous in-vitro studies of uncoating intermediates, it still has remained unclear whether this kind of uncoating intermediate exists in cells. In contrast to the global changes in the virion induced by heat or acid treatments, the infection in cells is

asymmetric when the virus binds to a single receptor and is supposed to release the RNA from a site towards the membrane. Recently, a local uncoating process of CVB3 was studied using a lipid bilayer nanodisc, where a CAR receptor was immobilized (Lee, H. *et al.* 2016). High resolution cryo-electron microscopy (cryo-EM) structure of the particle revealed the loss of pocket factor and extrusion of VP1. However, in contrast to the in vitro studies, which have shown that the RNA is released near the two-fold axis (Levy *et al.* 2010, Bostina *et al.* 2011), this study showed an opening at the three-fold axis (Lee, H. *et al.* 2016).

Although the uncoating step, where RNA is released from viral capsid, is fairly well characterized, the subsequent step, where RNA is released through endosomal membrane into the cytoplasm, is more poorly understood, and the trigger for the release has not been identified. So far, studies on Rhinovirus have shown that VP4 protein can independently induce permeability on lipid membranes of liposomes (Davis *et al.* 2008) and that VP4 forms a size-selective multimeric pore, which could serve as a channel for the release of the viral RNA (Panjwani *et al.* 2014). Furthermore, a cryo-electron tomograph suggested that long umbilical connectors mediate the transfer of poliovirus RNA through the membrane (Strauss *et al.* 2013), which was also supported by a more recent study where poliovirus RNA was protected from degradation by co-endosytoced ribonucleases (Groppelli *et al.* 2017). In addition, electron tomography of EV1 induced multivesicular bodies revealed increased permeability of the membranes after virus entry (Soonsawad *et al.* 2014).

Although the receptor serves as a trigger for uncoating with many enteroviruses, studies have shown that the uncoating does not occur immediately on the cell surface after receptor binding, but for example poliovirus is internalized before uncoating (Brandenburg *et al.* 2007). In addition, neutral red assay, where viral uncoating has been prevented by crosslinking the RNA, has shown that the uncoating of EV1 and CVA9 begins after 30-60 min post-infection (p.i.), suggesting that the viruses have already internalized into the cell (Siljamaki *et al.* 2013, Huttunen *et al.* 2014, Soonsawad *et al.* 2014). Thus, it has been suggested that an additional cue(s) for uncoating and genome release occurs. A recent study identified lipid-modifying enzyme PLA2G16 as an additional factor during RNA release of enteroviruses through the endosomal membrane (Staring *et al.* 2017). The exact mechanism how PLA2G16 affects RNA release is not known but, it was suggested to work as a cellular sensor during membrane damage at the viral entry sites, and subsequently initiate or maintain pore formation during RNA release (Staring *et al.* 2017).

2.1.3 Translation and polyprotein processing

Since enteroviruses have a small genome and encode only a limited number of viral proteins, they also need to rely on host cell factors during translation and replication. Thus, to ensure efficient infection, enteroviruses have evolved to utilize and modify host cell proteins to promote the infection. The translation and replication processes are highly conserved among enteroviruses, which offer a potential target for antiviral development. However, the lack of (broad-

spectrum) antiviral against enteroviruses indicates that the details of both viral and cellular factors during translation and replication, needs further elucidation.

After being released into the host cell cytoplasm, the RNA genome (7500 nt) of enteroviruses is translated as a single viral polyprotein (Fig. 4). In contrast to cellular cap dependent translation, the viral polyprotein is translated in a cap-independent manner via an internal ribosome entry site (IRES) at the 5′ non-coding region of the viral RNA (reviewed in Lozano and Martinez-Salas 2015). The positive strand RNA is translated in a 5′ to 3′ direction and cellular functions are also utilized as the translation machinery also involves cellular IRES trans-acting factors (ITAFs) (reviewed in Lee, K. M. *et al.* 2017). ITAFs are cellular proteins, which do not function in cap-dependent translation but help in the process of cap-independent translation by e.g. stabilizing the IRES in order to promote the binding of other canonical translation factors as well as ribosomes (Pilipenko *et al.* 2000). Several ITAFs have been associated with IRES-mediated translation of enteroviruses (Table 2). As an example, it has been shown that a cellular RNA binding protein, poly(rC) binding protein 2 (PCBP2), interacts with domain IV of poliovirus IRES (Blyn *et al.* 1996). Furthermore, the depletion of the PCBP2 protein from Hela cell extracts prevented the IRES-mediated translation of poliovirus (Blyn *et al.* 1997). In addition, another RNA binding protein, lupus autoantigen, was shown to be cleaved by viral protease 3C during poliovirus infection (Shiroki *et al.* 1999). The cleavage of this mainly nuclear protein resulted in the redistribution of the truncated form into the cytoplasm, where it could still enhance the initiation of translation.

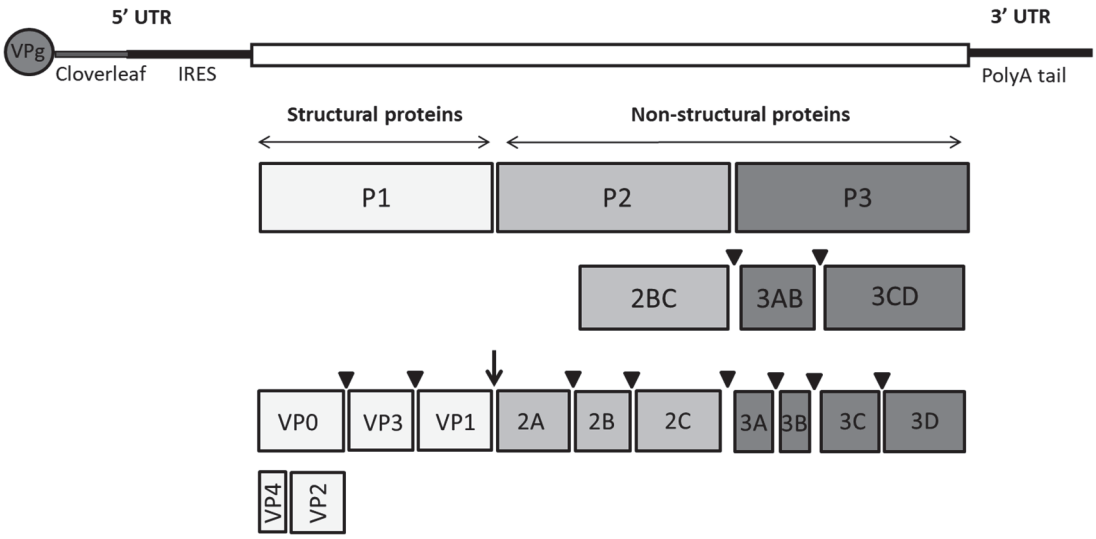

FIGURE 4 Schematic overview of enterovirus genome and the translated polyprotein. The image was modified from a review by Lin, Chen *et al.* 2009. The 5′ non-coding region contains six domains (I-VI) of which the first is a cloverleaf structure and the rest comprise the viral IRES. The 3′ non-coding region contains a poly A tail. In the coding region, three main precursor proteins and 11 mature proteins are shown. Arrow and arrow heads indicate cleavages carried out by viral proteases 2A and 3C/3CD, respectively. Abbreviations: VPg, viral protein genome linked; UTR, untranslated region; IRES, internal ribosome entry site.

The synthesized polyprotein consists of three regions P1-P3 of which P1 contains structural proteins, while P2 and P3 contain non-structural proteins, which are needed to promote the viral replication in different ways. P1 contains capsid proteins VP0-VP3, P2 proteins 2A-2C and P3 proteins 3A-3D. In order to release the individual proteins or some functional precursors such as 2BC, 3AB and 3CD, the polyprotein is next processed by viral proteases 2A, 3C and a precursor 3CD (reviewed in Palmenberg 1990). The primary cleavage between P1 and P2 regions is carried out by 2A protease cotranslationally, as soon as the required elements have been translated by the ribosomes (Toyoda *et al.* 1986, Palmenberg 1990). The release of 2A from the polyprotein is thus not prerequisite for the activity of 2A, but instead, the primary cleavage occurs in cis. However, also in-trans cleavage between P1-P2 has been reported for 2A in-vitro (Nicklin *et al.* 1987). Besides primary cleavage and maturation cleavage of VP0 into VP2 and VP4, the rest of the polyprotein cleavages are carried out either by 3C protease or its precursor 3CD (Hanecak *et al.* 1982, Ypma-Wong *et al.* 1988). It has been suggested that, like 2A, also 3C protease of poliovirus cleaves the P3 region in cis (Hanecak *et al.* 1984). However, also in trans cleavage action by 3C has been shown at several sites in the P2-P3 region in-vitro (Ypma-Wong and Semler 1987). It was shown that the processing of P2 region required only intact 3C in the P3 region. In contrast, the processing of P1 region required the whole P3 region to produce a protease capable of cleaving P1 into capsid proteins (Ypma-Wong and Semler 1987). Accordingly, it was shown later in-vitro that efficient processing of poliovirus P1 region is carried out by protein 3CD (Ypma-Wong 1988). The 3CD is a precursor of 3C protease and 3D polymerase and has been shown to function as a protease but lack polymerase activity (Harris, K. S. *et al.* 1992). Furthermore, the processing of P1 has been shown to be dependent on a cellular heat shock protein 90 (HSP90), which helps in the correct folding of P1 prior to processing (Geller *et al.* 2007). In addition to 3C mediated cleavage of 3CD into 3C and 3D, 2A protease has been shown to be responsible for an alternative cleavage pathway resulting in 3C' and 3D' proteins (Lee, C. K. and Wimmer 1988). However, the biological function of these alternate proteins is unclear, since it was shown that they are not essential for virus replication (Lee, C. K. and Wimmer 1988). In addition to polyprotein cleavage, enteroviral proteases also cleave different host cell proteins in order to enhance viral replication (reviewed in Laitinen *et al.* 2016).

TABLE 2 Cellular proteins related to IRES-mediated translation of enteroviruses, and their associated viral components. The table was modified from a review by Lin, Chen *et al.* 2009. Abbreviations: PTB, polypyrimidine tract-binding protein; nPTB, neural polypyrimidine tract-binding protein; PCBP, poly(rC) binding protein; Unr, upstream element binding protein; La, Lupus autoantigen; hnRNP, heterogeneous nuclear ribonucleoprotein; DRBP76:NF45heterodimer, dsRNA binding protein 76: NF45 heterodimer; FBP2, far upstream element binding protein 2; PABP, poly(A)-binding protein; PV, poliovirus; HRV, human rhinovirus; CVB3, Coxsackie virus B3; EV71, enterovirus 71.

Host protein	**Viral component**	**Virus**	**Reference**
PTB	IRES, 3C	PV	Hellen *et al.* 1993, Gutierrez-Escolano and del Angel 1996, Back *et al.* 2002
nPTB	IRES	PV	Guest *et al.* 2004
PCBP1	cloverleaf, IRES	PV, HRV	Gamarnik and Andino 1997, Choi *et al.* 2004
PCBP2	cloverleaf, IRES, 3CD, 3C	PV, HRV, CVB3	Blyn *et al.* 1996, Blyn *et al.* 1997, Walter, B. L. *et al.* 1999, Choi *et al.* 2004, Perera *et al.* 2007, Chase *et al.* 2014
Unr	IRES	PV, HRV	Hunt *et al.* 1999, Boussadia *et al.* 2003
La	IRES, 3C	PV, HRV, CVB3	Shiroki *et al.* 1999, Ray and Das 2002, Costa-Mattioli *et al.* 2004
hnRNP A1	IRES	HRV2, EV71	Cammas *et al.* 2007, Lin, Shih *et al.* 2009
Nucleolin/C23	IRES	PV, HRV	Izumi *et al.* 2001
DRBP76:NF45heterodimer	IRES	HRV2	Merrill *et al.* 2006, Merrill and Gromeier 2006
FBP2	IRES	EV71	Lin, Li *et al.* 2009
PABP	IRES	PV	Svitkin *et al.* 2001

2.1.4 Replication

Enterovirus replication occurs on rearranged host cell membranes, which are thought to originate from endoplasmic reticulum (ER), Golgi and components of autophagosomal membranes (Bienz *et al.* 1987, Schlegel *et al.* 1996, Jackson *et al.* 2005). The formation of these replication organelles may promote efficient replication by gathering viral and host proteins, which are important for replication. The replication complex has been shown to involve virus induced membranes (Bienz *et al.* 1992), viral proteins such as 2B, 2BC, 3A and 3D (Bienz *et al.* 1994, Schlegel *et al.* 1996, Suhy *et al.* 2000) as well as multiple host proteins (reviewed in Lin, Chen *et al.* 2009). Important viral proteins in membrane remodelling are 3A, 2B and 2BC, which participate in the process in several ways. The protein 3A recruits phosphatidylinositol-4-kinase IIIβ to the replication site and, in consequence, the local levels of phosphatidylinositol 4-phosphate (PI4P) lipids increase (Hsu *et al.* 2010). It has been suggested that PI4P lipids are important for both the formation of replication organelles and replication (Melia *et al.* 2017). In addition, the PI4P lipids may recruit other viral and host proteins which are important for replication. For example, in-vitro studies have shown that the viral RNA dependent RNA polymerase, 3D, preferentially binds to PI4P lipids (Hsu *et al.* 2010). In addition, cellular oxysterol binding protein mediates the exchange of PI4P with cholesterol, resulting in an increase of cholesterol content of replication membranes (Mesmin *et al.* 2013). As a consequence, the higher cholesterol content may induce membrane deformation which is required in the formation of replication organelles. Alternatively, the cholesterol may also redistribute to the membranes of replication from plasma membrane via recycling endosomes (Ilnytska *et al.* 2013). The viral protein 3A also recruits Golgi-specific Brefeldin A resistance factor 1 and indirectly GTPase ADP-ribosylation factor 1, which leads to the loss of the vesicle coat protein I and finally disturbance of the secretory pathway and protein secretion, as well as, to disassembly of the Golgi apparatus (Wessels, Duijsings, Lanke *et al.* 2006, Wessels, Duijsings, Niu *et al.* 2006). As a consequence, e.g. antiviral signalling proteins are not secreated on the cell surface, and hence, other cells are not alerted about viral infection. 2B protein, on the other hand, acts as a viroporin by releasing calcium stores from ER, resulting in the blockage of protein translocation from ER to Golgi and increased targeting of vesicles to the Golgi complex (Agirre *et al.* 2002, de Jong *et al.* 2006). The function of protein 2C is least understood, but it has been related to multiple steps during enterovirus infection, including replication. It has been shown to function as a helicase and an ATPase, and to play a role in membrane rearrangement, RNA binding and replication, as well as, uncoating and encapsidation (reviewed in van der Linden *et al.* 2015)

The key protein in enterovirus replication is viral polymerase 3D, which both catalyses uridylylation of the protein primer 3B (VPg) and RNA chain elongation (Flanegan and Baltimore 1977, Paul *et al.* 1998). Other essential elements for viral replication are cis acting RNA elements (CREs) located at the 5’ and 3’ non-coding regions, as well as, at the coding region of viral protein 2C

(CRE(2C)) (Andino *et al.* 1990, van Ooij *et al.* 2006). These CREs help in the initiation of the RNA synthesis by interacting with viral and cellular proteins to form a ribonucleoprotein complex, and playing a role in the uridylylation of the VPg. The 3D polymerase synthesizes negative strand copies in 3′ to 5′ direction and a replication intermediate, double-stranded RNA (dsRNA), is generated. The negative strand RNA serves as a template for new copies of positive strands and the uridylylated VPg serves as a primer in the synthesis of both strands (Pettersson *et al.* 1978).

Positive-stranded RNA viruses use the same RNA as a template for translation and replication. However, these two processes cannot occur at the same time since the RNA is translated from 5′ to 3′ direction, whereas 3D polymerase binds to the 3′ end of the RNA during replication. Thus, a switch mechanism between translation and replication must occur, and some candidates have been suggested to regulate such a mechanism. For example, studies on poliovirus suggested, that cellular polypyrimidine track binding (PTB) protein first functions as a cellular ITAF and enhances viral translation (Back *et al.* 2002). The cleavage of PTB by 3CD protease later during infection, however, decreases the levels of viral translation and possibly mediates as a switch to replication (Back *et al.* 2002). In addition, another RNA binding ITAF, PCBP2, has been shown to be involved in the switch between translation and replication. PCBP2 first binds to domain IV in the viral IRES during translation (Blyn *et al.* 1996, Blyn *et al.* 1997), but when the levels of viral protease 3CD (and 3C) increase, PCBP2 is cleaved and can no longer bind to the domain IV in the viral IRES resulting in decrease of translation (Perera *et al.* 2007, Chase *et al.* 2014). However, the cleaved PCPB2 can bind to domain I (cloverleaf) in the 5′ non-coding region and form a ternary complex with 3CD (Parsley *et al.* 1997). The formation of the complex can in turn promote viral replication by bridging the 5′ and 3′ termini (Herold and Andino 2001).

2.2 Cellular proteases vs. viral proteases

2.2.1 Classification and enzymatic function of proteases

Proteases are enzymes, which hydrolyse peptide bonds between amino acid residues in polypeptide chains of proteins. They can be found in all organisms from eukaryotes to prokaryotes and viruses and have also largely been utilized in biotechnology industry. Proteases are classified by the nature of the reaction they catalyse: endopeptidases (such as trypsin, papain, chymotrypsin and pepsin) attack internal peptide bonds of the target protein, whereas exopeptidases cleave the terminal amino acids from either amino or carboxy end of the polypeptide (reviewed in Rao *et al.* 1998). Endopeptidases are further divided into different classes by the nature of their catalytic site. 1) Serine, cysteine and threonine proteases carry out the catalysis in two steps. They use serine, cysteine or threonine at their catalytic site as a nucleophilic residue to

covalently attach into one of the protein fragments, releasing first half of the product. The temporary acyl-enzyme intermediate is then hydrolysed by active water in order to release the second product. 2) Aspartic proteases have two aspartic acid residues close together at their active site. These two aspartic acids are used in a one-step catalysis reaction, where activated water molecule performs a nucleophilic attack at the peptide bond. 3) Metalloproteases also perform a one-step catalysis using metal ions such as Zn^{2+} in the reaction (reviewed in Rao *et al.* 1998). Moreover, different classes of proteases can also be further grouped based on the similarity of their amino acid sequence and three-dimensional structure.

2.2.2 Cellular proteases

Proteases are a diverse group of proteins in cells, and their role can vary from non-specific degradative functions to highly specific proteolytic reactions resulting in new protein products. These specific reactions then regulate the localization, action and further interactions of many proteins, which in turn results in biological processes such as cell cycle progression, wound healing, haemostasis, neuronal outgrowth, immunity and apoptosis (Lopez-Otin and Bond 2008, Turk *et al.* 2012, Quiros *et al.* 2015, Reinhard *et al.* 2015). The importance of correct protease function is also manifested in many diseases such as cancer, neurodegenerative disorders and cardiovascular diseases (Lopez-Otin and Hunter 2010, Gordon *et al.* 2014, Nalivaeva *et al.* 2014, Gutierrez-Fernandez *et al.* 2015), which also makes proteases potential targets for drug development or candidates as diagnostic biomarkers (Turk 2006).

Proteases catalyse mainly irreversible reactions and hence their action needs to be tightly regulated in cells (reviewed in Lopez-Otin and Bond 2008). The regulation of proteases occurs via endogenous inhibitors, limitation of proteases into specific regions of the cell (such as mitochondria and lysosomes), regulation of gene expression, production of the proteases as non-active proenzymes, which subsequently are activated, or modification of proteases post-translationally (reviewed in Lopez-Otin and Bond 2008).

The majority of endogenous inhibitors of proteases are proteins and they can inhibit the action of target protease in different ways: by directly binding to the active site, by binding next to the active site and consequently blocking the substrate access or by binding regions that block the dimerization of the protease and further activity (Bode and Huber 2000). The activation of inactive proenzymes can be either autocatalytic or catalysed by other proteases. In addition, the activation might require other factors such as apoptosome platform for caspases (Riedl and Salvesen 2007), a protein cofactor such as tissue factor glycoprotein (Versteeg and Ruf 2006) or like in the case of calpain proteases, calcium ions (Hosfield *et al.* 1999, Suzuki *et al.* 2004).

2.2.2.1 Calpains

Calpains are cytoplasmic calcium dependent proteases, which function in neutral pH environment. They exist ubiquitously from higher organisms like humans to

micro-organisms. Calpains have been shown to have a role in many cellular functions such as cell cycle progression and signal transduction as well as cell proliferation, differentiation, apoptosis and membrane fusion (Saido *et al.* 1994, Sorimachi *et al.* 1997, Carafoli and Molinari 1998, Huang and Wang 2001, Sorimachi 2001). In addition, calpains have also been associated in different diseases such as muscular dystrophy, non-insulin dependent diabetes, cancer and Alzheimer's disease (Branca 2004, Carragher 2006). Fifteen different calpains are expressed in humans, which can be either ubiquitous or tissue specific. The proteolytic processing by calpains does not result in degradation of the target protein, but instead, formation of a protein product, which is different compared to the original substrate (reviewed in Ono and Sorimachi 2012). This feature differentiates calpains from other major proteolytic actors in the cell, namely proteasomes, autophagy and caspases. In addition, calpains themselves recognize their substrates whereas in proteasomal degradation and autophagy, the substrates are tagged by other systems before processing, and caspases recognize short amino acid sequences of the target protein (reviewed in Ono and Sorimachi 2012).

Calpains belong to the papain like superfamily of cysteine proteases. The best characterized calpains 1 and 2 are called conventional calpains, whereas other calpains are referred as unconventional calpains. Based on the structure, calpains are further classified as classical or non-classical. The 80 kDa catalytic subunit of classical calpains is composed of N-terminal anchor helix region, the CysPc protease domains PC1 and PC2, the C2 domain-like domain, and the penta-EF-hand domains, whereas in non-classical calpains some of these four domains are deleted or replaced (Sorimachi *et al.* 1993, Maki *et al.* 1997). In order to form a functional protease, conventional calpains also contain a 30 kDa regulatory subunit, which does not have catalytic activity but is suggested to function as a chaperone-like component (Yoshizawa *et al.* 1995). In addition, the function of conventional calpains as well as calpain 8 and 9 is regulated by an endogenous inhibitor protein called calpastatin (Lee, H. J. *et al.* 1999, Hata *et al.* 2007, Kiss *et al.* 2008). Calpastatin inhibits calpains by occupying the active site of calpains but escapes itself from cleavage by looping around the active site cysteine (Hanna *et al.* 2008).

The activity of calpains is regulated by calcium ions, which have been shown to bind to several domains of the protease, including the CysPc protease domain (Moldoveanu *et al.* 2002, Goll *et al.* 2003). This binding results in alignment of the active site and further covertion into an active enzyme. In-vitro studies have shown that the calcium concentration requirement differs between calpain 1 and 2 and hence they are also called micro- and milli-calpains, respectively. However, the activation of calpains in cells is still poorly understood, since the micromolar and even millimolar calcium levels, which are shown to activate calpains in vitro, are not available in living cells. Nevertheless, at least two theories have been suggested for calpain activation in cells. First, it is suggested that calpains get activated when increased calcium concentration in the cytoplasm triggers autolysis in the catalytic and regulatory subunits of calpains, which subsequently increases sensitivity to calpain and substrate

accessibility (Imajoh *et al.* 1986, Inomata *et al.* 1988). Second, it is proposed that due to increased calcium concentration, calpains are translocated to membranes, where different protein activators and phospholipids activate calpains. This activation does not require autolysis and decreases the calcium requirement to physiological levels (Suzuki *et al.* 1987, Pontremoli *et al.* 1988, Saido *et al.* 1991, Molinari *et al.* 1994, Melloni *et al.* 1998). In addition, it has been suggested that calpains could be activated in a cascade, where calpain 1 is first activated in the presence of micromolar calcium concentration, which then also leads in the activation of calpain 2 (Tompa *et al.* 1996).

In addition to the calpain activation in living cells, the other big question is related to calpain substrates. The substrate specificity of calpains is still unclear even though several approaches have been applied (Stabach *et al.* 1997, Tompa *et al.* 2004, Cuerrier *et al.* 2005). Instead of the amino acid sequence, the overall 3D structure of the target protein seems to play a more important role in the substrate recognition (Sakai *et al.* 1987, Stabach *et al.* 1997). In addition, the location of calpains may have a role in the selection of target when e.g. translocation of calpains to membranes may favor membrane associated proteins as substrates. It has been shown that calpains have a narrow and deep active cite in the protease domain, and hence, it has been suggested that calpains mainly process their target proteins in the inter-domain unstructured regions, which can fit in the active site cleft (Moldoveanu *et al.* 2004). Despite the lack of rules that govern calpain substrate specificity, in vitro studies have revealed multiple calpain substrates including kinases and phosphatases, cytoskeletal proteins, membrane associated proteins and transcriptional factors (reviewed in Goll *et al.* 2003, Rintanen *et al.* 2012).

2.2.3 Viral proteases

Viral proteases are encoded by several different types of viruses apart from their capsid complexity, existence of an envelope or genome type (Krausslich and Wimmer 1988). In general, the proteases encoded by viruses are highly specific and perform only limited catalysis on target proteins such as viral polyproteins. In addition, the viral proteases may cleave different host cell factors in order to promote the infection. Since the precise coordination and function of viral proteases is essential for virus replication and infectivity, they are one of the key targets for antiviral development. In addition, as enzymes are highly detailed structures, which need to carry out specific reactions, viral proteases are not as easily mutated as for example capsid proteins, further highlighting their potential as antiviral targets.

2.2.3.1 Enteroviral proteases

Enteroviruses encode three proteases: 2A, 3C and a precursor protein 3CD. P2 region encodes for 2A, whereas 3C and 3CD are encoded in the P3 region of the polyprotein. The first cleavage between P1 and P2 regions of the viral polyprotein occurs co-translationally and is carried out by 2A (Toyoda *et al.* 1986, Palmenberg 1990), while the remaining cleavages are carried out by 3C or 3CD (Ypma-Wong

et al. 1988, Palmenberg 1990). In addition to the viral polyprotein processing, enterovirus proteases have an important role in the manipulation of host cell system to favor infection. Namely, 2A and 3C proteases cleave different host proteins in order to shut-off host cell translation and transcription machinery, to escape from viral recognition pathways of the immune system and to induce cell death. Many host cell protein targets for enterovirus proteases have been identified (reviewed in Laitinen *et al.* 2016), and some of them are listed in the table below (Table 3).

Enterovirus proteases belong to the chymotrypsin like superfamily of proteases and have cysteine residue at the active site, which works as a nucleophile in the proteolysis reaction (Seipelt *et al.* 1999). The catalytic triad of 2A is composed of histidine, aspartic acid and cysteine, whereas 3C has glutamic acid instead of aspartic acid in the triad (Laitinen *et al.* 2016). The amino acid residues at the catalytic triad are fully conserved and other residues close to the catalytic site largely conserved between all species in enterovirus genus, indicating similarity in the cleavage action of enteroviral proteases (Laitinen *et al.* 2016). On the other hand, the sequences of 2A and 3C are only 20% identical although the tertiary structure of the proteases is very similar having two separate domains, which both participate in orienting the catalytic region (Laitinen *et al.* 2016).

The sequence specificity of enterovirus proteases was first studied with poliovirus showing that 2A cleaves between phenylalanine-glycine or tyrosine-glycine residues in the polyprotein (Toyoda *et al.* 1986), whereas 3C cleaves between glutamine-glycine (Krausslich and Wimmer 1988). However, these cleavage sites are not conserved between polyproteins of enterovirus species, and in addition, not all polyprotein sites with these residue pairs are cleaved, indicating that the cleavage activity is also dependent on surrounding amino acids. Accordingly, later studies have revealed that the most important residues at the cleavage site are P4, P2, P1, P1' and P2' (Blom *et al.* 1996, Seipelt *et al.* 1999). In addition, it was shown with another picornavirus, the foot-and-mouth disease virus (FMDV), that there was no strict order in the processing of structural proteins by 3C (Kristensen *et al.* 2018). This was shown using the P1-2A precursor, where different cleavage sites (VP0/VP3, VP3/VP1 and VP1/2A) were blocked one by one (Kristensen *et al.* 2018).

TABLE 3 Cellular targets of enteroviral proteases 2A and 3C. The table was modified from review by Laitinen *et al.* 2016. Abbreviations: eIF4GI, eukaryotic translation initiation factor 4GI; MDA5, melanoma differentiation-associated protein 5; IFN, interferon; PABP, poly A binding protein; Cst-64, cleavage stimulation factor 64; CREB-1, cyclic AMP responsive element binding protein 1; IRF7, interferon regulatory factor 7; MAVS, mitochondrial antiviral signalling protein; Oct, octamer binding transcription factor; RIG-I, retinoic acid-inducible gene I; TAF4B, transcription initiation factor TFIID subunit 4B; TBP, TATA-binding protein; TRIF, toll/IL-1 receptor domain-containing adaptor inducing interferon-beta; G3BP1, Ras-GTPase-activating protein-binding protein 1; CVB, coxsackie virus B; PV, poliovirus; EV, enterovirus; HRV, human rhinovirus.

	Host protein	**Consequence(s) of processing**	**Virus**	**Reference**
2A protease	Dystropin	Disruption of sarcolemma	CVB3	Badorff *et al.* 2000
	eIF4GI	Decline of host-cell protein synthesis	CVB4, PV, EV71	Lamphear and Rhoads 1996, Goldstaub *et al.* 2000, Kuo *et al.* 2002
	MDA5	Inhibition of type I IFN response	CVB3, EV71, PV	Barral *et al.* 2007, Feng *et al.* 2014
	IFN (α, β and ω) receptor 1	Antagonization of type I IFN signalling	EV71	Lu *et al.* 2012
	Nucleoporin 62	-	PV, HRV16	Castello *et al.* 2009, Walker *et al.* 2013
	Nucleoporin 98	Inhibition of nuclear import/export	PV, HRV2, HRV16	Castello *et al.* 2009, Walker *et al.* 2013, Park *et al.* 2015
	Nucleoporin 153	-	PV	Castello *et al.* 2009
	Serum response factor	Downregulation of cardiac-specific contractile and regulatory genes	CVB3	Wong *et al.* 2012
	PABP	Inhibition of host-cell protein synthesis	PV	Joachims *et al.* 1999, Rivera and Lloyd 2008

3C protease	Cst-64	Impair of cellular 3′-end pre-mRNA processing and polyadenylation.	EV71	Weng *et al.* 2009
	CREB-1	Inhibition of CREB-activated transcription	PV	Yalamanchili *et al.* 1997
	IRF7	Inhibition of IFN gene expression	EV71	Lei *et al.* 2013
	MAVS	Inhibition of types I and III IFN response, changes of mitochondria	CVB3	Mukherjee *et al.* 2011, Lind *et al.* 2016
	Nucleoporin 62	Relocation of cellular proteins and inhibition of nuclear import	HRV14	Gustin and Sarnow 2002, Walker *et al.* 2013
	Nucleoporin 153	Prevention of mRNA trafficking from nucleus to cytoplasm	HRV14, HRV16	Gustin and Sarnow 2002, Ghildyal *et al.* 2009, Walker *et al.* 2013
	Oct	Lost inhibition of transcriptional activation by the SV40 B enhancer	PV, HRV16	Amineva *et al.* 2004, Ramajayam *et al.* 2011
	RIG-I	Attenuation of virus recognition and the innate immune response	CVB3, EV71, PV, HRV16, Echo1	Barral *et al.* 2009, Feng *et al.* 2014
	TAF4B	Suppression of NF-κB response	PV	Neznanov *et al.* 2005
	TBP	Possibly inhibition of RNA polymerase II	PV	Das and Dasgupta 1993, Clark *et al.* 1993
	TRIF	Possibly suppression of the types I and III IFN signalling and apoptosis	CVB3	Mukherjee *et al.* 2011, Lind *et al.* 2016

PABP	Inhibition of host-cell protein synthesis	PV	Joachims *et al.* 1999, Kuyumcu-Martinez *et al.* 2002, Kuyumcu-Martinez *et al.* 2004, Rivera and Lloyd 2008
G3BP1	Inhibition of stress granule formation	PV	White *et al.* 2007

2.3 Cellular filaments in enterovirus infection

The cytoskeleton of a cell is composed of different filamentous structures, namely actin filaments, microtubules and intermediate filaments (reviewed in Fletcher and Mullins 2010). The cytoskeletal filaments are very dynamic and organize into networks, in a process, which is controlled by wide range of regulatory proteins. The main differences between the three filament types are related to their mechanical stiffness, assembly dynamics, polarization and associated molecular motors. The main functions of the cytoskeleton are to organize organs and other contents of the cell, to connect the cell to the surrounding environment, and to maintain the shape and drive the movements of the cell (reviewed in Fletcher and Mullins 2010). In addition, viruses, including enteroviruses, utilize cellular filaments in several steps of their lifecycle, from the first attachment to the last steps of egress and spread from cell to cell.

2.3.1 Actin filaments

Actin is a crucial player in many cellular functions and is found from both cytoplasm and the nucleus (Grummt 2006). Actin forms filaments (F-actin) but can also exist as a free monomer called G-actin. The monomers of G actin can polymerase into filamentous F-actin that can, in turn, rapidly depolymerize, a characteristic, which makes the actin a very dynamic structure. Actin participates in cell movement as well as in the maintenance of cell shape and is also a critical player in the membrane trafficking in the cells.

Actin has been shown to play a role in the most common internalization processes. F-actin dynamics is needed in many steps during clathrin-coated pit formation and invagination in clathrin mediated endocytosis (Merrifield *et al.* 2002, Merrifield *et al.* 2005, Yarar *et al.* 2005). In addition, caveolar/raft mediated endocytosis and micropinocytosis have been shown to be actin dependent (Pelkmans *et al.* 2002, Mercer and Helenius 2010). Since actin is so crucial player in many endocytic processes it is no surprise that also many viruses exploit actin

when entering the host cell. Even though studies using inhibitors against actin have shown contradictory results, there is an indication that also the infection of enterovirus B species is dependent on actin during entry (Pietiainen *et al.* 2004, Coyne and Bergelson 2006, Karjalainen *et al.* 2008, Heikkila *et al.* 2010, Delorme-Axford *et al.* 2013, Krieger *et al.* 2013). In addition, a comparative study of EV71 susceptible and resistant human rhabdomyosarcoma RD cell lines revealed that certain variant of beta-actin is needed for the infection of EV71 (Lui *et al.* 2013). Furthermore, enteroviruses have been shown to be dependent on regulators of actin dynamics, namely the members of Rho family GTPases Cdc42, RhoA and Rac1 (Coyne and Bergelson 2006, Karjalainen *et al.* 2008, Krieger *et al.* 2013, Huttunen *et al.* 2014).

2.3.2 Microtubules

Microtubules are polymers made of α- and β-tubulin dimers. Like actin, they are dynamic structures, constantly assembling and disassembling when tubulin dimers are added or removed. Microtubules originate from the microtubule organizing centre from where they radiate out towards the cell edges. Microtubules participate in many cellular functions such as cell migration, cell division as well as organelle and vesicle transport in the cells. The subunits of microtubules are structurally asymmetrical, which makes microtubules polarized polymers. This feature is important for the biological function of microtubules like for the interaction with motor proteins dynein and kinesin, which move preferentially in one direction along microtubule tracks during transport of different cargos like vesicles, organelles and protein complexes (reviewed in Hirokawa *et al.* 2009).

The role of microtubules in enterovirus infection has been studied using a microtubule destabilizing drug nocodazole. These studies have suggested that EV1 and CVA9 are not dependent on microtubules (Pietiainen *et al.* 2004, Heikkila *et al.* 2010, Huttunen *et al.* 2014), whereas CVB3 entry was shown to be inhibited with nocodazole in placental trophoblast cells (Delorme-Axford *et al.* 2013). In addition, the translocation of the poliovirus replication complexes from ER to perinuclear area has been shown to be dependent on microtubules, although the functionality of the replication complexes was not dependent on this translocation (Egger and Bienz 2005). Moreover, the 3C protease of poliovirus has been shown to cleave microtubule associated protein 4 (Joachims and Etchison 1992, Joachims *et al.* 1995).

2.3.3 Intermediate filaments

The third group of filaments, which comprise the cellular cytoskeleton, are intermediate filaments. There are 70 different genes that encode for intermediate filament proteins, which can be subcategorised into six types (I-VI). Most of the intermediate filament proteins locate in the cytoplasm such as keratin (type I and II), desmin (type III), vimentin (type III), synemin (type IV) and nestin (VI). The only exception to cytoplasmic intermediate filaments is lamins (type V), which

are nuclear proteins. The central building block of intermediate filament is a helical coiled-coil dimer, which is formed of two helical intertwined proteins (reviewed in Parry *et al.* 2007). The dimers assemble into tetramers, which further associate end to end to form protofilaments and finally filaments. Compared to actin and microtubules, intermediate filaments are highly flexible and stretchable (Kreplak *et al.* 2005, Block *et al.* 2015). The most important function of intermediate filaments is to give support to the cell, but they are also involved in signal transduction pathways, cytoplasmic organization of cell organelles and cell migration (Goldman *et al.* 2008, Leduc and Etienne-Manneville 2015, Etienne-Manneville 2018).

Vimentin is the major intermediate filament found in most of the cell types, and it forms a dynamic network system, similar to microtubules and actin (Yoon, M. *et al.* 1998). Vimentin has many tasks in cells such as providing mechanical support of the cytoplasm and localization of mitochondria as well as cell migration and adhesion of mesenchymal cells (Ivaska *et al.* 2007, Nekrasova *et al.* 2011, Buehler 2013, Guo *et al.* 2013). Vimentin has also been related to cancer as it has been shown that vimentin expression levels increase in invasive cells during cancer development and progression (Hendrix *et al.* 1997, Mendez *et al.* 2010, Zelenko *et al.* 2017, Richardson *et al.* 2018). Vimentin is regulated by several post-translational modifications such as phosphorylation, ubiquitylation, sumoylation and glycosylation (reviewed in Snider and Omary 2014). Vimentin is phosphorylated at multiple sites (Hyder *et al.* 2008) and in general, the phosphorylation events induce reorganization of the vimentin filaments in different biological processes, like cell migration (reviewed in Snider and Omary 2014).

Like many other intermediate filaments, also vimentin has a role in the infection of several enveloped and non-enveloped DNA and RNA viruses such as vaccinia virus (Ferreira *et al.* 1994), adenovirus (Belin and Boulanger 1987), herpes virus (Miller and Hertel 2009) and dengue virus (Kanlaya *et al.* 2010). In addition, vimentin rearrangements have been shown during the infection of a close relative of enteroviruses, FMDV, and a bovine enterovirus (Armer *et al.* 2008). Vimentin was also shown to rearrange during EV71 infection (Haolong *et al.* 2013), and interestingly, has also been suggested to serve as an attachment receptor for EV71 (Du *et al.* 2014). Moreover, the 2A protease of CVB4 has been shown to cleave another intermediate filament, namely cytokeratin 8, later within infection, during the onset of cytopathic effect (Seipelt *et al.* 2000).

3 AIMS OF THE STUDY

I To characterize the dense EV1 particle, isolated from infected cells using caesium chloride gradient, and study its role as an uncoating intermediate.

II To study the role of host cell calpain proteases in the polyprotein processing of enterovirus B species in-vitro.

III To study the role of host cell intermediate filament, vimentin, in the infection of enterovirus B species, especially during viral translation and replication.

4 SUMMARY OF THE METHODS

The methods used in this thesis are summarized in Table 4. Detailed description of the methods can be found in the original papers, which are indicated by Roman numerals.

TABLE 4 The methods used in the publications (indicated by Roman numerals) related to this thesis.

Method	Publication
Cell culture	I, II, III
Virus production and purification	I
Virus infection	I, II, III
Drug treatment	II, III
Immunofluorescence and confocal microscopy	I, II, III
Quantification of microscopic data	I, III
Western blotting	II, III
Thermal stability assay	I
Infectivity assay	I, III
Isotopic labeling	I, III
Electron microscopy	I
RT-qPCR	III
Gradient centrifugation	I
Baculo virus-insect cell protein expression	II
Mass spectrometry	II
Statistical testing	II, III

5 RESULTS AND DISCUSSION

5.1 Identification of a new EV1 particle form during infection

Originally, the novel uncoating intermediate particle of EV1 was discovered in this study when a new purification protocol for viral particles was used. In order to produce highly purified virus preparations for spectroscopic and biochemical assays, in addition to typical rate-zonal sucrose gradient centrifugation, we isolated viruses from infected cells using equilibrium density gradient centrifugation in caesium chloride (CsCl). Surprisingly, apart from the empty particle population with very low density, the CsCl gradient revealed two additional particle populations with distinct densities (I). The light particles banded at the density of 1.29 g cm^{-3}, while the dense particles had a density between 1.35 and 1.38 g cm^{-3} (I, Fig. 1A). Three differently sedimenting particle types have typically been separated during infection using sucrose gradient: intact particle, altered uncoating intermediate particle and RNA lacking empty particle with sedimentation rates of approximately 160S, 135S and 80S, respectively (Lonberg-Holm *et al.* 1975, Fricks and Hogle 1990, Gromeier and Wetz 1990, Ofori-Anyinam *et al.* 1993, Curry *et al.* 1996, Tuthill *et al.* 2006). In addition, enteroviruses have been separated in CsCl gradients and two distinct particle populations (light and dense) have been revealed with poliovirus, CVB5 and bovine enterovirus (Rowlands *et al.* 1975, Yamaguchi-Koll *et al.* 1975, Urakawa *et al.* 1987). However, the link between uncoating intermediate particles and dense particles from CsCl gradients has not been discussed earlier.

We showed that two particle populations with different densities appeared in CsCl gradient, regardless whether the viruses were first purified using sucrose gradient centrifugation or directly subjected to CsCl gradient (I, Fig. 1A). We also showed that an additional CsCl gradient centrifugation did not progressively increase the number of dense particles, indicating that the centrifugation itself did not cause the production of these particles (I, Fig. 1Aii). Furthermore, we showed that the formation of dense particles was not due to temperature increase, since the light particles did not transform into dense particles either at

RT or + 37 °C in a storage buffer 2 mM $MgCl_2$-PBS determined with CsCl gradient centrifugation (I, Fig. 1 B). In addition, a real-time spectroscopy assay showed that the fluorescence did not significantly increase during incubation of light particles at RT or + 37 °C for 180 min in a storage buffer (2 mM $MgCl_2$-PBS), indicating that the light particles were stable in these conditions (I, Fig. 1 C). In contrast, the incubation of light particles in water at + 37 °C resulted in clear fluorescence increase, indicating that the viral RNA became accessible to the RNA intercalating dye, sybr green II (SG II) (I, Fig. 1 C).

Next, we wanted to reveal the timeframe for dense particle formation during infection. We used radioactively labeled EV1 in order to sensitively detect different forms of EV1 particles during infection. The radioactive virus was purified using CsCl centrifugation and only intact, light particles were used as an input to infect the cells (I, Fig. 2D). The infection was stopped at different times post infection and the different particles from the infected cells were separated using either CsCl (I, Fig. 2A) or sucrose (I, Fig. 2C) gradient centrifugation. The results showed that binding the virus on ice for 1 h did not produce altered particles since only light virion peak in CsCl gradient or native virion peak in sucrose gradient, in fractions 14-18 from the top, were observed (I, Fig. 2A and C). In contrast, dense particle population in CsCl gradient or a widened peak in fractions 12-18 from the top in sucrose gradient, appeared after 30 min virus incubation on cells at 37 °C, and were evident at 120 min and 180 min p.i. as well. Interestingly, the sucrose gradient centrifugation did not produce a separate 135S peak typical for enteroviruses during uncoating, but instead, only a broadened native peak was formed next to 160S intact form, suggesting that this altered particle population was distinct from 135S particles described for enteroviruses. The correlation of the appearance of the dense particle peak in the CsCl gradient and the widened peak in the sucrose gradient suggested that the dense virus population was the same as the virus population inside the wide peak in sucrose gradient. Indeed, when the fractions of the wide peak from sucrose gradient were collected and subjected to CsCl gradient, both light (intact) particles and dense particles were detected, indicating that the widened peak in sucrose gradient contained two particle populations, which could be separated in CsCl gradient (I, Fig. 2E). Next, we wanted to compare the number of dense particles inside and outside cells. We infected cells with light (intact) virus and collected the viruses from cells after 2 h p.i. Particles derived from cells were then separated using CsCl gradient and different particle types (empty, light and dense) were quantified. The results showed that, in cells, over 50% of the light particles had transformed into dense particles (I, Fig. 2B). In contrast, if the light virus was directly subjected into CsCl centrifugation, over 80% of the light particles stayed intact, while the rest were either dense or empty particles. This indicated that, although some dense particles may form spontaneously, the formation of dense particles was clearly enhanced in cells and was not caused by centrifugation itself (I, Fig. 2B).

Altogether, we showed that an altered EV1 particle population was detected during early infection as a widened peak next to the 160S virus form in

the sucrose gradient. These particles could be separated from the intact particles in CsCl gradient centrifugation, producing a separate dense particle population in addition to intact, light virions. These dense particles were distinct from 135S particles and may represent a novel form of EV1 uncoating intermediate particle.

5.1.1 Characterization of the dense particle

Next, we wanted to further characterize the dense EV1 particles. Earlier studies have suggested that the dense particles have similar RNA to protein ratio compared to the light (intact) particles and that the different densities of light and dense particles can be explained by increased permeability of dense particles, which allows the interaction of Cs^+ ions with the RNA (Yamaguchi-Koll *et al.* 1975). First, we observed that the dense particles of EV1 indeed are more porous since a RNA intercalating dye SG II, could penetrate the capsid of dense particles (I, Fig. 3A). In a thermal stability assay, SG II dye was added with the virus at RT after which the temperature was gradually increased and the stability of the virus evaluated according to the melting temperature, as previously described (Walter, T. S. *et al.* 2012). In contrast to the dense particles, which showed permeability already at RT, light (intact) virions were not permeable to the dye in the beginning, and the melting temperature of 53 °C could be determined. This result supported our earlier observation that intact, light particles had structurally changed during infection and allowed small molecules such as SG II and Cs^+ ions to penetrate the capsid of dense particles, leading to increased density in the CsCl gradient (I, Fig. 2A and 3A).

Since we observed that dense particles have a more open structure compared to intact (light) particles, and earlier studies of dense particles showed that they were more sensitive to RNase A (Yamaguchi-Koll *et al.* 1975, Wiegers *et al.* 1977), we also tested the sensitivity of the light and dense particles to RNase A. Interestingly, the results showed that the infectivity of neither light nor dense particles was compromised due to RNase A treatment before infection (I, Fig. 3B). This suggested that the pores on the dense particle capsid were not large enough for the RNase A enzyme to reach the RNA, nor was RNA externalized from these particles.

One of the reported feature of the uncoating intermediate, expanded or 135S particles of enteroviruses is that they seem to lack the inner capsid protein VP4 (Crowell and Philipson 1971, Belnap *et al.* 2000, Bubeck *et al.* 2005, Seitsonen *et al.* 2012). It has been shown that, during uncoating and RNA release, VP4 protein is externalized and it is suggested to form a multimeric pore on the endosomal membrane through which the RNA can be released (Strauss *et al.* 2013, Panjwani *et al.* 2014). We studied the protein composition of the light and dense EV1 particles by labelling the methionins and cysteines of the capsid proteins with radioactive sulphur. SDS-PAGE analysis showed that both the light and dense virus particles contained their VP4 protein (I, Fig. 3C). Although the protein signal in general was lower for dense particles compared to light particles, the share of VP4 protein from all capsid proteins was very similar for both of the particle types, 4.5% and 4.3% for light and dense particles, respectively. This

result also corresponded well with the theoretical calculation of the methionins and cysteines in VP4 compared to all methoinins and cysteines present in capsid proteins, which was 4.3%. Furthermore, the existence of the VP4 protein in the EV1 dense particle also explained why only a minor shift of the peak was detected in the sucrose gradient during infection (I, Fig. 2C and E). Thus, in contrast to uncoating intermediate particles typically described for other enteroviruses, we suggest that this uncoating intermediate of EV1 is different and still contains VP4 protein and cannot be termed as a 135S particle. Recently it was also shown with an acid labile enterovirus D68, that an intermediate particle is formed during the transition from native virion to an altered (135S) particle in-vitro (Liu *et al.* 2018). Cryo-EM structure revealed that also this particle still contained VP4 protein and was more open compared to native virion, showing an opening at the two-fold axis. Altogether these studies thus suggest that, there are multiple structural uncoating intermediates during enterovirus infection.

5.1.2 The dense particle is infectious and can bind to its receptor

Previous studies on uncoating intermediates of enteroviruses have suggested that the infectivity of the virus in cell cultures decreases substantially upon conversion from intact to the 135S particle (Curry *et al.* 1996, Organtini *et al.* 2014). The lack of VP4 capsid protein may explain this because of its important role in genome release (Danthi *et al.* 2003, Panjwani *et al.* 2014). In addition, it has been shown earlier that the uncoating intermediate particles of some enteroviruses detach from the receptor, suggesting that the conformational change in these particles leads to poorer receptor binding (Lonberg-Holm *et al.* 1975, Goodfellow *et al.* 2005). In the light of these earlier studies, we also wanted to study the infectivity of the dense EV1 particle. We used three different infection methods to determine the infectivity of light and dense particles within short, intermediate and long timescale (I, Fig. 5). First, the number of infected cells was calculated after 6 h p.i. by immunolabeling the capsid protein VP1 (I, Fig. 5A). Next, the infectivity was determined based on the appearance of cytopathic effect (CPE) at 24 h p.i. when the viable cells were stained with crystal violet and the absorbance of the stain was measured (I, Fig. 5C). Finally, the 50% tissue culture infective dose per millilitre (TCID50/ml) was determined using end-point dilution method (I, Fig. 5B). All the infectivity tests described above showed high infectivity for both light and dense EV1 particles, although the infectivity of the dense particles was slightly lower compared to the light particles.

While for some enteroviruses it has been shown that the receptor induces a conformational change into an uncoating intermediate particle (Tsang *et al.* 2001, Coyne and Bergelson 2006, Yamayoshi *et al.* 2013, Liu *et al.* 2015, Wei *et al.* 2016), we and others have already earlier suggested that, for EV1 and CVA9, the trigger for uncoating is not the interaction with their receptors $\alpha_2\beta_1$ and $\alpha_v\beta_3$ integrins, respectively (Xing *et al.* 2004, Shakeel *et al.* 2013). Here, we also confirmed using a thermal stability assay that the binding domain of the $\alpha_2\beta_1$ integrin receptor, I-domain, stabilized the intact EV1 particle rather than induced uncoating (I, Fig. 6A). Furthermore, we were able to show that the dense EV1 particle was also able

to bind the I-domain (I, Fig. 6B and C). This was shown with an infection assay, where the light and dense particles were incubated with varying amounts of I-domain and subsequently bound on cells on ice. After the unbound virus was washed away, the infection proceeded for 24 h, and viable cells were stained with crystal violet (I, Fig. 6B). Like with light particles, the infection caused by dense particles was compromised when the particles were first incubated with the I-domain. This suggested that the receptor binding sites were already occupied with the I-domain when the particles were added to cells, and thus, the viruses were not able to bind to the receptor. Moreover, we showed qualitatively, using transmission electron microscopy, that I-domain was bound on light and dense particles, and that the infection was not inhibited because of virus particle disruption (I, Fig. 6C). Interestingly, two recent studies showed that the infection of several echoviruses, including EV1, was dependent on neonatal Fc receptor (Morosky *et al.* 2019, Zhao *et al.* 2019). Furthermore, while DAF has been shown to act as an attachment receptor for many echoviruses, the Fc receptor was shown to induce uncoating of echovirus 6 in an acidic environment (Zhao *et al.* 2019). In contrast to echovirus 6, EV1 has been shown to internalize into pH neutral multivesicular bodies via attachment to $\alpha_2\beta_1$ integrin receptor (Xing *et al.* 2004, Karjalainen *et al.* 2011). Whether the Fc receptor also functions as an uncoating receptor for EV1 and contributes to the formation of the altered, dense particle characterized here, remains to be studied.

5.1.3 Heat treatment does not mimic the formation of dense particles during infection

Depending on the enterovirus species, the trigger for uncoating has been suggested to be either low pH or receptor binding. For structural studies, the uncoating intermediate particles have typically been formed by treating the intact particles in an acidic environment, or in the case of acid stabile viruses, heating them at elevated temperatures with or without receptor engagement (Garriga *et al.* 2012, Harutyunyan *et al.* 2013, Ren *et al.* 2013, Shingler *et al.* 2013, Butan *et al.* 2014). Furthermore, the heat-converted uncoating intermediate of poliovirus was suggested to mimic the cell-derived uncoating intermediate (Curry *et al.* 1996). In the case of EV1, we showed that the heat treatment (5 min at 50 °C in PBS supplemented with 2 mM $MgCl_2$) did not produce a similar shift of peaks in the sucrose gradient as observed when the native virus was incubated on cells (I, Fig. 4Ai and 2C). Furthermore, separation of the heat-treated particles in CsCl gradient led to the disappearance of the intact, light virion peak at 1.31 g cm^{-3}, while the dense virion peak did not accumulate, indicating that the heat treatment did not convert the intact, light virus particles into dense virus particles (I, Fig. 4Aii). It is also possible that the heat caused a rupture of the virions so quickly that we missed the appearance of a possible dense intermediate in the gradient. Indeed, we showed using transmission electron microscopy that heat-treatment produced morphologically different particles, whereas light and dense particles derived from cells, shared similar morphology of an intact virus (I, Fig. 4B). In contrast to light and dense virus particles, the heat-converted particles

often showed an additional protrusion in the vicinity of the capsid, suggesting that the heat treatment led to virus opening which was distinct from the opening that occurred during infection in cells (I, Fig. 4B). In addition, the existence of these protrusions probably enhanced formation of virus aggregations, supported also by the fact that CsCl gradient separation of heat-treated particles resulted in an appearance of a transparent ''smear'' on the tube walls (I, data not shown). Also earlier studies of heat-treated enteroviruses have shown that the profiles in sucrose gradient differ, suggesting differences in the response to heating between different virus species (Airaksinen *et al.* 2001).

Thus, we suggest that the formation of the uncoating intermediate of EV1, the dense particle, cannot be mimicked by heating the intact EV1 particle at temperatures higher than physiological temperature. However, our recent in vitro studies show that a porous EV1 particle can be formed by treating the intact particle with bovine serum albumin alone or in combination with high potassium and low sodium and calcium concentrations at + 37 °C (Ruokolainen *et al.* 2019). This particle was shown to be permeable to SG II dye, resistant to RNase A treatment and still infectious. Furthermore, cryo-EM structure of the particle revealed that the pocket factor was lost, particle was expanded by 4 % and openings were formed near the two-fold axis (Ruokolainen *et al.* 2019). In contrast to the dense particles derived from cells, these albumin- and ion treated particles had at least partially lost VP4 protein, which also resulted in a clear shift of the intact virus peak in sucrose gradient (Ruokolainen *et al.* 2019). The formation of uncoating intermediate particles during infection may differ from in vitro derived uncoating intermediate particles, since in contrast to the global changes induced by physical factors, the changes of the virus particles during infection may be more local and linked to receptor binding. This was also demonstrated by recent cryo-EM studies with CVB3, where the CAR receptor was immobilized on lipid bilayer nanodisc, resulting in asymmetric changes of the virus particle (Lee, H. *et al.* 2016).

All in all, our results showed that, in addition to the native virus, another infectious EV1 particle is found from cells during infection. This particle still contains all capsid proteins but has a more open structure in comparison to the native virion. This more permeable structure enables its separation from the native virion in CsCl gradient, but does not prevent receptor binding or infection. Thus, this intermediate particle is distinct from 135S particle and may represent a novel uncoating intermediate.

5.2 Host cell calpains can cleave structural proteins from the enterovirus polyprotein

Earlier results from our research group have shown that host cell calpain proteases are important during enterovirus infection (Upla *et al.* 2008). It was shown that inhibitors and small interfering RNAs (siRNAs) against calpains

prevented the infection of enteroviruses. In addition, attempts to inhibit binding or uptake with calpain inhibitor were not successful, indicating that calpain action occurred after entry. This deduction was also supported when calpain inhibitor could prevent the infection even after microinjection of viral RNA into the cells. Furthermore, the effective time window of calpain inhibitor at 3 h p.i. pinpointed the action of calpains at the time when the translation and replication start to accelerate (Upla *et al.* 2008). Calpains also got activated during infection at 3 h p.i., further suggesting the role of calpains after entry, during early translation/replication. However, the mechanistic understanding of calpain action remained unclear, and prompted us to study the role of calpains in more detail.

5.2.1 The infection of enteroviruses can be prevented with calpain inhibitor but not with 2A inhibitor

First, we showed that the infection of three serotypes from the enterovirus B species, EV1, CVB3 and CVB1, could be prevented using calpain inhibitor (II, Fig. 1). The infection was determined after 6 h p.i. in adenocarcinomic human alveolar basal epithelial (A549) cells by immunolabeling the VP1 protein and visualizing the newly synthetized capsid protein using confocal microscopy (II Fig. 1A). In addition, the levels of VP1 from the whole cell population were studied using western blotting (II, Fig. 1B). Both studies clearly showed that the infection of all three viruses was prevented when calpain inhibitor was used. On the other hand, the results also showed that the infection could not be prevented using an inhibitor against 2A viral protease. This inhibitor, called elastatinal, did not supress the infection, but instead, VP1 levels remained the same as in control infection with all three viruses (II, Fig. 1A and B).

Since both calpains and enteroviral proteases have cysteine as their catalytically active amino acid, and since calpain inhibitor has earlier been shown to inhibit the action of 2A (Molla *et al.* 1993), we also wanted to test the cross-reactivity of calpain inhibitor on viral proteases. We carried out an in-vitro reaction, where the actions of 2A and 3C were studied by detecting the levels of their known cellular targets, poly A binding protein (PABP) and Ras-GTPase-activating protein-binding protein 1 (G3BP1), respectively (II, Fig. 2). A549 cell homogenate was incubated with purified enteroviral proteases with or without the calpain inhibitor, and the cleavage action of 2A and 3C was revealed using western blotting. The results showed that both 2A and 3C were inhibited with calpain inhibitor: the levels of PABP were the same as in control without 2A protease, and the 3C induced cleavage product of G3BP1 did not appear in the presence of calpain inhibitor (II, Fig. 2). Additionally, we showed in-vitro that the 2A protease inhibitor, elastatinal, which did not prevent the infection of the three tested enteroviruses (II, Fig. 1), prevented the action of viral protease 2A against cellular targets but not that of 3C (II, Fig. 2). It has been shown that 2A makes the first cleavage by cleaving itself out from the P1 region in-cis already during translation (Toyoda *et al.* 1986, Sommergruber *et al.* 1989, Palmenberg 1990, Laitinen *et al.* 2016). Probably elastatinal was unable to prevent infection because

it was not able to bind to 2A and prevent its action, while 2A was still attached to the polyprotein. In addition, interestingly it was shown with another picornavirus, namely FMDV, that the cleavage between P1 and 2A is not necessary to produce empty capsids and infectious virions (Gullberg *et al.* 2013). In the study, the cells were transfected with an expression cassette containing 3C protease and P1-2A, which was mutated to prevent the cleavage action between P1 and 2A. In addition, to study the effect on the virus infectivity, the mutation was introduced into the full-length FMDV infectious cDNA clone.

The results thus showed that the infection of three tested enterovirus B serotypes, namely EV1, CVB3 and CVB1, could be prevented using calpain inhibitor. Furthermore, this inhibitor was shown to inhibit viral proteases 2A and 3C in-vitro, thus indicating that the use of the inhibitor in cell experiments might be problematic. However, the cross-reactivity of calpain inhibitor with viral proteases also brought out the potential of the inhibitor as an efficient antiviral.

5.2.2 Calpains can release VP1 and VP3 proteins by cleaving the P1 region of enteroviral polyprotein in-vitro

The exact role of calpains in enterovirus infection remained unsolved in our earlier studies (Upla *et al.* 2008). However, the time of action for calpains inferred to infection steps taking place after RNA release, when the translation and replication start to accelerate. This was also proven by the experiment where the infection was halted after microinjection of the viral RNA into the cytoplasm during calpain inhibitor treatment. This showed that calpain inhibitors had targets in the cytoplasm in the early replication/translation phase. According to the dogma, after translation, before replication takes place, the enteroviral polyprotein is processed by viral proteases 2A, 3C and precursor 3CD in order to release proteins needed for capsid assembly and replication. The first cleavage between P1 and P2 is done by 2A protease in cis already co-translationally (Toyoda *et al.* 1986, Sommergruber *et al.* 1989, Palmenberg 1990, Laitinen *et al.* 2016), while the other cleavages are then thought to be carried out by proteases 3C and 3CD (Ypma-Wong *et al.* 1988, Palmenberg 1990). Considering the time window of calpain action in enterovirus infection, and the nature of calpains as processing rather than degradative cysteine proteases, we hypothesized that calpains could take part in the polyprotein processing of enteroviruses. However, since our preliminary data showed that calpain inhibitor cross-reacted with viral proteases, we had to study the action of calpains and viral proteases separately. In order to do so, we produced the P1 region of CVB1 polyprotein in sf9 cells using baculovirus system (II, Fig. 3A). In addition, since our preliminary studies showed that the 2A inhibitor elastatinal could not inhibit the infection in cells, we also wanted to study the possible role of calpains in P1 cleavage out from the whole polyprotein. Hence, to study the cleavage site between P1 and 2A, a construct with P1 followed by a mutated 2A without protease activity (P1-2A*), was produced (II, Fig. 3A). The P1 or P1-2A* lysate derived from insect cells was incubated with purified calpain proteases 1 and 2 or viral proteases 2A and 3C in an in-vitro reaction, and the results were evaluated using western blotting. The

results showed that the addition of calpains decreased the amount of P1 (II, Fig. 3 B and C) and, more importantly, that the amounts of VP1 and VP3 proteins increased (II, Fig. 3 B, D and E). Although both calpains 1 and 2 could release VP1 and VP3 proteins from the P1 polyprotein, the results were statistically significant only for calpain 2, suggesting that calpain 2 was more potent at cleaving the P1, at least in vitro. Additionally, our positive control, 3C protease, could release VP1 and VP3 proteins, and the results were statistically significant (II, Fig. 3 B, D and E). On the other hand, our results showed that neither of the calpains could cleave between P1 and 2A in the P1-2A* construct, since bands corresponding to P1 or VP1 did not appear (II, Fig. 3B). However, calpains were able to release VP3 protein from the P1-2A* construct, further indicating that the cleavage sites between VP0-VP3 and VP3-VP1 could be processed by calpains (II, Fig. 3B and E). Additionally, we showed that 2A protease could not process the cleavage site between P1 and 2A, when it was introduced in trans (II, Fig. 3 B, D and E). Altogether, our results showed that calpains could cleave the P1 region of enterovirus polyprotein in-vitro, and release VP1 and VP3 capsid proteins, like 3C. These results raise up a question, whether the role of calpains in enterovirus polyprotein processing has gone unnoticed earlier, because it has been difficult to separate the action of viral and calpain proteases in cell assays. As we and others have shown, calpain inhibitors also cross-react with viral protases (Molla *et al.* 1993), which creates a challenge in infection assays, carried out in cells. However, to verify the role of calpains in polyprotein processing during enterovirus infection, additional studies are needed.

To further demonstrate the cleavage action of calpains 1 and 2, we carried out a titration assay for the proteases (II, Fig. 4A). By incubating the P1 construct with increasing concentrations of calpains, we showed that the appearance of VP1 protein was dependent on calpain concentration, since VP1 only appeared when higher calpain concentrations were used. However, lower amounts of calpains were able to produce a cleavage product corresponding to an intermediate containing both VP1 and VP3. This intermediate was also evident in control reaction, where calpains were not added. However, the appearance of the VP1+VP3 intermediate in control reaction was calcium dependent, since the intermediate only appeared if excess calcium was added into the in-vitro reaction, suggesting a presence of calcium dependent protease in the insect cell derived lysate. Furthermore, since calpains have been shown to be calcium dependent proteases, we also studied the role of calcium in calpain activation during P1 processing. We showed that the cleavage action of calpain 2 was calcium dependent, since calpain 2 was not able to release VP1 out from P1 if excess calcium was not added or if it was chelated with egtazic acid (EGTA) (II, Fig. 4A). In contrast, calpain 1 was able to release VP1 out of the P1 even without excess calcium, suggesting that the amount of calcium in the P1 lysate was enough to activate calpain 1. Interestingly, the addition of EGTA in the presence of calpain 1 induced the disappearance of the whole P1 band, because of an unknown reason. The difference between calcium sensitivity of calpain 1 and 2 was not surprising, since it is known from in-vitro studies that the calcium requirement for calpain 1 and 2 differs. Based on in vitro assays, calpain 1 is

supposed to need micromolar, whereas calpain 2 needs millimolar concentrations of calcium to get activated (Goll *et al.* 2003). The calcium requirement in vivo, however, is still under investigation to understand how calpains get activated in cells, where such high concentrations of calcium do not exist (Goll *et al.* 2003). Nevertheless, the trigger for increased calcium levels during enterovirus infection could be the viruses themselves, since enteroviruses have been shown to increase the amount of cytosolic calcium during infection by releasing calcium from ER and inducing plasma membrane permeability (Aldabe *et al.* 1997, van Kuppeveld *et al.* 1997). In addition, Bozym et al. showed that calcium levels increased during CVB3 infection at 2-3 h p.i. (Bozym *et al.* 2011) and our earlier studies showed calpain activation at 3-4 h p.i. (Upla *et al.* 2008).

Finally, we used calpain inhibitor in an in-vitro reaction to further show that the appearance of VP1 and VP3 proteins was due to calpain action. P1 construct was incubated with calpain 1 and 2 in the presence or absence of calpain inhibitor (II, Fig. 4B and C). Again, both calpains produced cleavage products corresponding to VP1 and VP3, if the inhibitor was not added. In contrast, the presence of calpain inhibitor prevented the formation of these cleavage products, further confirming that the processing was due to calpain action. All in all, our results thus showed that the P1 region of enterovirus B species can be processed by calpains in vitro, resulting in the release of capsid proteins VP3 and VP1.

5.2.3 Calpains cleave near the VP3-VP1 cleavage site

Our results showed that calpains were able to cleave P1 and produce VP1 and VP3 as cleavage products similarly as viral protease 3C. Because the cleavage sites between VP0-VP3 and VP3-VP1 used by calpains may differ from those used by 3C protease, we wanted to study these cleavage sites in more detail. Unfortunately, due to low water solubility, we could not produce a suitable peptide for the cleavage site of VP0-VP3, but we used a 30 amino acid synthetic peptide covering the cleavage site between VP3-VP1 (NH2-MLKDTPFIRQDNFYQGPVEESVERAMVRVA-COOH). This peptide, which also included the putative cleavage site of 3C, was used in an in-vitro assay where purified calpain proteases or viral protease 3C was incubated with the peptide. To reveal the exact cleavage sites for the proteases, the results were analysed using SWATH-MS mass spectrometry analysis (II Fig. 6A). The analysis revealed that the highest intensities of cleavage products produced by both calpains corresponded to sequences, which resulted from cleavage at (NH2-) MLKDTPFIRQDNF/YQGPVEESVERAMVRVA (-COOH). In turn, the cleavage site used by 3C protease was the one reported in the literature (NH2-) MLKDTPFIRQDNFYQ/GPVEESVERAMVRVA (-COOH), which was only two amino acids apart from that used by calpains. Although, the in-vitro cleavage assays showed that calpain 2 released more VP1 and VP3 out from the P1 (II, Fig. 3), here the mass spectrometry analysis clearly showed that also calpain 1 was able to cleave P1 from the exact same location as calpain 2. As discussed above, the calcium requirement of calpain 1 and 2 differs in-vitro and does not resemble in-vivo conditions, and hence, it may be difficult to draw clear conclusions of

calpain preference from in-vitro assays. Whether calpains can cleave from other 3C or 3CD specific cleavage sites at the P2 and P3 regions remain to be studied.

Moreover, we used this synthetic peptide in a competition assay to reveal whether its excess can inhibit calpains from the processing of P1. When purified calpains were incubated with P1 construct in the presence of excess peptide, the amount of cleavage product corresponding to VP1 was clearly less, compared to the control without the peptide (II, Fig. 6B). This indicated that the peptide included a sequence motif, which was processed by calpains, and that its excess hindered calpains from cleaving the P1 construct. Altogether, these results thus showed that calpains can specifically cleave at the cleavage site between VP3 and VP1, and that the cleavage site was only two amino acids apart from that used by 3C. However, it will be important to study in the future, whether the capsid proteins produced by calpains can be used in the production of pentamers and subsequently in the assembly of infectious virions.

5.2.4 Discussion of the role of calpain proteases during enterovirus infection

As a proof of principle, we showed here that host cell calpain proteases can process enterovirus P1 polyprotein and release VP1 and VP3 proteins in-vitro. Does this happen in cells as well? Our earlier studies already clearly showed the importance of calpains during enterovirus infection (Upla *et al.* 2008). Although, calpain inhibitors might be problematic in cell assays, the inhibition of calpains with specific siRNAs clearly decreased the infection of EV1 (Upla *et al.* 2008). In addition, the fact that calpains got activated at the time when translation and replication start to accelerate suggested a role for calpains at this stage of infection (Upla *et al.* 2008).

Also a few other studies have connected calpains to enterovirus infection. It has been shown that calpains could work in trafficking of CVB3 containing vesicles inside cells during infection, or later in infection in CVB induced necrosis or autophagy (Yoon, S. Y. *et al.* 2008, Bozym *et al.* 2010, Bozym *et al.* 2011, Li *et al.* 2014). These above-mentioned studies were carried out using calpain inhibitors, which might complicate the interpretation of the results because of cross-reactivity with viral proteases. In addition, we have earlier shown using autophagosomal marker LC3 that EV1 does not need or induce autophagy during its infection (Rintanen *et al.* 2012). This suggests that there are differences between enterovirus serotypes and that, at least for EV1, the role of calpains is not related to autophagy. On the other hand, as calpains are very abundant proteases in cells, whose activity is controlled by altering calcium concentrations, the participation of calpains in multiple steps of enterovirus infection might be possible.

In addition to enteroviruses, calpains have been suggested to have a role in the infection of other viruses as well, such as influenza, herpesvirus, chikungunya and some other picornaviruses (Debiasi *et al.* 1999, DeBiasi *et al.* 2001, Zheng *et al.* 2014, Karpe *et al.* 2016, Howe *et al.* 2016, Blanc *et al.* 2016). Interestingly, calpain 2 has also been associated in the cleavage of hepatitis C virus non-structural protein (Kalamvoki and Mavromara 2004). Furthermore, the

polyprotein processing of other positive-sense RNA viruses has been shown to involve cellular proteases in addition to viral proteases. For example, the studies of hepatitis C and dengue virus have shown that the cellular signal peptidases or furins cleave the viral polyprotein in the ER to release mature structural proteins (McLauchlan *et al.* 2002, Perera and Kuhn 2008). However, to our knowledge, the role of calpains, or other cytoplasmic proteases, has not been suggested in the viral polyprotein processing earlier.

It is not far-fetched to speculate that enteroviruses, and also other viruses, may have adapted to use readily available host cell proteases to favour their infection. In the study by Lawson and Semler it was shown that during enterovirus infection, 3C and 3CD were more active in membranous fraction, while P1 and its processing still occurred in the soluble fraction (Lawson and Semler 1992). In addition, their in-vitro assay showed that P1 was processed already before 3CD protease was detected (Lawson and Semler 1992). It may be that viral proteases mostly process P1, which is found from the replication membranes, while calpains could promote the processing of P1 in the cytosol. On the other hand, it may also be that over time the role of viral proteases in cleavage of host factors became more important to promote apoptosis and suppress immunological responses (Laitinen *et al.* 2016), while calpains have become a back-up system for viral polyprotein cleavage. In addition to lytic infections, enteroviruses are also known to cause persistent infections, where the viruses can stay silent in tissues without causing cell death (Alidjinou *et al.* 2014, Flynn *et al.* 2017, Bouin *et al.* 2019). In order not to cause apoptosis, the viral proteases are most likely downregulated, but calpains could still promote polyprotein processing and subsequently allow low levels of capsid protein production and replication. However, whether calpain proteases truly function in infected cells and take part in polyprotein processing, remains to be shown.

Altogether, our results showed that host cell calpain proteases can process the P1 region of enterovirus polyprotein, and as a result, release capsid proteins. Moreover, we showed a high cross-reactivity of calpain inhibitors with viral proteases in this study, which highlights their potential also as future antivirals.

5.3 Vimentin dynamics are needed for efficient production of enteroviral non-structural proteins

In addition to other cellular filaments, also the dynamics of intermediate filament vimentin, have been associated with several viral infections (Chen *et al.* 1986, Risco *et al.* 2002, Stefanovic *et al.* 2005, Bhattacharya *et al.* 2007, Gladue *et al.* 2013, Fay and Pante 2013, Meckes *et al.* 2013, Teo and Chu 2014). Additionally, our earlier studies showed that the cell susceptibility to EV1 infection correlated with vimentin organization (Turkki *et al.* 2013). In some of these earlier studies, vimentin has been reported to form cage like structures around replicating genome or viral proteins. However, the trigger or mechanism of action for

vimentin rearrangements has not been revealed yet. Thus, here we have studied the role of vimentin dynamics during the infection of enterovirus B species in more detail.

5.3.1 Vimentin rearranges around dsRNA during replication, triggered by viral protein synthesis

First, the vimentin rearrangements were studied by immunolabeling enterovirus capsid protein VP1 and vimentin, and the results were visualized using confocal microscopy. The analysis revealed that, at later stages of infection (4-6 h p.i.), vimentin formed a ball-like structure in the perinuclear area of CVB3 (III, Fig. 1A), EV1, CVB1 and CVA9 (III, Fig. 1C) infected cells. In addition, it was observed that VP1 did not co-localize with vimentin, but instead, was abundant in other parts of the cytoplasm. Further studies then showed that vimentin was associated with the replicating RNA, since immunolabeling of the replication intermediate, dsRNA, together with vimentin showed dsRNA inside the vimentin cage (III, Fig. 1D). A time-course study showed that the vimentin cages started to appear and contained dsRNA at around 3 h p.i. but were more evident and compact between 4-6 h p.i. (III, Fig. 1E and 2A). The results also showed that the redistribution of vimentin was not due to rounding of the cells, since cells were still attached to the coverslips and cell outlines did not match with those of the vimentin cages (III, Fig. 1A, C and E). In addition, immunolabeling of tubulin together with vimentin showed that not all cellular filaments were rearranged, since tubulin showed normal filamentous morphology all over the cytoplasm during CVB3 infection (III, Fig. 1B). When the intensity of capsid and dsRNA label per cell was quantified, the amount of capsid and dsRNA per cell gradually increased from 3 to 6 h p.i. (III, Fig. 2B). However, quantification of cells positive for CVB3 capsids or dsRNA showed that at 3 h p.i. there were more cells positive for dsRNA than capsid production, 60% and 20%, respectively. Then the number of capsid and dsRNA containing cells increased clearly at 4 h p.i. and did not change that much anymore until the last detected time-point, 6 h p.i. (III, Fig. 2B). The schedule for vimentin rearrangements in infected cells followed the schedule of capsid production, since as the number of cells positive for capsid production increased, so did the number of cells that showed vimentin rearrangements (III, Fig. 2B). Although the number of replication positive cells was evident already at 3 h p.i. the number of cells having dsRNA inside compact vimentin structures was not yet evident at 3 h p.i. indicating that replication preceded the formation of vimentin rearrangements (III, Fig. 2B). Our results thus suggested that replication was not dependent on vimentin rearrangements and the appearance of vimentin cages was more related to viral protein production.

Next, we sought to determine the trigger for vimentin rearrangements in more detail. In order to test whether the presence of viral particles and their internalization was sufficient to trigger vimentin rearrangements or if translation and replication were needed, we used infection incompetent neutral-red (NR) and UV-inactivated viruses in our studies. The uncoating and subsequent replication of NR-CVB3 was prevented by crosslinking the genome inside the

capsid with light, as described earlier (Brandenburg *et al.* 2007, Siljamaki *et al.* 2013, Huttunen *et al.* 2014, Soonsawad *et al.* 2014). The light inactivation was carried out at different times p.i. and vimentin rearrangements were visualized using confocal microscopy (III, Fig. 3A). The quantification of the results showed that vimentin rearrangements did not form if the NR-CVB3 was inactivated with light at 20 min and 1 h p.i. but at 3 h p.i. when replication had already started, the vimentin cages started to appear (III, Fig. 3A). In addition, the infection with UV-inactivated EV1 did not induce vimentin rearrangements, in contrast to control infection, where EV1 induced the formation of vimentin cages at 5 h p.i. This was confirmed by immunolabeling and microscopy (III, Fig. 3B).

As our results indicated that the presence of the virus particle or its internalization did not trigger vimentin rearrangements, we next wanted to study the role of replication and translation as a trigger. First, to study the effect of replication on vimentin cage formation, we used guanidine hydrochloride (GuHCl). GuHCl has been shown to inhibit the action of 2C protein and subsequently to prevent the initiation of negative strand RNA synthesis (Barton and Flanegan 1997, Pfister and Wimmer 1999, Banerjee *et al.* 2004). Our results showed that addition of 2 mM GuHCl during early infection inhibited CVB3 infection completely, which was detected by immunolabeling of VP1 protein (data not shown). Furthermore, vimentin cages did not form during GuHCl treatment. Thus, by inhibiting replication, GuHCl also affected translation, although it has not been shown to impair translation per se. To further study whether dsRNA has a direct role in vimentin rearrangements, we transfected the cells with low and high concentrations of a dsRNA analog, poly-IC. The results showed that Poly-IC did not induce vimentin rearrangements (III, data not shown), suggesting that dsRNA did not itself trigger vimentin cage formation. Next, we inhibited the protein synthesis using cycloheximide and puromycin (Barton *et al.* 1999). We confirmed the functionality of the synthesis inhibitors by detecting the virus induced CPE (III, Fig. 3C), levels of VP1 (III, Fig. 3E) and replication using qPCR (III, Fig. 3F). Our results also showed that vimentin rearrangements did not occur in the presence of these translation inhibitors (III, Fig. 3D). Furthermore, we disturbed the protein synthesis by using VER155008 and geldanamycin inhibitors against cellular chaperones, HSP70 and HSP90, respectively. These inhibitors, especially VER155008, increased the cell viability compared to control infection and inhibited the formation of vimentin cages (III, Fig. 3G and H). In addition, the levels of dsRNA and VP1 decreased in the presence of these inhibitors (III, Fig. 3I and J). Altogether, our results thus showed that the formation of vimentin cages during enterovirus infection was dependent on viral protein synthesis rather than virus internalization or the presence of viral particles or dsRNA.

5.3.2 Inhibition of vimentin rearrangements allows efficient infection but postpones cell death

In order to study vimentin dynamics during enterovirus infection in more detail, we used a drug called β,β'-Iminodipropionitrile (IDPN), which has earlier been

shown to cause disruption of vimentin (Galigniana *et al.* 1998). First, we confirmed that IDPN did not affect drastically to A549 cell viability (III, Fig. 4A), or vimentin morphology by itself (III, Fig. 4B). Next, we showed that IDPN rescued the cells from CVB3 infection, since the cell viability of infected, IDPN treated cells was clearly higher compared to infected cells without the drug (III, Fig. 4C). Surprisingly, the production of progeny viruses was, however, not affected by inhibition of vimentin rearrangements, since the number of infectious virions, determined with end-point assay, was the same with or without IDPN treatment (III, Fig. 4D). In addition, qPCR analysis showed that the amount of positive sense RNA gradually increased during CVB3 infection both with and without IDPN treatment. Only a slight decrease in replication was observed during IDPN treatment (III, Fig. 4E). This was evident also when dsRNA was immunolabeled and visualized with confocal microscopy, but more importantly, the visualization revealed different localization of dsRNA in IDPN treated versus non-treated cells during infection (III, Fig. 4F). In IDPN treated cells, where vimentin dynamics was prevented, the dsRNA was not concentrated in the perinuclear region, but instead, was more spread around the whole cytoplasm.

5.3.3 Vimentin cage contains replicating RNA, cellular membranes and viral non-structural proteins but not viral structural proteins

The findings that the replicating viral RNA located in vimentin cages, and that the localization changed when vimentin dynamics was inhibited with IDPN, prompted us to study also other components that might be associated with vimentin cages. First, we inspected the viral 3D polymerase, and showed that it associated with the vimentin cage during normal infection. Like dsRNA, also 3D polymerase was more spread out in the whole cytoplasm during IDPN treatment (III, Fig. 5A). In addition, these confocal microscopy studies showed that the expression of 3D polymerase was lower with IDPN treatment compared to normal infection. Similarly, another non-structural protein, viral protease 2A, was associated with vimentin during normal infection, but was more evenly distributed in the cytoplasm upon IDPN treatment (III, Fig. 5B) altogether suggesting that several players associated with replication/translation were associated with the vimentin cage. In addition, vimentin has previously been shown to co-immunoprecipitate another non-structural protein of picornaviruses, namely 2C of the FMDV virus (Gladue *et al.* 2013) further adding to the list of vimentin associated non-structural proteins.

In contrast to non-structural proteins, we showed that the localization of the structural protein VP1 did not associate with vimentin (III, Fig. 5C). In addition, the localization and expression levels of VP1 did not show a major change when the cells were treated with IDPN during infection. However, when we evaluated the localization of cellular components during infection with and without IDPN treatment, we observed that luminal ER marker, protein disulfide-isomerase, and cis-Golgi matrix protein, GM130, were associated with vimentin cages during normal infection but were more spread out when vimentin rearrangements were inhibited with IDPN (III, Fig. 5D and E).

The replication of positive-strand RNA viruses typically takes place on host cell membranes which are rearranged during virus infection. For enteroviruses it has been shown that the replication starts on single membrane tubular structures which are converted into double membrane vesicles later during infection (Limpens *et al.* 2011, Belov *et al.* 2012). As we observed that the replicating RNA as well as viral non-structural proteins and components from ER and Golgi associated with vimentin cage, it is likely that vimentin rearrangements have a role in the formation or support of replication organelles. Moreover, we showed that inhibition of vimentin rearrangements also resulted in more dispersed localization of these above mentioned components. Although we showed the effect of vimentin cage formation during the replication of enterovirus B species, considering the universal nature of replication process among different enterovirus species, it is likely that also other species would show similar results. In addition, earlier studies with EV71 from the enterovirus A species also connected vimentin with formation of replication centers (Haolong *et al.* 2013). Like the vimentin cages, the replication organelles of enteroviruses mostly occupy the perinuclear region of the cell (Limpens *et al.* 2011, Belov *et al.* 2012). In addition, the schedule for the formation of replication organelles coinsides with the formation of vimentin cages, further suggesting that vimentin helps in the organization of the replication area of enteroviruses. Furthermore, it can be speculated that sequestering of the replication area by vimentin cage may also protect the virus from innate immune responses of the cell. It would be interesting to study in the future, whether vimentin cage e.g. hampers the cellular pattern recognition receptors from recoqnizing foreign components, such as dsRNA, during enterovirus infection (Mogensen 2009).

5.3.4 Inhibition of vimentin dynamics affects the levels and activity of viral non-structural proteins

As the confocal microscopy studies suggested a difference in the levels and location of non-structural versus structural proteins upon IDPN treatment, we next wanted to quantify this observation. First, we observed that the levels of VP1 were about 40% lower in IDPN treated cells as compared to normal infection detected by western blotting (III, Fig. 6A). This observation was in line with the earlier observation that replication was slightly decreased during IDPN treatment (III, Fig. 4E). In contrast, when the levels of non-structural proteins 3D, 2A and 3C were compared to VP1, it was evident that they decreased more drastically upon IDPN treatment being 1%, 20% or 10% of the VP1 signal (set to 100%) for 3D, 2A and 3C, respectively (III, Fig. 6A). Since there was a clear decrease in the production of non-structural proteins, it was quite unexpected that the number of infectious virions did not change during IDPN treatment (III, Fig. 4D). However, as we showed that the production of structural proteins and RNA is not much affected during IDPN treatment, it may be that in this short time-scale (6 h p.i.) the lower number of non-structural proteins does not have an effect on viral yields. At later timepoints, however, it is likely that low amount of viral non-structural proteins also affects the number of infectious virions.

In addition to the cleavage of enterovirus polyprotein, the viral proteases 2A and 3C cleave several host cell proteins related to host cell shut-off, apoptosis and immunological responses (Kuo *et al.* 2002, Chau *et al.* 2007, White *et al.* 2007, Rivera and Lloyd 2008, Dougherty *et al.* 2015, Laitinen *et al.* 2016). In order to study the activity of 2A and 3C proteases, we next detected the levels of some of their cellular targets. The levels of host cell PABP and G3BP1 were clearly affected during IDPN treatment compared to normal infection, since they were not cleaved if IDPN was added during infection, supporting also the observation of lower 2A and 3C protease levels (III, Fig. 6B). As the cleavage of these and other cellular factors has been shown to promote apoptosis, we also studied cell viability and measured the levels of caspase activation upon IDPN treatment. Our results showed that cell viability increased (III, Fig. 6C) and caspase activation was clearly decreased (III, Fig. 6D) upon IDPN treatment compared to normal infection. This result of caspase activation was in line with both the lower expression and subsequent cleavage action of viral proteases (III, Fig. 6A and B), explaining also the lack of CPE in IDPN treated infected cells. Interestingly, although the PABP cleavage was affected by low levels of 2A viral protease, another substrate for 2A, eukaryotic translation initiation factor 4 G (eIF4G), was not as drastically affected. This protein, which is related to the host cell shut-off during enterovirus infection, was cleaved even during IDPN treatment when 2A levels were low (III, Fig. 6E), suggesting that a shut off was taking place in IDPN treated infected cells. Indeed, when we studied the host cell shut-off using metabolic labeling, we confirmed the shut-off even upon IDPN treatment in infected cells (III, Fig. 6F). It has been shown earlier that eIF4G is cleaved already at an early stage during poliovirus infection, leading to a decreased synthesis of host proteins (Etchison *et al.* 1982). Evidently, in our studies, the low 2A protease activity left was able to induce host cell shut-off by rapidly cleaving the eIF4G even during IDPN treatment.

Finally, to confirm that the observed changes in cell viability were not related to ER stress response, we studied ER stress markers and reactive oxygen species during infection. Our results showed that the levels of ER stress markers did not change upon infection or IDPN treatment (III, Fig. 6G). In addition, the levels of reactive oxygen species were very similar in control and infected cells with or without IDPN treatment (III, Fig. 6H). Altogether, these results thus suggested that the postponed cell death during IDPN treatment was related to low expression and activity of viral proteases instead of ER stress response. As enteroviral proteases are important contributors in the viral pathogenicity (Laitinen *et al.* 2016), understanding of the regulators of their function is important. The downregulation of viral protease action may prevent the essential events leading to enterovirus induced diseases such as encephalitis, cardiomyopathy and meningitis (Verma *et al.* 2009, Tapparel *et al.* 2013, Gaaloul *et al.* 2014, Laitinen *et al.* 2016, Bouin *et al.* 2019).

5.3.5 Inhibition of vimentin dynamics affects the synthesis of non-structural proteins rather than their degradation

All in all, our results suggested that the inhibition of vimentin dynamics with IDPN affected more specifically the viral non-structural than structural proteins, also leading to prolonged cell survival. These results prompted the question how the structural and non-structural proteins could have a different fate. Enteroviruses are known to translate their polyprotein as a single unit, but could the different parts of the polyprotein be differentially synthesized, processed, or even degraded? It was shown by others earlier that the virus core protein of hepatitis C virus was protected from proteasomal degradation by vimentin (Nitahara-Kasahara *et al.* 2009). Hence, we first set out to study if viral proteins were degraded during IDPN treatment by carrying out an infection time series with or without IDPN (III, Fig. 7A). The western blot results showed that 2A and 3D proteins appeared during normal infection at 5-6 h p.i. but were not visible in IDPN treated infected cells. However, VP1 was observed both with and without IDPN treatment, although to less extent during IDPN treatment. This suggested that rather than being degraded, the non-structural proteins were not produced to same extent in IDPN treated compared to non-treated infected cells already from the beginning. To further confirm that degradation was not the explanation for lower levels of non-structural proteins, we used a specific inhibitor of proteasomal degradation, called bortezomib. The western blot results showed that, the addition of bortezomib during IDPN treatment in infected cells did not restore the non-structural proteins or VP1, further confirming that the lower protein levels upon IDPN treatment were not due to proteasomal degradation (III, Fig. 7B, lanes 2, 5 and 6). In addition to proteasomal degradation, we wanted to test whether cytoplasmic calpain proteases would have a role in the observed protein levels. As suggested by us (II), calpains may take part in the enterovirus polyprotein processing and might hence contribute to the phenomena observed here as well. Indeed, the addition of calpain inhibitor on top of IDPN during infection totally prevented viral protein production (III, Fig. 7B, lane 4). This and our earlier observations (II) thus suggest that the production of VP1 and RNA was possibly enhanced by calpains, even if non-structural proteins were quite heavily downregulated during IDPN treatment. The protein production was totally abolished when also calpains were inhibited, supporting the hypothesis that calpains may have a role in the polyprotein processing.

Next, we studied the effect of cellular heat shock proteins HSP70 and HSP90 using western blotting (III, Fig. 7B). HSP70 protein has earlier been suggested to have a universal role in the life cycle of different viruses (Mayer 2005), and has been associated with for example rabies and dengue virus infections (Lahaye *et al.* 2012, Taguwa *et al.* 2015). HSP90, on the other hand, has been shown to protect the viral components of EV71 and poliovirus from proteasomal degradation (Geller *et al.* 2007, Tsou *et al.* 2013). Our results showed that the inhibition of HSP70 with VER155008 totally abolished virus protein synthesis and infection (III, Fig. 7B lane 10). More importantly, we showed that HSP90 inhibitor, geldanamycin, prevented P1 processing into VP1, whereas the processing of non-

structural proteins was not much affected (III, Fig. 7B lanes 11 and 12). This observation was totally the opposite compared to IDPN treatment, which mostly affected the non-structural rather than structural proteins. It has been shown in earlier studies that HSP90 binds to P1 and affects its processing (Geller *et al.* 2007, Newman *et al.* 2018). Thus, in the light of earlier and our results here, it could be speculated that viral structural and non-structural proteins are processed differently during infection. In fact, Lawson and Semler (Lawson and Semler 1992) showed in their metabolic labeling assay that most of the P1 and structural proteins accumulate in cytosolic fraction, while P2-P3 and non-structural proteins were found from the membrane bound fraction, supposedly associated with replication membranes. In addition, they showed that the processing of P1 compared to P2 and P3, was different, since active processing of P2 and P3 occurred during early infection in membranous fraction, but did not much occur in the soluble fraction, while P1 was processed in the soluble fraction for longer periods. So, perhaps the non-structural proteins are more affected by vimentin dynamics, while P1 processing is more affected by HSP90. In addition, as our results showed, also calpain proteases might contribute to the processing of P1 (II).

Thus, we showed that the inhibition of vimentin dynamics resulted in lower production of the non-structural proteins, in contrast to structural proteins. In addition, we showed that this difference was not due to selective degradation of non-structural proteins, which raises the question how structural and non-structural proteins can be differently produced? It has been shown earlier that the release of P1 from the rest of the polyprotein occurs quickly during translation. This cleavage is carried out by 2A protease, which cleaves between itself and P1 during translation, as soon as the required components have been translated (Toyoda *et al.* 1986, Palmenberg 1990). So, it may be that after the release of P1, the synthesis of P2-P3 region is dependent on a compact replication area and vimentin cage. In contrast, the production of P1 is less affected by vimentin cage formation. However, future studies are needed to reveal the mechanistic basis of these phenomena in more detail. One possibility could be the different non-canonical translation mechanisms, which are commonly used by RNA viruses (Firth and Brierley 2012). These mechanisms such as ribosomal frameshifting have also been reported for some picornaviruses (Donnelly *et al.* 2001, Loughran *et al.* 2011). In general, non-canonical translation can result in different ratios of viral proteins, often allowing greater production of structural proteins (Dinman 2012, Napthine *et al.* 2017). Whether such mechanisms are contributing to the observed different ratios of non-structural and structural protein synthesis and processing observed here, remains to be shown.

Altogether, these results thus showed that enteroviral protein synthesis induced the formation of vimentin cages, which contained replicating RNA and non-structural viral proteins. The inhibition of vimentin dynamics and cage formation with IDPN resulted in lower production of non-structural proteins in contrast to structural proteins, which was not due to degradation of the non-structural proteins. Finally, we suggest that the loss of vimentin cage results in poorly organized replication area leading to a more diffuse pattern of dsRNA

and non-structural proteins. This results in less efficient synthesis of non-structural proteins, leading also to higher cell viability. In contrast, the structural proteins in the soluble pool are produced almost normally and are much less affected by perturbed vimentin structure (III, Fig. 8).

6 CONCLUDING REMARKS

The main conclusions of this thesis are:

I We demonstrated that, in addition to native virus, another infectious EV1 particle form, possibly an uncoating intermediate, is found during infection. This particle has a higher density in CsCl gradient because of a more open structure compared to the native virus. Further characterization of this dense particle showed that it still contains VP4 protein and is capable of binding to the receptor $\alpha_2\beta_1$ integrin and cause infection. Finally, the formation of this dense particle cannot be mimicked by heating the native particle in elevated temperatures.

II Proteolytic processing of structural proteins from the enteroviral polyprotein can be carried out by cellular calpain proteases in-vitro. Furthermore, prevention of calpain action by calpain inhibitors also prevents the action of viral proteases, which highlights their potential as future antivirals.

III Enterovirus infection induces drastic vimentin rearrangements during replication, which is triggered by viral protein synthesis. The formed vimentin cages contain replication membranes, originating from the ER and Golgi, as well as viral RNA and viral non-structural proteins, but less of the structural proteins. Moreover, the inhibition of vimentin rearrangements does not drastically affect structural proteins, but results in less efficient production of non-structural proteins, leading also to prolonged host cell survival.

Thus, this thesis shed light on both viral and cellular factors, which contribute to the infection of enteroviruses after entry, during uncoating and translation/replication (Fig. 5).

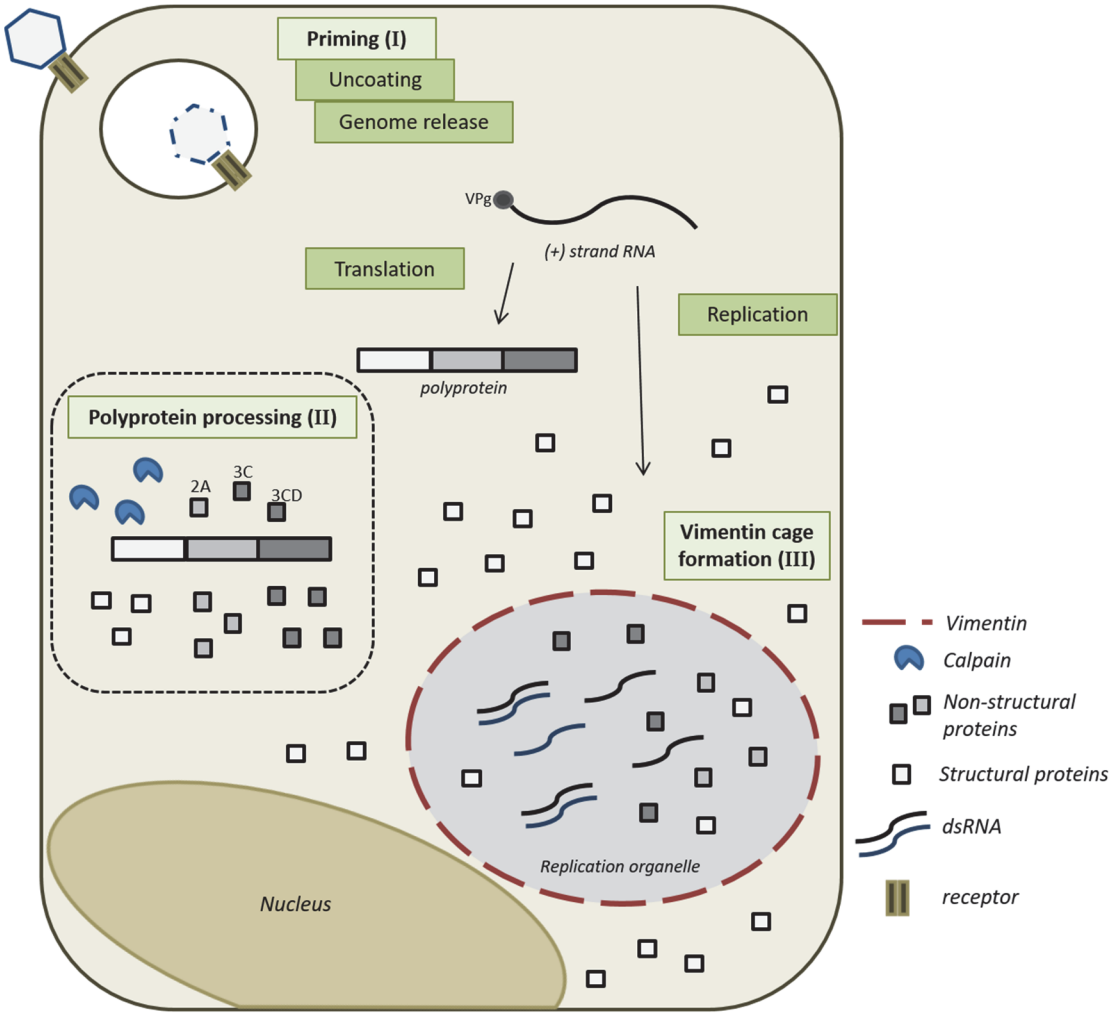

FIGURE 5 A summary of the conclusions of the thesis. The respective original papers are indicated by Roman numerals I-III. After attachment and internalization, EV1 capsid goes through minor structural changes, which allows entry of small molecules. In this so called **priming (I)** step, the virus has a more open structure compared to native virion, but still contains all capsid proteins. Furthermore, the virus is still in an infectious state and is able to bind to its receptor. After priming, the uncoating occurs and the viral RNA is externalized from the capsid, and subsequently released into the host cell cytoplasm. The positive-sense RNA is next translated as a single polyprotein, which is cleaved by viral proteases 2A, 3C and 3CD. In addition, studies in-vitro suggest that cytoplasmic, cellular calpain proteases may contribute to the **polyprotein processing (II)** by cleaving the structural proteins out of the enteroviral polyprotein. In addition to translation, the viral RNA is also replicated and during translation/replication the enteroviral protein synthesis triggers vimentin rearrangements leading to **vimentin cage formation (III)**. The vimentin cage supports the replication organelle and contains replicating viral RNA, components of ER and Golgi, and viral non-structural proteins, but less of the structural proteins. The non-structural proteins are efficiently produced only if vimentin cage is formed, while the production of structural proteins in the cytoplasm is less dependent on the vimentin rearrangements and cage formation.

Acknowledgements

This work was carried out at the University of Jyväskylä at the Department of Biological and Environmental Sciences and NanoScience center, Division of Cell and Molecular Biology. The thesis was funded by Jane and Aatos Erkko foundation and Ellen and Artturi Nyyssönen foundation.

I would like to acknowledge all the people involved in my PhD journey. First, I would like to thank my supervisor Varpu Marjomäki for all her support and help over these years. Your presence and positive attitude in all circumstances enabled me to enjoy the good days, but most importantly, also to get through and move forward during the more challenging days. In addition, I thank for all the trust and responsibility you have given me, and also all the opportunities you have provided during my PhD studies, such as conference trips abroad and research visit to South Africa.

Next, I would like to acknowledge the reviewers of this thesis: Professor Kalle Saksela and Docent Tero Ahola. Your feedback and suggestions were very valuble to me. I would also like to thank Doctor Marco Vignuzzi for accepting the invitation to serve as my opponent. Furthermore, I would like to acknowledge my thesis committee members Doctor Jost Enninga and Docent Giuseppe Balistreri. Thank you for all the valuable discussions and advices over the years. Thank you also to all my co-authors in the papers. Without you this would have not been possible.

I would also like to thank my collegues in South Africa. The two months research visit to Pretoria was exciting and amazing and I left from there with a lot of good memories (and luckily also some results!). Most importantly, I would like to thank Professor Musa Mhlanga for giving me the opportunity to work in his lab. In addition, I would like to thank Jerolen for help and fun moments in the lab. Furthermore, your kindness made me feel very welcomed. I want to also thank other lab members Ezio, Maria, Stephanie, Janine and Loretta for company and help.

Next I would like to expresss the biggest thanks to my awesome collegues: the Marjomäki group. People have come and gone, but I feel very privileged that I have had such a great group of people as my collegues over the years. Thank you all the previous members: Lassi, Moona, Artur, Maria, Mari, Marie, Helena and Paula for teaching me, and also, for all the important discussions and funny moments in the lab, and in different activities and conferences. Thank you also for the current members: Visa, Dhanik, Sailee and Ville. Discussions at lunch and in the office have been so important and your support has meant a lot. In addition, thanks for your great company in all the funny activities, dinners and conference trips. I would also like to thank our students and especially those who I have been supervising: Juuli, William, Niko and Tino. It has been very refreshing, instructive and fun being your supervisor, so thank you for that opportunity. However, ultimately I see you as my collegues and I also thank for all the great discussions about science and life in general. In addition, I would like to thank our technicians in the department, Arja Mansikkaviita, Alli

Liukkonen, Petri Papponen and Laura Pitkänen, for helping in practical things in the lab.

Furthermore, I would like to thank all the collegues outside Marjomäki group, so people from B- and C-corridors. We have had enjoyable moments either just chatting in the corridors or playing super football, curling and megazone among others. In addition, we have had such fun time organizing the Researcher's night during the past couple of years! I would especially like to thank my girl team Kati, Pilvi and Alli. Thank you for all the discussions, as well as for the time spent outside the department. I'm happy to say that you girls have become more than collegues, you are my friends. In addition, I want to thank Mari for her friendship also during her post-Marjomäki group era. It is a privilege to find collegues with whom the friendship goes beyond work!

Next, I would like to thank all my other friends and family. Thank you for giving me something else to think about than cells and viruses. Although it might be hard to understand what I actually do for work, still, I have always felt your support and love. So thank you Aino, Sami and Antti; Anette, Saara and Anne; and all the friends that Ilari has brought in my life. The biggest thanks go also to both Myllynen and Laajala families. Thank you 'Laajalan klaani' for support and all the fun times in Haapajärvi and Oulu. Thanks also to my little sisters Hanna and Noora and especially my parents, äiskä and iskä. You have supported me in all the things I have decided to do and always believed in me even if I have had doubts myself. Thank you also to my uncle's family, so Risto, Anja, Tiia and Mikko, especially for providing a summer cottage and the best company to spend midsummers and other summer weekends. That is the place where work stress can be forgotten, at the latest.

Last but not least, I would like to express my deepest gratitude to my husband Ilari. Your love and support have meant everything to me. You have encouraged me during both ups and downs of this PhD journey and relieved my stress with your wise words and calm attitude when I have needed it. But most importantly, somehow, you have always been able to make me laugh even during the hardest days! Besides being my husband you are also my best friend.

YHTEENVETO (RÉSUMÉ IN FINNISH)

Enterovirusten tehokasta avautumista ja replikaatiota edistävät solu- ja virustekijät

Virukset ovat mikroskooppisia partikkeleita, jotka koostuvat perimäaineksesta ja sitä ympäröivästä proteiinikuoresta. Lisäksi joillakin viruksilla on proteiinikuoren ympärillä lipidivaippa. Virukset eivät kykene elämään itsenäisesti, vaan niiden lisääntyminen on täysin riippuvaista isäntäsolusta, jonka proteiinisynteesiin liittyviä koneistoja ja muita tekijöitä virus käyttää hyväkseen.

Enterovirukset ovat halkaisijaltaan noin 30 nm kokoisia vaipattomia viruksia, joiden perimäaineksena toimii RNA molekyyli. Ne aiheuttavat useimmiten oireettomia tai lieviä sairauksia, mutta voivat aiheuttaa myös vakavampia tauteja. Infektion aikana enterovirus tunkeutuu isäntäsoluun, minkä jälkeen sen proteiinikuori avautuu ja RNA vapautuu isäntäsolun solulimaan. Solulimassa enteroviruksen RNA toimii mallina proteiinisynteesissä, jossa kaikki viruksen proteiinit tuotetaan yhtenä polyproteiinina. Jälkikäteen polyproteiini pilkotaan yksittäisiksi proteiineiksi, joita tarvitaan uusien virusten proteiinikuoren kokoamiseen ja muihin infektiota edistäviin prosesseihin. Proteiinisynteesin lisäksi viruksen RNA:ta monistetaan ja perimäaines pakataan uusiin valmistuviin viruspartikkeleihin, jotka vapautetaan ulos solusta, mikä useimmiten johtaa isäntäsolun kuolemaan.

Enterovirusten perimä sisältää koodin vain rajoitettuun määrään proteiineja, joten virukset ovat mukautuneet evoluution aikana hyödyntämään isäntäsolun proteiineja ja muita tekijöitä. Monet näistä solutekijöistä, kuten myös infektioon vaikuttavista virustekijöistä tunnetaan. Silti edelleen yksi virustutkimuksen päätavoite on tunnistaa uusia tärkeitä infektiota edistäviä tekijöitä. Tätä tietoa voidaan käyttää hyväksi viruslääkkeiden kehittelyssä, sillä esimerkiksi enteroviruksia vastaan ei ole vielä toimivaa lääkettä. Nykyään erityisesti solutekijöihin kohdistuvia lääkkeitä pidetään potentiaalisina vaihtoehtoina virusinfektioiden estämiseen, sillä ne voisivat mahdollisesti toimia useampia viruksen serotyyppejä vastaan. Lisäksi, vaikka virukset tuottavat mutaatioita nopeasti välttääkseen viruksen kuoreen kiinnittyviä lääkkeitä, muuntautuminen on hankalampaa kun viruksen täytyy tuottaa mutaatioita, jotka auttavat kehittämään vaihtoehtoisia keinoja välttää solutekijöitä, jotka ovat alun perin tärkeitä viruksen infektioreitillä.

Tämä väitös koostuu kolmesta osatyöstä, joissa tutkittiin sekä virus- että solutekijöitä, jotka vaikuttavat enterovirusten tehokkaaseen infektioon. Ensimmäisessä osatyössä tutkittiin infektiovaihetta, jossa viruksen proteiinikuori avautuu. Toisessa ja kolmannessa osatyössä puolestaan tutkittiin solutekijöitä, jotka ovat osallisena enterovirusten infektiossa viruksen proteiinien synteesin ja perimäaineksen monistumisen aikana.

Ensimmäisessä osatyössä löysimme ja kuvailimme uuden echovirus 1 (EV1) partikkelin, joka muodostui infektion aikana. Tämän partikkelin muodostuminen ajoittui infektiovaiheeseen, jossa viruksen proteiinikuori avautuu ja RNA vapautuu kuoresta ulos. Tällaisia niin kutsuttuja välimuotoisia partikkeleita on kuvailtu enteroviruksista ennenkin, mutta me osoitimme, että EV1 partikkeli ei ollut

ominaisuuksiltaan tyypillinen enterovirusten välimuotopartikkeli. Verrattuna natiiviin viruspartikkeliin, tämä välimuotopartikkeli oli rakenteeltaan avoimempi, mutta proteiinikuori sisälsi silti edelleen kaikki rakenneproteiinit. Lisäksi osoitimme, että toisin kuin aiemmin kuvatut välimuotopartikkelit, tämä partikkeli pystyi edelleen sitoutumaan reseptoriproteiiniin solun pinnalla ja aikaansaamaan tehokkaan infektion.

Toisessa osatyössä osoitimme in vitro -kokeilla, että proteiinisynteesissä tuotettu viruksen polyproteiini voidaan pilkkoa yksittäisiksi viruksen proteiineiksi viruksen omien entsyymien lisäksi myös solun kalpaiini-entsyymien avulla. Lisäksi näytimme, että kalpaiini-entsyymejä vastaan kehitetty inhibiittori esti myös viruksen entsyymien toiminnan. Tämä tulos osoitti, että kalpaiini-inhibiittoria voitaisiin mahdollisesti käyttää viruslääkkeenä enterovirusinfektioita vastaan.

Kolmannessa osatyössä näytimme, että enterovirusinfektio saa aikaan voimakkaita muutoksia solun välimuotoisia säikeitä muodostavassa vimentiiniproteiinissa. Normaalisti koko soluliman kattava vimentiiniverkosto tiivistyi ja muodosti häkkimäisen rakenteen tuman läheisyyteen infektion aikana. Tarkempi tarkastelu osoitti, että tämän vimentiinihäkin muodostumisen laukaisi viruksen proteiinien synteesi ja että vimentiinihäkki sisälsi monistuvaa viruksen RNA:ta ja ei-rakenteellisia proteiineja, mutta ei rakenneproteiineja. Lisäksi osoitimme, että vimentiinirakenne on tärkeä nimenomaan ei-rakenteellisten proteiinien tuotossa, sillä vimentiinihäkin muodostumisen estäminen johti ei-rakenteellisten proteiinien heikompaan tuottoon verrattuna rakenneproteiineihin. Ei-rakenteellisten proteiinien heikompi tuotto puolestaan lisäsi isäntäsolujen elävyyttä vähentämällä apoptoosia.

Viruksia vastaan voidaan pääasiassa taistella kahdella tavalla: lääkkeillä tai rokotteilla. Rokotteiden kehittäminen yli sataa eri enterovirus-serotyyppiä vastaan on työlästä, ja siksi enterovirustutkimuksessa panostetaan yhä enemmän toimivien, erityisesti laajakirjoisten, viruslääkkeiden löytymiseen. Tämä edellyttää myös syvällistä ymmärrystä erilaisista enterovirusinfektioon vaikuttavista tekijöistä ja korostaa perustavalaatuisen virustutkimuksen tärkeyttä, mitä myös tämä väitöstyö edustaa.

REFERENCES

Agirre A., Barco A., Carrasco L. & Nieva J.L. 2002. Viroporin-mediated membrane permeabilization. Pore formation by nonstructural poliovirus 2B protein. *J Biol Chem* 277: 40434-40441.

Airaksinen A., Somerharju P. & Hovi T. 2001. Variation in liposome binding among enteroviruses. *Virology* 279: 539-545.

Aldabe R., Irurzun A. & Carrasco L. 1997. Poliovirus protein 2BC increases cytosolic free calcium concentrations. *J Virol* 71: 6214-6217.

Alidjinou E.K., Sane F., Engelmann I., Geenen V. & Hober D. 2014. Enterovirus persistence as a mechanism in the pathogenesis of type 1 diabetes. *Discov Med* 18: 273-282.

Amineva S.P., Aminev A.G., Palmenberg A.C. & Gern J.E. 2004. Rhinovirus 3C protease precursors 3CD and 3CD' localize to the nuclei of infected cells. *J Gen Virol* 85: 2969-2979.

Andino R., Rieckhof G.E. & Baltimore D. 1990. A functional ribonucleoprotein complex forms around the 5' end of poliovirus RNA. *Cell* 63: 369-380.

Armer H., Moffat K., Wileman T., Belsham G.J., Jackson T., Duprex W.P., Ryan M. & Monaghan P. 2008. Foot-and-mouth disease virus, but not bovine enterovirus, targets the host cell cytoskeleton via the nonstructural protein 3Cpro. *J Virol* 82: 10556-10566.

Back S.H., Kim Y.K., Kim W.J., Cho S., Oh H.R., Kim J.E. & Jang S.K. 2002. Translation of polioviral mRNA is inhibited by cleavage of polypyrimidine tract-binding proteins executed by polioviral 3C(pro). *J Virol* 76: 2529-2542.

Badorff C., Berkely N., Mehrotra S., Talhouk J.W., Rhoads R.E. & Knowlton K.U. 2000. Enteroviral protease 2A directly cleaves dystrophin and is inhibited by a dystrophin-based substrate analogue. *J Biol Chem* 275: 11191-11197.

Baggen J., Thibaut H.J., Strating, J R P M & van Kuppeveld, F J M. 2018. The life cycle of non-polio enteroviruses and how to target it. *Nat Rev Microbiol* 16: 368-381.

Baggen J., Thibaut H.J., Staring J., Jae L.T., Liu Y., Guo H., Slager J.J., de Bruin J.W., van Vliet A.L., Blomen V.A., Overduin P., Sheng J., de Haan C.A., de Vries E., Meijer A., Rossmann M.G., Brummelkamp T.R. & van Kuppeveld F.J. 2016. Enterovirus D68 receptor requirements unveiled by haploid genetics. *Proc Natl Acad Sci U S A* 113: 1399-1404.

Baggen J., Hurdiss D.L., Zocher G., Mistry N., Roberts R.W., Slager J.J., Guo H., van Vliet, A L W, Wahedi M., Benschop K., Duizer E., de Haan, C A M, de Vries E., Casasnovas J.M., de Groot R.J., Arnberg N., Stehle T., Ranson N.A., Thibaut H.J. & van Kuppeveld, F J M. 2018. Role of enhanced receptor engagement in the evolution of a pandemic acute hemorrhagic conjunctivitis virus. *Proc Natl Acad Sci U S A* 115: 397-402.

Banerjee R., Weidman M.K., Echeverri A., Kundu P. & Dasgupta A. 2004. Regulation of poliovirus 3C protease by the 2C polypeptide. *J Virol* 78: 9243-9256.

Barral P.M., Sarkar D., Fisher P.B. & Racaniello V.R. 2009. RIG-I is cleaved during picornavirus infection. *Virology* 391: 171-176.

Barral P.M., Morrison J.M., Drahos J., Gupta P., Sarkar D., Fisher P.B. & Racaniello V.R. 2007. MDA-5 is cleaved in poliovirus-infected cells. *J Virol* 81: 3677-3684.

Barton D.J. & Flanegan J.B. 1997. Synchronous replication of poliovirus RNA: initiation of negative-strand RNA synthesis requires the guanidine-inhibited activity of protein 2C. *J Virol* 71: 8482-8489.

Barton D.J., Morasco B.J. & Flanegan J.B. 1999. Translating ribosomes inhibit poliovirus negative-strand RNA synthesis. *J Virol* 73: 10104-10112.

Basavappa R., Syed R., Flore O., Icenogle J.P., Filman D.J. & Hogle J.M. 1994. Role and mechanism of the maturation cleavage of VP0 in poliovirus assembly: structure of the empty capsid assembly intermediate at 2.9 A resolution. *Protein Sci* 3: 1651-1669.

Belin M.T. & Boulanger P. 1987. Processing of vimentin occurs during the early stages of adenovirus infection. *J Virol* 61: 2559-2566.

Belnap D.M., Filman D.J., Trus B.L., Cheng N., Booy F.P., Conway J.F., Curry S., Hiremath C.N., Tsang S.K., Steven A.C. & Hogle J.M. 2000. Molecular tectonic model of virus structural transitions: the putative cell entry states of poliovirus. *J Virol* 74: 1342-1354.

Belov G.A., Nair V., Hansen B.T., Hoyt F.H., Fischer E.R. & Ehrenfeld E. 2012. Complex dynamic development of poliovirus membranous replication complexes. *J Virol* 86: 302-312.

Bergelson J.M., Shepley M.P., Chan B.M., Hemler M.E. & Finberg R.W. 1992. Identification of the integrin VLA-2 as a receptor for echovirus 1. *Science* 255: 1718-1720.

Bergelson J.M., Chan M., Solomon K.R., St John N.F., Lin H. & Finberg R.W. 1994. Decay-accelerating factor (CD55), a glycosylphosphatidylinositol-anchored complement regulatory protein, is a receptor for several echoviruses. *Proc Natl Acad Sci U S A* 91: 6245-6248.

Bhattacharya B., Noad R.J. & Roy P. 2007. Interaction between Bluetongue virus outer capsid protein VP2 and vimentin is necessary for virus egress. *Virol J* 4: 7.

Bienz K., Egger D. & Pfister T. 1994. Characteristics of the poliovirus replication complex. *Arch Virol Suppl* 9: 147-157.

Bienz K., Egger D. & Pasamontes L. 1987. Association of polioviral proteins of the P2 genomic region with the viral replication complex and virus-induced membrane synthesis as visualized by electron microscopic immunocytochemistry and autoradiography. *Virology* 160: 220-226.

Bienz K., Egger D., Pfister T. & Troxler M. 1992. Structural and functional characterization of the poliovirus replication complex. *J Virol* 66: 2740-2747.

Blanc F., Furio L., Moisy D., Yen H.L., Chignard M., Letavernier E., Naffakh N., Mok C.K. & Si-Tahar M. 2016. Targeting host calpain proteases decreases influenza A virus infection. *Am J Physiol Lung Cell Mol Physiol* 310: 689.

Block J., Schroeder V., Pawelzyk P., Willenbacher N. & Koster S. 2015. Physical properties of cytoplasmic intermediate filaments. *Biochim Biophys Acta* 1853: 3053-3064.

Blom N., Hansen J., Blaas D. & Brunak S. 1996. Cleavage site analysis in picornaviral polyproteins: discovering cellular targets by neural networks. *Protein Sci* 5: 2203-2216.

Blyn L.B., Towner J.S., Semler B.L. & Ehrenfeld E. 1997. Requirement of poly(rC) binding protein 2 for translation of poliovirus RNA. *J Virol* 71: 6243-6246.

Blyn L.B., Swiderek K.M., Richards O., Stahl D.C., Semler B.L. & Ehrenfeld E. 1996. Poly(rC) binding protein 2 binds to stem-loop IV of the poliovirus RNA 5' noncoding region: identification by automated liquid chromatography-tandem mass spectrometry. *Proc Natl Acad Sci U S A* 93: 11115-11120.

Bochkov Y.A., Watters K., Ashraf S., Griggs T.F., Devries M.K., Jackson D.J., Palmenberg A.C. & Gern J.E. 2015. Cadherin-related family member 3, a childhood asthma susceptibility gene product, mediates rhinovirus C binding and replication. *Proc Natl Acad Sci U S A* 112: 5485-5490.

Bode W. & Huber R. 2000. Structural basis of the endoproteinase-protein inhibitor interaction. *Biochim Biophys Acta* 1477: 241-252.

Bostina M., Levy H., Filman D.J. & Hogle J.M. 2011. Poliovirus RNA is released from the capsid near a twofold symmetry axis. *J Virol* 85: 776-783.

Bouin A., Gretteau P.A., Wehbe M., Renois F., N'Guyen Y., Leveque N., Vu M.N., Tracy S., Chapman N.M., Bruneval P., Fornes P., Semler B.L. & Andreoletti L. 2019. Enterovirus Persistence in Cardiac Cells of Patients With Idiopathic Dilated Cardiomyopathy Is Linked to 5' Terminal Genomic RNA-Deleted Viral Populations With Viral-Encoded Proteinase Activities. *Circulation* 139: 2326-2338.

Boussadia O., Niepmann M., Creancier L., Prats A.C., Dautry F. & Jacquemin-Sablon H. 2003. Unr is required in vivo for efficient initiation of translation from the internal ribosome entry sites of both rhinovirus and poliovirus. *J Virol* 77: 3353-3359.

Bozym R.A., Morosky S.A., Kim K.S., Cherry S. & Coyne C.B. 2010. Release of intracellular calcium stores facilitates coxsackievirus entry into polarized endothelial cells. *PLoS Pathog* 6: e1001135.

Bozym R.A., Patel K., White C., Cheung K.H., Bergelson J.M., Morosky S.A. & Coyne C.B. 2011. Calcium signals and calpain-dependent necrosis are essential for release of coxsackievirus B from polarized intestinal epithelial cells. *Mol Biol Cell* 22: 3010-3021.

Branca D. 2004. Calpain-related diseases. *Biochem Biophys Res Commun* 322: 1098-1104.

Brandenburg B., Lee L.Y., Lakadamyali M., Rust M.J., Zhuang X. & Hogle J.M. 2007. Imaging poliovirus entry in live cells. *PLoS Biol* 5: e183.

Bubeck D., Filman D.J., Cheng N., Steven A.C., Hogle J.M. & Belnap D.M. 2005. The structure of the poliovirus 135S cell entry intermediate at 10-angstrom resolution reveals the location of an externalized polypeptide that binds to membranes. *J Virol* 79: 7745-7755.

Buehler M.J. 2013. Mechanical players-The role of intermediate filaments in cell mechanics and organization. *Biophys J* 105: 1733-1734.

Butan C., Filman D.J. & Hogle J.M. 2014. Cryo-electron microscopy reconstruction shows poliovirus 135S particles poised for membrane interaction and RNA release. *J Virol* 88: 1758-1770.

Cammas A., Pileur F., Bonnal S., Lewis S.M., Leveque N., Holcik M. & Vagner S. 2007. Cytoplasmic relocalization of heterogeneous nuclear ribonucleoprotein A1 controls translation initiation of specific mRNAs. *Mol Biol Cell* 18: 5048-5059.

Carafoli E. & Molinari M. 1998. Calpain: a protease in search of a function? *Biochem Biophys Res Commun* 247: 193-203.

Carragher N.O. 2006. Calpain inhibition: a therapeutic strategy targeting multiple disease states. *Curr Pharm Des* 12: 615-638.

Carrillo-Tripp M., Shepherd C.M., Borelli I.A., Venkataraman S., Lander G., Natarajan P., Johnson J.E., Brooks C.L. & Reddy V.S. 2009. VIPERdb2: an enhanced and web API enabled relational database for structural virology. *Nucleic Acids Res* 37: 436.

Castello A., Izquierdo J.M., Welnowska E. & Carrasco L. 2009. RNA nuclear export is blocked by poliovirus 2A protease and is concomitant with nucleoporin cleavage. *J Cell Sci* 122: 3799-3809.

Chase A.J., Daijogo S. & Semler B.L. 2014. Inhibition of poliovirus-induced cleavage of cellular protein PCBP2 reduces the levels of viral RNA replication. *J Virol* 88: 3192-3201.

Chau D.H., Yuan J., Zhang H., Cheung P., Lim T., Liu Z., Sall A. & Yang D. 2007. Coxsackievirus B3 proteases 2A and 3C induce apoptotic cell death through mitochondrial injury and cleavage of eIF4GI but not DAP5/p97/NAT1. *Apoptosis* 12: 513-524.

Chen M., Goorha R. & Murti K.G. 1986. Interaction of frog virus 3 with the cytomatrix. IV. Phosphorylation of vimentin precedes the reorganization of intermediate filaments around the virus assembly sites. *J Gen Virol* 67 (Pt 5): 915-922.

Choi K., Kim J.H., Li X., Paek K.Y., Ha S.H., Ryu S.H., Wimmer E. & Jang S.K. 2004. Identification of cellular proteins enhancing activities of internal ribosomal entry sites by competition with oligodeoxynucleotides. *Nucleic Acids Res* 32: 1308-1317.

Clark M.E., Lieberman P.M., Berk A.J. & Dasgupta A. 1993. Direct cleavage of human TATA-binding protein by poliovirus protease 3C in vivo and in vitro. *Mol Cell Biol* 13: 1232-1237.

Costa-Mattioli M., Svitkin Y. & Sonenberg N. 2004. La autoantigen is necessary for optimal function of the poliovirus and hepatitis C virus internal ribosome entry site in vivo and in vitro. *Mol Cell Biol* 24: 6861-6870.

Coyne C.B. & Bergelson J.M. 2006. Virus-induced Abl and Fyn kinase signals permit coxsackievirus entry through epithelial tight junctions. *Cell* 124: 119-131.

Crowell R.L. & Philipson L. 1971. Specific alterations of coxsackievirus B3 eluted from HeLa cells. *J Virol* 8: 509-515.

Cuerrier D., Moldoveanu T. & Davies P.L. 2005. Determination of peptide substrate specificity for mu-calpain by a peptide library-based approach: the importance of primed side interactions. *J Biol Chem* 280: 40632-40641.

Curry S., Chow M. & Hogle J.M. 1996. The poliovirus 135S particle is infectious. *J Virol* 70: 7125-7131.

Danthi P., Tosteson M., Li Q.H. & Chow M. 2003. Genome delivery and ion channel properties are altered in VP4 mutants of poliovirus. *J Virol* 77: 5266-5274.

Das S. & Dasgupta A. 1993. Identification of the cleavage site and determinants required for poliovirus 3CPro-catalyzed cleavage of human TATA-binding transcription factor TBP. *J Virol* 67: 3326-3331.

Davis M.P., Bottley G., Beales L.P., Killington R.A., Rowlands D.J. & Tuthill T.J. 2008. Recombinant VP4 of human rhinovirus induces permeability in model membranes. *J Virol* 82: 4169-4174.

de Jong A.S., Visch H.J., de Mattia F., van Dommelen M.M., Swarts H.G., Luyten T., Callewaert G., Melchers W.J., Willems P.H. & van Kuppeveld F.J. 2006. The coxsackievirus 2B protein increases efflux of ions from the endoplasmic reticulum and Golgi, thereby inhibiting protein trafficking through the Golgi. *J Biol Chem* 281: 14144-14150.

DeBiasi R.L., Edelstein C.L., Sherry B. & Tyler K.L. 2001. Calpain inhibition protects against virus-induced apoptotic myocardial injury. *J Virol* 75: 351-361.

Debiasi R.L., Squier M.K., Pike B., Wynes M., Dermody T.S., Cohen J.J. & Tyler K.L. 1999. Reovirus-induced apoptosis is preceded by increased cellular calpain activity and is blocked by calpain inhibitors. *J Virol* 73: 695-701.

Delorme-Axford E., Sadovsky Y. & Coyne C.B. 2013. Lipid raft- and SRC family kinase-dependent entry of coxsackievirus B into human placental trophoblasts. *J Virol* 87: 8569-8581.

Dinman J.D. 2012. Mechanisms and implications of programmed translational frameshifting. *Wiley Interdiscip Rev RNA* 3: 661-673.

Donnelly M.L., Luke G., Mehrotra A., Li X., Hughes L.E., Gani D. & Ryan M.D. 2001. Analysis of the aphthovirus 2A/2B polyprotein 'cleavage' mechanism indicates not a proteolytic reaction, but a novel translational effect: a putative ribosomal 'skip'. *J Gen Virol* 82: 1013-1025.

Dougherty J.D., Tsai W.C. & Lloyd R.E. 2015. Multiple Poliovirus Proteins Repress Cytoplasmic RNA Granules. *Viruses* 7: 6127-6140.

Du N., Cong H., Tian H., Zhang H., Zhang W., Song L. & Tien P. 2014. Cell surface vimentin is an attachment receptor for enterovirus 71. *J Virol* 88: 5816-5833.

Egger D. & Bienz K. 2005. Intracellular location and translocation of silent and active poliovirus replication complexes. *J Gen Virol* 86: 707-718.

Etchison D., Milburn S.C., Edery I., Sonenberg N. & Hershey J.W. 1982. Inhibition of HeLa cell protein synthesis following poliovirus infection correlates with the proteolysis of a 220,000-dalton polypeptide associated with eucaryotic initiation factor 3 and a cap binding protein complex. *J Biol Chem* 257: 14806-14810.

Etienne-Manneville S. 2018. Cytoplasmic Intermediate Filaments in Cell Biology. *Annu Rev Cell Dev Biol* 34: 1-28.

Fay N. & Pante N. 2013. The intermediate filament network protein, vimentin, is required for parvoviral infection. *Virology* 444: 181-190.

Feng Q., Langereis M.A., Lork M., Nguyen M., Hato S.V., Lanke K., Emdad L., Bhoopathi P., Fisher P.B., Lloyd R.E. & van Kuppeveld F.J. 2014. Enterovirus 2Apro targets MDA5 and MAVS in infected cells. *J Virol* 88: 3369-3378.

Ferreira L.R., Moussatche N. & Moura Neto V. 1994. Rearrangement of intermediate filament network of BHK-21 cells infected with vaccinia virus. *Arch Virol* 138: 273-285.

Firth A.E. & Brierley I. 2012. Non-canonical translation in RNA viruses. *J Gen Virol* 93: 1385-1409.

Flanegan J.B. & Baltimore D. 1977. Poliovirus-specific primer-dependent RNA polymerase able to copy poly(A). *Proc Natl Acad Sci U S A* 74: 3677-3680.

Fletcher D.A. & Mullins R.D. 2010. Cell mechanics and the cytoskeleton. *Nature* 463: 485-492.

Flynn C.T., Kimura T., Frimpong-Boateng K., Harkins S. & Whitton J.L. 2017. Immunological and pathological consequences of coxsackievirus RNA persistence in the heart. *Virology* 512: 104-112.

Fricks C.E. & Hogle J.M. 1990. Cell-induced conformational change in poliovirus: externalization of the amino terminus of VP1 is responsible for liposome binding. *J Virol* 64: 1934-1945.

Gaaloul I., Riabi S., Harrath R., Hunter T., Hamda K.B., Ghzala A.B., Huber S. & Aouni M. 2014. Coxsackievirus B detection in cases of myocarditis, myopericarditis, pericarditis and dilated cardiomyopathy in hospitalized patients. *Mol Med Rep* 10: 2811-2818.

Galigniana M.D., Scruggs J.L., Herrington J., Welsh M.J., Carter-Su C., Housley P.R. & Pratt W.B. 1998. Heat shock protein 90-dependent (geldanamycin-inhibited) movement of the glucocorticoid receptor through the cytoplasm to the nucleus requires intact cytoskeleton. *Mol Endocrinol* 12: 1903-1913.

Gamarnik A.V. & Andino R. 1997. Two functional complexes formed by KH domain containing proteins with the 5' noncoding region of poliovirus RNA. *RNA* 3: 882-892.

Garriga D., Pickl-Herk A., Luque D., Wruss J., Caston J.R., Blaas D. & Verdaguer N. 2012. Insights into minor group rhinovirus uncoating: the X-ray structure of the HRV2 empty capsid. *PLoS Pathog* 8: e1002473.

Geller R., Vignuzzi M., Andino R. & Frydman J. 2007. Evolutionary constraints on chaperone-mediated folding provide an antiviral approach refractory to development of drug resistance. *Genes Dev* 21: 195-205.

Ghildyal R., Jordan B., Li D., Dagher H., Bardin P.G., Gern J.E. & Jans D.A. 2009. Rhinovirus 3C protease can localize in the nucleus and alter active and passive nucleocytoplasmic transport. *J Virol* 83: 7349-7352.

Gladue D.P., O'Donnell V., Baker-Branstetter R., Holinka L.G., Pacheco J.M., Fernandez Sainz I., Lu Z., Ambroggio X., Rodriguez L. & Borca M.V. 2013. Foot-and-mouth disease virus modulates cellular vimentin for virus survival. *J Virol* 87: 6794-6803.

Goldman R.D., Grin B., Mendez M.G. & Kuczmarski E.R. 2008. Intermediate filaments: versatile building blocks of cell structure. *Curr Opin Cell Biol* 20: 28-34.

Goldstaub D., Gradi A., Bercovitch Z., Grosmann Z., Nophar Y., Luria S., Sonenberg N. & Kahana C. 2000. Poliovirus 2A protease induces apoptotic cell death. *Mol Cell Biol* 20: 1271-1277.

Goll D.E., Thompson V.F., Li H., Wei W. & Cong J. 2003. The calpain system. *Physiol Rev* 83: 731-801.

Gomez Yafal A., Kaplan G., Racaniello V.R. & Hogle J.M. 1993. Characterization of poliovirus conformational alteration mediated by soluble cell receptors. *Virology* 197: 501-505.

Goodfellow I.G., Evans D.J., Blom A.M., Kerrigan D., Miners J.S., Morgan B.P. & Spiller O.B. 2005. Inhibition of coxsackie B virus infection by soluble forms of its receptors: binding affinities, altered particle formation, and competition with cellular receptors. *J Virol* 79: 12016-12024.

Gordon L.B., Rothman F.G., Lopez-Otin C. & Misteli T. 2014. Progeria: a paradigm for translational medicine. *Cell* 156: 400-407.

Greve J.M., Davis G., Meyer A.M., Forte C.P., Yost S.C., Marlor C.W., Kamarck M.E. & McClelland A. 1989. The major human rhinovirus receptor is ICAM-1. *Cell* 56: 839-847.

Gromeier M. & Wetz K. 1990. Kinetics of poliovirus uncoating in HeLa cells in a nonacidic environment. *J Virol* 64: 3590-3597.

Groppelli E., Levy H.C., Sun E., Strauss M., Nicol C., Gold S., Zhuang X., Tuthill T.J., Hogle J.M. & Rowlands D.J. 2017. Picornavirus RNA is protected from cleavage by ribonuclease during virion uncoating and transfer across cellular and model membranes. *PLoS Pathog* 13: e1006197.

Grummt I. 2006. Actin and myosin as transcription factors. *Curr Opin Genet Dev* 16: 191-196.

Guest S., Pilipenko E., Sharma K., Chumakov K. & Roos R.P. 2004. Molecular mechanisms of attenuation of the Sabin strain of poliovirus type 3. *J Virol* 78: 11097-11107.

Gullberg M., Polacek C., Botner A. & Belsham G.J. 2013. Processing of the VP1/2A junction is not necessary for production of foot-and-mouth disease virus empty capsids and infectious viruses: characterization of "self-tagged" particles. *J Virol* 87: 11591-11603.

Guo M., Ehrlicher A.J., Mahammad S., Fabich H., Jensen M.H., Moore J.R., Fredberg J.J., Goldman R.D. & Weitz D.A. 2013. The role of vimentin intermediate filaments in cortical and cytoplasmic mechanics. *Biophys J* 105: 1562-1568.

Gustin K.E. & Sarnow P. 2002. Inhibition of nuclear import and alteration of nuclear pore complex composition by rhinovirus. *J Virol* 76: 8787-8796.
Gutierrez-Escolano L. & del Angel R.M. 1996. Nuclear proteins bind to poliovirus 5' untranslated region. *Arch Med Res* 27: 413-419.
Gutierrez-Fernandez A., Soria-Valles C., Osorio F.G., Gutierrez-Abril J., Garabaya C., Aguirre A., Fueyo A., Fernandez-Garcia M.S., Puente X.S. & Lopez-Otin C. 2015. Loss of MT1-MMP causes cell senescence and nuclear defects which can be reversed by retinoic acid. *EMBO J* 34: 1875-1888.
Hanecak R., Semler B.L., Anderson C.W. & Wimmer E. 1982. Proteolytic processing of poliovirus polypeptides: antibodies to polypeptide P3-7c inhibit cleavage at glutamine-glycine pairs. *Proc Natl Acad Sci U S A* 79: 3973-3977.
Hanecak R., Semler B.L., Ariga H., Anderson C.W. & Wimmer E. 1984. Expression of a cloned gene segment of poliovirus in E. coli: evidence for autocatalytic production of the viral proteinase. *Cell* 37: 1063-1073.
Hanna R.A., Campbell R.L. & Davies P.L. 2008. Calcium-bound structure of calpain and its mechanism of inhibition by calpastatin. *Nature* 456: 409-412.
Haolong C., Du N., Hongchao T., Yang Y., Wei Z., Hua Z., Wenliang Z., Lei S. & Po T. 2013. Enterovirus 71 VP1 activates calmodulin-dependent protein kinase II and results in the rearrangement of vimentin in human astrocyte cells. *PLoS One* 8: e73900.
Harris K.G. & Coyne C.B. 2014. Death waits for no man--does it wait for a virus? How enteroviruses induce and control cell death. *Cytokine Growth Factor Rev* 25: 587-596.
Harris K.S., Reddigari S.R., Nicklin M.J., Hammerle T. & Wimmer E. 1992. Purification and characterization of poliovirus polypeptide 3CD, a proteinase and a precursor for RNA polymerase. *J Virol* 66: 7481-7489.
Harutyunyan S., Kumar M., Sedivy A., Subirats X., Kowalski H., Kohler G. & Blaas D. 2013. Viral uncoating is directional: exit of the genomic RNA in a common cold virus starts with the poly-(A) tail at the 3'-end. *PLoS Pathog* 9: e1003270.
Hata S., Doi N., Kitamura F. & Sorimachi H. 2007. Stomach-specific calpain, nCL-2/calpain 8, is active without calpain regulatory subunit and oligomerizes through C2-like domains. *J Biol Chem* 282: 27847-27856.
Heikkila O., Susi P., Tevaluoto T., Harma H., Marjomaki V., Hyypia T. & Kiljunen S. 2010. Internalization of coxsackievirus A9 is mediated by {beta}2-microglobulin, dynamin, and Arf6 but not by caveolin-1 or clathrin. *J Virol* 84: 3666-3681.
Hellen C.U., Witherell G.W., Schmid M., Shin S.H., Pestova T.V., Gil A. & Wimmer E. 1993. A cytoplasmic 57-kDa protein that is required for translation of picornavirus RNA by internal ribosomal entry is identical to the nuclear pyrimidine tract-binding protein. *Proc Natl Acad Sci U S A* 90: 7642-7646.

Hendrix M.J., Seftor E.A., Seftor R.E. & Trevor K.T. 1997. Experimental co-expression of vimentin and keratin intermediate filaments in human breast cancer cells results in phenotypic interconversion and increased invasive behavior. *Am J Pathol* 150: 483-495.

Herold J. & Andino R. 2001. Poliovirus RNA replication requires genome circularization through a protein-protein bridge. *Mol Cell* 7: 581-591.

Hirokawa N., Noda Y., Tanaka Y. & Niwa S. 2009. Kinesin superfamily motor proteins and intracellular transport. *Nat Rev Mol Cell Biol* 10: 682-696.

Hober D. & Sauter P. 2010. Pathogenesis of type 1 diabetes mellitus: interplay between enterovirus and host. *Nat Rev Endocrinol* 6: 279-289.

Hofer F., Gruenberger M., Kowalski H., Machat H., Huettinger M., Kuechler E. & Blaas D. 1994. Members of the low density lipoprotein receptor family mediate cell entry of a minor-group common cold virus. *Proc Natl Acad Sci U S A* 91: 1839-1842.

Hosfield C.M., Elce J.S., Davies P.L. & Jia Z. 1999. Crystal structure of calpain reveals the structural basis for Ca(2+)-dependent protease activity and a novel mode of enzyme activation. *EMBO J* 18: 6880-6889.

Howe C.L., LaFrance-Corey R.G., Mirchia K., Sauer B.M., McGovern R.M., Reid J.M. & Buenz E.J. 2016. Neuroprotection mediated by inhibition of calpain during acute viral encephalitis. *Sci Rep* 6: 28699.

Hsu N.Y., Ilnytska O., Belov G., Santiana M., Chen Y.H., Takvorian P.M., Pau C., van der Schaar H., Kaushik-Basu N., Balla T., Cameron C.E., Ehrenfeld E., van Kuppeveld F.J. & Altan-Bonnet N. 2010. Viral reorganization of the secretory pathway generates distinct organelles for RNA replication. *Cell* 141: 799-811.

Huang Y. & Wang K.K. 2001. The calpain family and human disease. *Trends Mol Med* 7: 355-362.

Hunt S.L., Hsuan J.J., Totty N. & Jackson R.J. 1999. unr, a cellular cytoplasmic RNA-binding protein with five cold-shock domains, is required for internal initiation of translation of human rhinovirus RNA. *Genes Dev* 13: 437-448.

Huttunen M., Waris M., Kajander R., Hyypia T. & Marjomaki V. 2014. Coxsackievirus A9 infects cells via nonacidic multivesicular bodies. *J Virol* 88: 5138-5151.

Hyder C.L., Pallari H.M., Kochin V. & Eriksson J.E. 2008. Providing cellular signposts--post-translational modifications of intermediate filaments. *FEBS Lett* 582: 2140-2148.

Ilnytska O., Santiana M., Hsu N.Y., Du W.L., Chen Y.H., Viktorova E.G., Belov G., Brinker A., Storch J., Moore C., Dixon J.L. & Altan-Bonnet N. 2013. Enteroviruses harness the cellular endocytic machinery to remodel the host cell cholesterol landscape for effective viral replication. *Cell Host Microbe* 14: 281-293.

Imajoh S., Kawasaki H. & Suzuki K. 1986. Limited autolysis of calcium-activated neutral protease (CANP): reduction of the Ca2+-requirement is due to the NH2-terminal processing of the large subunit. *J Biochem* 100: 633-642.

Inomata M., Kasai Y., Nakamura M. & Kawashima S. 1988. Activation mechanism of calcium-activated neutral protease. Evidence for the existence of intramolecular and intermolecular autolyses. *J Biol Chem* 263: 19783-19787.

Ivaska J., Pallari H.M., Nevo J. & Eriksson J.E. 2007. Novel functions of vimentin in cell adhesion, migration, and signaling. *Exp Cell Res* 313: 2050-2062.

Izumi R.E., Valdez B., Banerjee R., Srivastava M. & Dasgupta A. 2001. Nucleolin stimulates viral internal ribosome entry site-mediated translation. *Virus Res* 76: 17-29.

Jackson W.T., Giddings T.H., Taylor M.P., Mulinyawe S., Rabinovitch M., Kopito R.R. & Kirkegaard K. 2005. Subversion of cellular autophagosomal machinery by RNA viruses. *PLoS Biol* 3: e156.

Joachims M. & Etchison D. 1992. Poliovirus infection results in structural alteration of a microtubule-associated protein. *J Virol* 66: 5797-5804.

Joachims M., Van Breugel P.C. & Lloyd R.E. 1999. Cleavage of poly(A)-binding protein by enterovirus proteases concurrent with inhibition of translation in vitro. *J Virol* 73: 718-727.

Joachims M., Harris K.S. & Etchison D. 1995. Poliovirus protease 3C mediates cleavage of microtubule-associated protein 4. *Virology* 211: 451-461.

Kalamvoki M. & Mavromara P. 2004. Calcium-dependent calpain proteases are implicated in processing of the hepatitis C virus NS5A protein. *J Virol* 78: 11865-11878.

Kanlaya R., Pattanakitsakul S.N., Sinchaikul S., Chen S.T. & Thongboonkerd V. 2010. Vimentin interacts with heterogeneous nuclear ribonucleoproteins and dengue nonstructural protein 1 and is important for viral replication and release. *Mol Biosyst* 6: 795-806.

Karjalainen M., Rintanen N., Lehkonen M., Kallio K., Maki A., Hellstrom K., Siljamaki V., Upla P. & Marjomaki V. 2011. Echovirus 1 infection depends on biogenesis of novel multivesicular bodies. *Cell Microbiol* 13: 1975-1995.

Karjalainen M., Kakkonen E., Upla P., Paloranta H., Kankaanpaa P., Liberali P., Renkema G.H., Hyypia T., Heino J. & Marjomaki V. 2008. A Raft-derived, Pak1-regulated entry participates in alpha2beta1 integrin-dependent sorting to caveosomes. *Mol Biol Cell* 19: 2857-2869.

Karpe Y.A., Pingale K.D. & Kanade G.D. 2016. Activities of proteasome and m-calpain are essential for Chikungunya virus replication. *Virus Genes* 52: 716-721.

Kiss R., Kovacs D., Tompa P. & Perczel A. 2008. Local structural preferences of calpastatin, the intrinsically unstructured protein inhibitor of calpain. *Biochemistry* 47: 6936-6945.

Krausslich H.G. & Wimmer E. 1988. Viral proteinases. *Annu Rev Biochem* 57: 701-754.

Kreplak L., Bar H., Leterrier J.F., Herrmann H. & Aebi U. 2005. Exploring the mechanical behavior of single intermediate filaments. *J Mol Biol* 354: 569-577.

Krieger S.E., Kim C., Zhang L., Marjomaki V. & Bergelson J.M. 2013. Echovirus 1 entry into polarized Caco-2 cells depends on dynamin, cholesterol, and cellular factors associated with macropinocytosis. *J Virol* 87: 8884-8895.

Kristensen T., Newman J., Guan S.H., Tuthill T.J. & Belsham G.J. 2018. Cleavages at the three junctions within the foot-and-mouth disease virus capsid precursor (P1-2A) by the 3C protease are mutually independent. *Virology* 522: 260-270.

Kuo R.L., Kung S.H., Hsu Y.Y. & Liu W.T. 2002. Infection with enterovirus 71 or expression of its 2A protease induces apoptotic cell death. *J Gen Virol* 83: 1367-1376.

Kuyumcu-Martinez N.M., Joachims M. & Lloyd R.E. 2002. Efficient cleavage of ribosome-associated poly(A)-binding protein by enterovirus 3C protease. *J Virol* 76: 2062-2074.

Kuyumcu-Martinez N.M., Van Eden M.E., Younan P. & Lloyd R.E. 2004. Cleavage of poly(A)-binding protein by poliovirus 3C protease inhibits host cell translation: a novel mechanism for host translation shutoff. *Mol Cell Biol* 24: 1779-1790.

Laajala M. & Marjomaki V. 2019. A Common Receptor Found for Echoviruses. *Trends Microbiol* 27: 475-477.

Lahaye X., Vidy A., Fouquet B. & Blondel D. 2012. Hsp70 protein positively regulates rabies virus infection. *J Virol* 86: 4743-4751.

Lai J.K., Sam I.C. & Chan Y.F. 2016. The Autophagic Machinery in Enterovirus Infection. *Viruses* 8: 10.3390/v8020032.

Laitinen O.H., Svedin E., Kapell S., Nurminen A., Hytonen V.P. & Flodstrom-Tullberg M. 2016. Enteroviral proteases: structure, host interactions and pathogenicity. *Rev Med Virol* 26: 251-267.

Lamphear B.J. & Rhoads R.E. 1996. A single amino acid change in protein synthesis initiation factor 4G renders cap-dependent translation resistant to picornaviral 2A proteases. *Biochemistry* 35: 15726-15733.

Lawson M.A. & Semler B.L. 1992. Alternate poliovirus nonstructural protein processing cascades generated by primary sites of 3C proteinase cleavage. *Virology* 191: 309-320.

Leduc C. & Etienne-Manneville S. 2015. Intermediate filaments in cell migration and invasion: the unusual suspects. *Curr Opin Cell Biol* 32: 102-112.

Lee C.K. & Wimmer E. 1988. Proteolytic processing of poliovirus polyprotein: elimination of 2Apro-mediated, alternative cleavage of polypeptide 3CD by in vitro mutagenesis. *Virology* 166: 405-414.

Lee H., Shingler K.L., Organtini L.J., Ashley R.E., Makhov A.M., Conway J.F. & Hafenstein S. 2016. The novel asymmetric entry intermediate of a picornavirus captured with nanodiscs. *Sci Adv* 2: e1501929.

Lee H.J., Tomioka S., Kinbara K., Masumoto H., Jeong S.Y., Sorimachi H., Ishiura S. & Suzuki K. 1999. Characterization of a human digestive tract-specific calpain, nCL-4, expressed in the baculovirus system. *Arch Biochem Biophys* 362: 22-31.

Lee K.M., Chen C.J. & Shih S.R. 2017. Regulation Mechanisms of Viral IRES-Driven Translation. *Trends Microbiol* 25: 546-561.

Lei X., Xiao X., Xue Q., Jin Q., He B. & Wang J. 2013. Cleavage of interferon regulatory factor 7 by enterovirus 71 3C suppresses cellular responses. *J Virol* 87: 1690-1698.

Levy H.C., Bostina M., Filman D.J. & Hogle J.M. 2010. Catching a virus in the act of RNA release: a novel poliovirus uncoating intermediate characterized by cryo-electron microscopy. *J Virol* 84: 4426-4441.

Li M., Wang X., Yu Y., Yu Y., Xie Y., Zou Y., Ge J., Peng T. & Chen R. 2014. Coxsackievirus B3-induced calpain activation facilitates the progeny virus replication via a likely mechanism related with both autophagy enhancement and apoptosis inhibition in the early phase of infection: an in vitro study in H9c2 cells. *Virus Res* 179: 177-186.

Limpens R.W., van der Schaar, H M, Kumar D., Koster A.J., Snijder E.J., van Kuppeveld F.J. & Barcena M. 2011. The transformation of enterovirus replication structures: a three-dimensional study of single- and double-membrane compartments. *MBio* 2: 10.1128/mBio.0016-11. Print 2011.

Lin J.Y., Li M.L. & Shih S.R. 2009. Far upstream element binding protein 2 interacts with enterovirus 71 internal ribosomal entry site and negatively regulates viral translation. *Nucleic Acids Res* 37: 47-59.

Lin J.Y., Chen T.C., Weng K.F., Chang S.C., Chen L.L. & Shih S.R. 2009. Viral and host proteins involved in picornavirus life cycle. *J Biomed Sci* 16: 10-103.

Lin J.Y., Shih S.R., Pan M., Li C., Lue C.F., Stollar V. & Li M.L. 2009. hnRNP A1 interacts with the 5' untranslated regions of enterovirus 71 and Sindbis virus RNA and is required for viral replication. *J Virol* 83: 6106-6114.

Lind K., Svedin E., Domsgen E., Kapell S., Laitinen O.H., Moll M. & Flodstrom-Tullberg M. 2016. Coxsackievirus counters the host innate immune response by blocking type III interferon expression. *J Gen Virol* 97: 1368-1380.

Liu Y., Sheng J., van Vliet, A L W, Buda G., van Kuppeveld, F J M & Rossmann M.G. 2018. Molecular basis for the acid-initiated uncoating of human enterovirus D68. *Proc Natl Acad Sci U S A* 115: E12209-E12217.

Liu Y., Sheng J., Baggen J., Meng G., Xiao C., Thibaut H.J., van Kuppeveld F.J. & Rossmann M.G. 2015. Sialic acid-dependent cell entry of human enterovirus D68. *Nat Commun* 6: 8865.

Lonberg-Holm K., Gosser L.B. & Kauer J.C. 1975. Early alteration of poliovirus in infected cells and its specific inhibition. *J Gen Virol* 27: 329-342.

Lopez-Otin C. & Hunter T. 2010. The regulatory crosstalk between kinases and proteases in cancer. *Nat Rev Cancer* 10: 278-292.

Lopez-Otin C. & Bond J.S. 2008. Proteases: multifunctional enzymes in life and disease. *J Biol Chem* 283: 30433-30437.

Loughran G., Firth A.E. & Atkins J.F. 2011. Ribosomal frameshifting into an overlapping gene in the 2B-encoding region of the cardiovirus genome. *Proc Natl Acad Sci U S A* 108: 1111.

Lozano G. & Martinez-Salas E. 2015. Structural insights into viral IRES-dependent translation mechanisms. *Curr Opin Virol* 12: 113-120.

Lu J., Yi L., Zhao J., Yu J., Chen Y., Lin M.C., Kung H.F. & He M.L. 2012. Enterovirus 71 disrupts interferon signaling by reducing the level of interferon receptor 1. *J Virol* 86: 3767-3776.

Lui Y.L., Lin Z., Lee J.J., Chow V.T., Poh C.L. & Tan E.L. 2013. Beta-actin variant is necessary for Enterovirus 71 replication. *Biochem Biophys Res Commun* 433: 607-610.

Maki M., Narayana S.V. & Hitomi K. 1997. A growing family of the Ca2+-binding proteins with five EF-hand motifs. *Biochem J* 328 (Pt 2): 718-720.

Marjomaki V., Pietiainen V., Matilainen H., Upla P., Ivaska J., Nissinen L., Reunanen H., Huttunen P., Hyypia T. & Heino J. 2002. Internalization of echovirus 1 in caveolae. *J Virol* 76: 1856-1865.

Martino T.A., Petric M., Weingartl H., Bergelson J.M., Opavsky M.A., Richardson C.D., Modlin J.F., Finberg R.W., Kain K.C., Willis N., Gauntt C.J. & Liu P.P. 2000. The coxsackie-adenovirus receptor (CAR) is used by reference strains and clinical isolates representing all six serotypes of coxsackievirus group B and by swine vesicular disease virus. *Virology* 271: 99-108.

Mayer M.P. 2005. Recruitment of Hsp70 chaperones: a crucial part of viral survival strategies. *Rev Physiol Biochem Pharmacol* 153: 1-46.

McLauchlan J., Lemberg M.K., Hope G. & Martoglio B. 2002. Intramembrane proteolysis promotes trafficking of hepatitis C virus core protein to lipid droplets. *EMBO J* 21: 3980-3988.

Meckes D.G., Menaker N.F. & Raab-Traub N. 2013. Epstein-Barr virus LMP1 modulates lipid raft microdomains and the vimentin cytoskeleton for signal transduction and transformation. *J Virol* 87: 1301-1311.

Melia C.E., van der Schaar, H M, Lyoo H., Limpens, R W A L, Feng Q., Wahedi M., Overheul G.J., van Rij R.P., Snijder E.J., Koster A.J., Barcena M. & van Kuppeveld, F J M. 2017. Escaping Host Factor PI4KB Inhibition: Enterovirus Genomic RNA Replication in the Absence of Replication Organelles. *Cell Rep* 21: 587-599.

Melloni E., Michetti M., Salamino F. & Pontremoli S. 1998. Molecular and functional properties of a calpain activator protein specific for mu-isoforms. *J Biol Chem* 273: 12827-12831.

Mendelsohn C.L., Wimmer E. & Racaniello V.R. 1989. Cellular receptor for poliovirus: molecular cloning, nucleotide sequence, and expression of a new member of the immunoglobulin superfamily. *Cell* 56: 855-865.

Mendez M.G., Kojima S. & Goldman R.D. 2010. Vimentin induces changes in cell shape, motility, and adhesion during the epithelial to mesenchymal transition. *FASEB J* 24: 1838-1851.

Mercer J. & Helenius A. 2010. Apoptotic mimicry: phosphatidylserine-mediated macropinocytosis of vaccinia virus. *Ann N Y Acad Sci* 1209: 49-55.

Merrifield C.J., Perrais D. & Zenisek D. 2005. Coupling between clathrin-coated-pit invagination, cortactin recruitment, and membrane scission observed in live cells. *Cell* 121: 593-606.

Merrifield C.J., Feldman M.E., Wan L. & Almers W. 2002. Imaging actin and dynamin recruitment during invagination of single clathrin-coated pits. *Nat Cell Biol* 4: 691-698.

Merrill M.K. & Gromeier M. 2006. The double-stranded RNA binding protein 76:NF45 heterodimer inhibits translation initiation at the rhinovirus type 2 internal ribosome entry site. *J Virol* 80: 6936-6942.

Merrill M.K., Dobrikova E.Y. & Gromeier M. 2006. Cell-type-specific repression of internal ribosome entry site activity by double-stranded RNA-binding protein 76. *J Virol* 80: 3147-3156.

Mesmin B., Bigay J., Moser von Filseck J., Lacas-Gervais S., Drin G. & Antonny B. 2013. A four-step cycle driven by PI(4)P hydrolysis directs sterol/PI(4)P exchange by the ER-Golgi tether OSBP. *Cell* 155: 830-843.

Miller M.S. & Hertel L. 2009. Onset of human cytomegalovirus replication in fibroblasts requires the presence of an intact vimentin cytoskeleton. *J Virol* 83: 7015-7028.

Milstone A.M., Petrella J., Sanchez M.D., Mahmud M., Whitbeck J.C. & Bergelson J.M. 2005. Interaction with coxsackievirus and adenovirus receptor, but not with decay-accelerating factor (DAF), induces A-particle formation in a DAF-binding coxsackievirus B3 isolate. *J Virol* 79: 655-660.

Mogensen T.H. 2009. Pathogen recognition and inflammatory signaling in innate immune defenses. *Clin Microbiol Rev* 22: 24-73, Table of Contents.

Moldoveanu T., Campbell R.L., Cuerrier D. & Davies P.L. 2004. Crystal structures of calpain-E64 and -leupeptin inhibitor complexes reveal mobile loops gating the active site. *J Mol Biol* 343: 1313-1326.

Moldoveanu T., Hosfield C.M., Lim D., Elce J.S., Jia Z. & Davies P.L. 2002. A Ca(2+) switch aligns the active site of calpain. *Cell* 108: 649-660.

Molinari M., Anagli J. & Carafoli E. 1994. Ca(2+)-activated neutral protease is active in the erythrocyte membrane in its nonautolyzed 80-kDa form. *J Biol Chem* 269: 27992-27995.

Molla A., Hellen C.U. & Wimmer E. 1993. Inhibition of proteolytic activity of poliovirus and rhinovirus 2A proteinases by elastase-specific inhibitors. *J Virol* 67: 4688-4695.

Morosky S., Wells A.I., Lemon K., Evans A.S., Schamus S., Bakkenist C.J. & Coyne C.B. 2019. The neonatal Fc receptor is a pan-echovirus receptor. *Proc Natl Acad Sci U S A* 116: 3758-3763.

Muehlenbachs A., Bhatnagar J. & Zaki S.R. 2015. Tissue tropism, pathology and pathogenesis of enterovirus infection. *J Pathol* 235: 217-228.

Mukherjee A., Morosky S.A., Delorme-Axford E., Dybdahl-Sissoko N., Oberste M.S., Wang T. & Coyne C.B. 2011. The coxsackievirus B 3C protease cleaves MAVS and TRIF to attenuate host type I interferon and apoptotic signaling. *PLoS Pathog* 7: e1001311.

Nalivaeva N.N., Belyaev N.D., Kerridge C. & Turner A.J. 2014. Amyloid-clearing proteins and their epigenetic regulation as a therapeutic target in Alzheimer's disease. *Front Aging Neurosci* 6: 235.

Napthine S., Ling R., Finch L.K., Jones J.D., Bell S., Brierley I. & Firth A.E. 2017. Protein-directed ribosomal frameshifting temporally regulates gene expression. *Nat Commun* 8: 15582.

Nekrasova O.E., Mendez M.G., Chernoivanenko I.S., Tyurin-Kuzmin P.A., Kuczmarski E.R., Gelfand V.I., Goldman R.D. & Minin A.A. 2011. Vimentin intermediate filaments modulate the motility of mitochondria. *Mol Biol Cell* 22: 2282-2289.

Nelsen-Salz B., Eggers H.J. & Zimmermann H. 1999. Integrin alpha(v)beta3 (vitronectin receptor) is a candidate receptor for the virulent echovirus 9 strain Barty. *J Gen Virol* 80 (Pt 9): 2311-2313.

Newman J., Asfor A.S., Berryman S., Jackson T., Curry S. & Tuthill T.J. 2018. The Cellular Chaperone Heat Shock Protein 90 Is Required for Foot-and-Mouth Disease Virus Capsid Precursor Processing and Assembly of Capsid Pentamers. *J Virol* 92: 10.1128/JVI.0141-17. Print 2018 Mar 1.

Neznanov N., Chumakov K.M., Neznanova L., Almasan A., Banerjee A.K. & Gudkov A.V. 2005. Proteolytic cleavage of the p65-RelA subunit of NF-kappaB during poliovirus infection. *J Biol Chem* 280: 24153-24158.

Nicklin M.J., Krausslich H.G., Toyoda H., Dunn J.J. & Wimmer E. 1987. Poliovirus polypeptide precursors: expression in vitro and processing by exogenous 3C and 2A proteinases. *Proc Natl Acad Sci U S A* 84: 4002-4006.

Nishimura Y. & Shimizu H. 2012. Cellular receptors for human enterovirus species a. *Front Microbiol* 3: 105.

Nishimura Y., Shimojima M., Tano Y., Miyamura T., Wakita T. & Shimizu H. 2009. Human P-selectin glycoprotein ligand-1 is a functional receptor for enterovirus 71. *Nat Med* 15: 794-797.

Nitahara-Kasahara Y., Fukasawa M., Shinkai-Ouchi F., Sato S., Suzuki T., Murakami K., Wakita T., Hanada K., Miyamura T. & Nishijima M. 2009. Cellular vimentin content regulates the protein level of hepatitis C virus core protein and the hepatitis C virus production in cultured cells. *Virology* 383: 319-327.

Nurani G., Lindqvist B. & Casasnovas J.M. 2003. Receptor priming of major group human rhinoviruses for uncoating and entry at mild low-pH environments. *J Virol* 77: 11985-11991.

Ofori-Anyinam O., Vrijsen R., Kronenberger P. & Boeye A. 1993. Effect of a capsid-stabilizing pyridazinamine, R 78206, on the eclipse and intracellular location of poliovirus. *J Virol* 67: 2367-2369.

Ono Y. & Sorimachi H. 2012. Calpains: an elaborate proteolytic system. *Biochim Biophys Acta* 1824: 224-236.

Organtini L.J., Makhov A.M., Conway J.F., Hafenstein S. & Carson S.D. 2014. Kinetic and structural analysis of coxsackievirus B3 receptor interactions and formation of the A-particle. *J Virol* 88: 5755-5765.

Palmenberg A.C. 1990. Proteolytic processing of picornaviral polyprotein. *Annu Rev Microbiol* 44: 603-623.

Panjwani A., Strauss M., Gold S., Wenham H., Jackson T., Chou J.J., Rowlands D.J., Stonehouse N.J., Hogle J.M. & Tuthill T.J. 2014. Capsid protein VP4 of

human rhinovirus induces membrane permeability by the formation of a size-selective multimeric pore. *PLoS Pathog* 10: e1004294.

Park N., Schweers N.J. & Gustin K.E. 2015. Selective Removal of FG Repeat Domains from the Nuclear Pore Complex by Enterovirus 2A(pro). *J Virol* 89: 11069-11079.

Parry D.A., Strelkov S.V., Burkhard P., Aebi U. & Herrmann H. 2007. Towards a molecular description of intermediate filament structure and assembly. *Exp Cell Res* 313: 2204-2216.

Parsley T.B., Towner J.S., Blyn L.B., Ehrenfeld E. & Semler B.L. 1997. Poly (rC) binding protein 2 forms a ternary complex with the 5'-terminal sequences of poliovirus RNA and the viral 3CD proteinase. *RNA* 3: 1124-1134.

Paul A.V., van Boom J.H., Filippov D. & Wimmer E. 1998. Protein-primed RNA synthesis by purified poliovirus RNA polymerase. *Nature* 393: 280-284.

Pelkmans L., Puntener D. & Helenius A. 2002. Local actin polymerization and dynamin recruitment in SV40-induced internalization of caveolae. *Science* 296: 535-539.

Perera R. & Kuhn R.J. 2008. Structural proteomics of dengue virus. *Curr Opin Microbiol* 11: 369-377.

Perera R., Daijogo S., Walter B.L., Nguyen J.H. & Semler B.L. 2007. Cellular protein modification by poliovirus: the two faces of poly(rC)-binding protein. *J Virol* 81: 8919-8932.

Pettersson R.F., Ambros V. & Baltimore D. 1978. Identification of a protein linked to nascent poliovirus RNA and to the polyuridylic acid of negative-strand RNA. *J Virol* 27: 357-365.

Pfister T. & Wimmer E. 1999. Characterization of the nucleoside triphosphatase activity of poliovirus protein 2C reveals a mechanism by which guanidine inhibits poliovirus replication. *J Biol Chem* 274: 6992-7001.

Pietiainen V., Marjomaki V., Upla P., Pelkmans L., Helenius A. & Hyypia T. 2004. Echovirus 1 endocytosis into caveosomes requires lipid rafts, dynamin II, and signaling events. *Mol Biol Cell* 15: 4911-4925.

Pilipenko E.V., Pestova T.V., Kolupaeva V.G., Khitrina E.V., Poperechnaya A.N., Agol V.I. & Hellen C.U. 2000. A cell cycle-dependent protein serves as a template-specific translation initiation factor. *Genes Dev* 14: 2028-2045.

Pons-Salort M., Parker E.P. & Grassly N.C. 2015. The epidemiology of non-polio enteroviruses: recent advances and outstanding questions. *Curr Opin Infect Dis* 28: 479-487.

Pontremoli S., Melloni E., Michetti M., Salamino F., Sparatore B. & Horecker B.L. 1988. An endogenous activator of the Ca2+-dependent proteinase of human neutrophils that increases its affinity for Ca2+. *Proc Natl Acad Sci U S A* 85: 1740-1743.

Prchla E., Kuechler E., Blaas D. & Fuchs R. 1994. Uncoating of human rhinovirus serotype 2 from late endosomes. *J Virol* 68: 3713-3723.

Quiros P.M., Langer T. & Lopez-Otin C. 2015. New roles for mitochondrial proteases in health, ageing and disease. *Nat Rev Mol Cell Biol* 16: 345-359.

Ramajayam R., Tan K.P. & Liang P.H. 2011. Recent development of 3C and 3CL protease inhibitors for anti-coronavirus and anti-picornavirus drug discovery. *Biochem Soc Trans* 39: 1371-1375.

Rao M.B., Tanksale A.M., Ghatge M.S. & Deshpande V.V. 1998. Molecular and biotechnological aspects of microbial proteases. *Microbiol Mol Biol Rev* 62: 597-635.

Ray P.S. & Das S. 2002. La autoantigen is required for the internal ribosome entry site-mediated translation of Coxsackievirus B3 RNA. *Nucleic Acids Res* 30: 4500-4508.

Reinhard S.M., Razak K. & Ethell I.M. 2015. A delicate balance: role of MMP-9 in brain development and pathophysiology of neurodevelopmental disorders. *Front Cell Neurosci* 9: 280.

Ren J., Wang X., Hu Z., Gao Q., Sun Y., Li X., Porta C., Walter T.S., Gilbert R.J., Zhao Y., Axford D., Williams M., McAuley K., Rowlands D.J., Yin W., Wang J., Stuart D.I., Rao Z. & Fry E.E. 2013. Picornavirus uncoating intermediate captured in atomic detail. *Nat Commun* 4: 1929.

Richardson A.M., Havel L.S., Koyen A.E., Konen J.M., Shupe J., Wiles W.G., Martin W.D., Grossniklaus H.E., Sica G., Gilbert-Ross M. & Marcus A.I. 2018. Vimentin Is Required for Lung Adenocarcinoma Metastasis via Heterotypic Tumor Cell-Cancer-Associated Fibroblast Interactions during Collective Invasion. *Clin Cancer Res* 24: 420-432.

Riedl S.J. & Salvesen G.S. 2007. The apoptosome: signalling platform of cell death. *Nat Rev Mol Cell Biol* 8: 405-413.

Rintanen N., Karjalainen M., Alanko J., Paavolainen L., Maki A., Nissinen L., Lehkonen M., Kallio K., Cheng R.H., Upla P., Ivaska J. & Marjomaki V. 2012. Calpains promote alpha2beta1 integrin turnover in nonrecycling integrin pathway. *Mol Biol Cell* 23: 448-463.

Risco C., Rodriguez J.R., Lopez-Iglesias C., Carrascosa J.L., Esteban M. & Rodriguez D. 2002. Endoplasmic reticulum-Golgi intermediate compartment membranes and vimentin filaments participate in vaccinia virus assembly. *J Virol* 76: 1839-1855.

Rivera C.I. & Lloyd R.E. 2008. Modulation of enteroviral proteinase cleavage of poly(A)-binding protein (PABP) by conformation and PABP-associated factors. *Virology* 375: 59-72.

Roivainen M., Alfthan G., Jousilahti P., Kimpimaki M., Hovi T. & Tuomilehto J. 1998. Enterovirus infections as a possible risk factor for myocardial infarction. *Circulation* 98: 2534-2537.

Roivainen M., Piirainen L., Hovi T., Virtanen I., Riikonen T., Heino J. & Hyypia T. 1994. Entry of coxsackievirus A9 into host cells: specific interactions with alpha v beta 3 integrin, the vitronectin receptor. *Virology* 203: 357-365.

Rossmann M.G., He Y. & Kuhn R.J. 2002. Picornavirus-receptor interactions. *Trends Microbiol* 10: 324-331.

Rowlands D.J., Shirley M.W., Sangar D.V. & Brown F. 1975. A high density component in several vertebrate enteroviruses. *J Gen Virol* 29: 223-234.

Royston L. & Tapparel C. 2016. Rhinoviruses and Respiratory Enteroviruses: Not as Simple as ABC. *Viruses* 8: 10.3390/v8010016.

Ruokolainen V., Domanska A., Laajala M., Pelliccia M., Butcher S.J. & Marjomaki V. 2019. Extracellular albumin and endosomal ions prime enterovirus particles for uncoating that can be prevented by fatty acid saturation. *J Virol* .

Saido T.C., Sorimachi H. & Suzuki K. 1994. Calpain: new perspectives in molecular diversity and physiological-pathological involvement. *FASEB J* 8: 814-822.

Saido T.C., Mizuno K. & Suzuki K. 1991. Proteolysis of protein kinase C by calpain: effect of acidic phospholipids. *Biomed Biochim Acta* 50: 485-489.

Sakai K., Akanuma H., Imahori K. & Kawashima S. 1987. A unique specificity of a calcium activated neutral protease indicated in histone hydrolysis. *J Biochem* 101: 911-918.

Schlegel A., Giddings T.H., Ladinsky M.S. & Kirkegaard K. 1996. Cellular origin and ultrastructure of membranes induced during poliovirus infection. *J Virol* 70: 6576-6588.

Seipelt J., Liebig H.D., Sommergruber W., Gerner C. & Kuechler E. 2000. 2A proteinase of human rhinovirus cleaves cytokeratin 8 in infected HeLa cells. *J Biol Chem* 275: 20084-20089.

Seipelt J., Guarne A., Bergmann E., James M., Sommergruber W., Fita I. & Skern T. 1999. The structures of picornaviral proteinases. *Virus Res* 62: 159-168.

Seitsonen J.J., Shakeel S., Susi P., Pandurangan A.P., Sinkovits R.S., Hyvonen H., Laurinmaki P., Yla-Pelto J., Topf M., Hyypia T. & Butcher S.J. 2012. Structural analysis of coxsackievirus A7 reveals conformational changes associated with uncoating. *J Virol* 86: 7207-7215.

Shakeel S., Seitsonen J.J., Kajander T., Laurinmaki P., Hyypia T., Susi P. & Butcher S.J. 2013. Structural and functional analysis of coxsackievirus A9 integrin alphavbeta6 binding and uncoating. *J Virol* 87: 3943-3951.

Shakeel S., Dykeman E.C., White S.J., Ora A., Cockburn J.J.B., Butcher S.J., Stockley P.G. & Twarock R. 2017. Genomic RNA folding mediates assembly of human parechovirus. *Nat Commun* 8: z.

Shingler K.L., Yoder J.L., Carnegie M.S., Ashley R.E., Makhov A.M., Conway J.F. & Hafenstein S. 2013. The enterovirus 71 A-particle forms a gateway to allow genome release: a cryoEM study of picornavirus uncoating. *PLoS Pathog* 9: e1003240.

Shiroki K., Isoyama T., Kuge S., Ishii T., Ohmi S., Hata S., Suzuki K., Takasaki Y. & Nomoto A. 1999. Intracellular redistribution of truncated La protein produced by poliovirus 3Cpro-mediated cleavage. *J Virol* 73: 2193-2200.

Siljamaki E., Rintanen N., Kirsi M., Upla P., Wang W., Karjalainen M., Ikonen E. & Marjomaki V. 2013. Cholesterol dependence of collagen and echovirus 1 trafficking along the novel alpha2beta1 integrin internalization pathway. *PLoS One* 8: e55465.

Snider N.T. & Omary M.B. 2014. Post-translational modifications of intermediate filament proteins: mechanisms and functions. *Nat Rev Mol Cell Biol* 15: 163-177.

Sommergruber W., Zorn M., Blaas D., Fessl F., Volkmann P., Maurer-Fogy I., Pallai P., Merluzzi V., Matteo M. & Skern T. 1989. Polypeptide 2A of human rhinovirus type 2: identification as a protease and characterization by mutational analysis. *Virology* 169: 68-77.

Soonsawad P., Paavolainen L., Upla P., Weerachatyanukul W., Rintanen N., Espinoza J., McNerney G., Marjomaki V. & Cheng R.H. 2014. Permeability changes of integrin-containing multivesicular structures triggered by picornavirus entry. *PLoS One* 9: e108948.

Sorimachi H. 2001. Muscular dystrophy and calpain. *Tanpakushitsu Kakusan Koso* 46: 1772-1780.

Sorimachi H., Ishiura S. & Suzuki K. 1997. Structure and physiological function of calpains. *Biochem J* 328 (Pt 3): 721-732.

Sorimachi H., Ishiura S. & Suzuki K. 1993. A novel tissue-specific calpain species expressed predominantly in the stomach comprises two alternative splicing products with and without Ca(2+)-binding domain. *J Biol Chem* 268: 19476-19482.

Stabach P.R., Cianci C.D., Glantz S.B., Zhang Z. & Morrow J.S. 1997. Site-directed mutagenesis of alpha II spectrin at codon 1175 modulates its mu-calpain susceptibility. *Biochemistry* 36: 57-65.

Staring J., von Castelmur E., Blomen V.A., van den Hengel, L G, Brockmann M., Baggen J., Thibaut H.J., Nieuwenhuis J., Janssen H., van Kuppeveld F.J., Perrakis A., Carette J.E. & Brummelkamp T.R. 2017. PLA2G16 represents a switch between entry and clearance of Picornaviridae. *Nature* 541: 412-416.

Stefanovic S., Windsor M., Nagata K.I., Inagaki M. & Wileman T. 2005. Vimentin rearrangement during African swine fever virus infection involves retrograde transport along microtubules and phosphorylation of vimentin by calcium calmodulin kinase II. *J Virol* 79: 11766-11775.

Strauss M., Levy H.C., Bostina M., Filman D.J. & Hogle J.M. 2013. RNA transfer from poliovirus 135S particles across membranes is mediated by long umbilical connectors. *J Virol* 87: 3903-3914.

Suhy D.A., Giddings T.H. & Kirkegaard K. 2000. Remodeling the endoplasmic reticulum by poliovirus infection and by individual viral proteins: an autophagy-like origin for virus-induced vesicles. *J Virol* 74: 8953-8965.

Suzuki K., Hata S., Kawabata Y. & Sorimachi H. 2004. Structure, activation, and biology of calpain. *Diabetes* 53 Suppl 1: 12.

Suzuki K., Imajoh S., Emori Y., Kawasaki H., Minami Y. & Ohno S. 1987. Calcium-activated neutral protease and its endogenous inhibitor. Activation at the cell membrane and biological function. *FEBS Lett* 220: 271-277.

Svitkin Y.V., Imataka H., Khaleghpour K., Kahvejian A., Liebig H.D. & Sonenberg N. 2001. Poly(A)-binding protein interaction with elF4G stimulates picornavirus IRES-dependent translation. *RNA* 7: 1743-1752.

Taguwa S., Maringer K., Li X., Bernal-Rubio D., Rauch J.N., Gestwicki J.E., Andino R., Fernandez-Sesma A. & Frydman J. 2015. Defining Hsp70 Subnetworks in Dengue Virus Replication Reveals Key Vulnerability in Flavivirus Infection. *Cell* 163: 1108-1123.

Tapparel C., Siegrist F., Petty T.J. & Kaiser L. 2013. Picornavirus and enterovirus diversity with associated human diseases. *Infect Genet Evol* 14: 282-293.

Teo C.S. & Chu J.J. 2014. Cellular vimentin regulates construction of dengue virus replication complexes through interaction with NS4A protein. *J Virol* 88: 1897-1913.

Thibaut H.J., Lacroix C., De Palma A.M., Franco D., Decramer M. & Neyts J. 2016. Toward antiviral therapy/prophylaxis for rhinovirus-induced exacerbations of chronic obstructive pulmonary disease: challenges, opportunities, and strategies. *Rev Med Virol* 26: 21-33.

Tompa P., Baki A., Schad E. & Friedrich P. 1996. The calpain cascade. Mu-calpain activates m-calpain. *J Biol Chem* 271: 33161-33164.

Tompa P., Buzder-Lantos P., Tantos A., Farkas A., Szilagyi A., Banoczi Z., Hudecz F. & Friedrich P. 2004. On the sequential determinants of calpain cleavage. *J Biol Chem* 279: 20775-20785.

Toyoda H., Nicklin M.J., Murray M.G., Anderson C.W., Dunn J.J., Studier F.W. & Wimmer E. 1986. A second virus-encoded proteinase involved in proteolytic processing of poliovirus polyprotein. *Cell* 45: 761-770.

Tsang S.K., McDermott B.M., Racaniello V.R. & Hogle J.M. 2001. Kinetic analysis of the effect of poliovirus receptor on viral uncoating: the receptor as a catalyst. *J Virol* 75: 4984-4989.

Tsou Y.L., Lin Y.W., Chang H.W., Lin H.Y., Shao H.Y., Yu S.L., Liu C.C., Chitra E., Sia C. & Chow Y.H. 2013. Heat shock protein 90: role in enterovirus 71 entry and assembly and potential target for therapy. *PLoS One* 8: e77133.

Turk B. 2006. Targeting proteases: successes, failures and future prospects. *Nat Rev Drug Discov* 5: 785-799.

Turk B., Turk D. & Turk V. 2012. Protease signalling: the cutting edge. *EMBO J* 31: 1630-1643.

Turkki P., Makkonen K.E., Huttunen M., Laakkonen J.P., Yla-Herttuala S., Airenne K.J. & Marjomaki V. 2013. Cell susceptibility to baculovirus transduction and echovirus infection is modified by protein kinase C phosphorylation and vimentin organization. *J Virol* 87: 9822-9835.

Tuthill T.J., Bubeck D., Rowlands D.J. & Hogle J.M. 2006. Characterization of early steps in the poliovirus infection process: receptor-decorated liposomes induce conversion of the virus to membrane-anchored entry-intermediate particles. *J Virol* 80: 172-180.

Upla P., Marjomaki V., Nissinen L., Nylund C., Waris M., Hyypia T. & Heino J. 2008. Calpain 1 and 2 are required for RNA replication of echovirus 1. *J Virol* 82: 1581-1590.

Urakawa T., Hamada N. & Shingu M. 1987. Isolation and antigenic characterization of dense particles of swine enteroviruses. *Kurume Med J* 34: 65-73.

van der Linden L., Wolthers K.C. & van Kuppeveld F.J. 2015. Replication and Inhibitors of Enteroviruses and Parechoviruses. *Viruses* 7: 4529-4562.

van Kuppeveld F.J., Hoenderop J.G., Smeets R.L., Willems P.H., Dijkman H.B., Galama J.M. & Melchers W.J. 1997. Coxsackievirus protein 2B modifies

endoplasmic reticulum membrane and plasma membrane permeability and facilitates virus release. *EMBO J* 16: 3519-3532.

van Ooij M.J., Vogt D.A., Paul A., Castro C., Kuijpers J., van Kuppeveld F.J., Cameron C.E., Wimmer E., Andino R. & Melchers W.J. 2006. Structural and functional characterization of the coxsackievirus B3 CRE(2C): role of CRE(2C) in negative- and positive-strand RNA synthesis. *J Gen Virol* 87: 103-113.

Verma N.A., Zheng X.T., Harris M.U., Cadichon S.B., Melin-Aldana H., Khetsuriani N., Oberste M.S. & Shulman S.T. 2009. Outbreak of life-threatening coxsackievirus B1 myocarditis in neonates. *Clin Infect Dis* 49: 759-763.

Versteeg H.H. & Ruf W. 2006. Emerging insights in tissue factor-dependent signaling events. *Semin Thromb Hemost* 32: 24-32.

Walker E.J., Younessi P., Fulcher A.J., McCuaig R., Thomas B.J., Bardin P.G., Jans D.A. & Ghildyal R. 2013. Rhinovirus 3C protease facilitates specific nucleoporin cleavage and mislocalisation of nuclear proteins in infected host cells. *PLoS One* 8: e71316.

Walter B.L., Nguyen J.H., Ehrenfeld E. & Semler B.L. 1999. Differential utilization of poly(rC) binding protein 2 in translation directed by picornavirus IRES elements. *RNA* 5: 1570-1585.

Walter T.S., Ren J., Tuthill T.J., Rowlands D.J., Stuart D.I. & Fry E.E. 2012. A plate-based high-throughput assay for virus stability and vaccine formulation. *J Virol Methods* 185: 166-170.

Wei W., Guo H., Chang J., Yu Y., Liu G., Zhang N., Willard S.H., Zheng S. & Yu X.F. 2016. ICAM-5/Telencephalin Is a Functional Entry Receptor for Enterovirus D68. *Cell Host Microbe* 20: 631-641.

Weng K.F., Li M.L., Hung C.T. & Shih S.R. 2009. Enterovirus 71 3C protease cleaves a novel target CstF-64 and inhibits cellular polyadenylation. *PLoS Pathog* 5: e1000593.

Wessels E., Duijsings D., Lanke K.H., van Dooren S.H., Jackson C.L., Melchers W.J. & van Kuppeveld F.J. 2006. Effects of picornavirus 3A Proteins on Protein Transport and GBF1-dependent COP-I recruitment. *J Virol* 80: 11852-11860.

Wessels E., Duijsings D., Niu T.K., Neumann S., Oorschot V.M., de Lange F., Lanke K.H., Klumperman J., Henke A., Jackson C.L., Melchers W.J. & van Kuppeveld F.J. 2006. A viral protein that blocks Arf1-mediated COP-I assembly by inhibiting the guanine nucleotide exchange factor GBF1. *Dev Cell* 11: 191-201.

White J.P., Cardenas A.M., Marissen W.E. & Lloyd R.E. 2007. Inhibition of cytoplasmic mRNA stress granule formation by a viral proteinase. *Cell Host Microbe* 2: 295-305.

Wiegers K.J., Yamaguchi-Koll U. & Drzeniek R. 1977. Differences in the physical properties of dense and standard poliovirus particles. *J Gen Virol* 34: 465-473.

Williams C.H., Kajander T., Hyypia T., Jackson T., Sheppard D. & Stanway G. 2004. Integrin alpha v beta 6 is an RGD-dependent receptor for coxsackievirus A9. *J Virol* 78: 6967-6973.

Wong J., Zhang J., Yanagawa B., Luo Z., Yang X., Chang J., McManus B. & Luo H. 2012. Cleavage of serum response factor mediated by enteroviral protease 2A contributes to impaired cardiac function. *Cell Res* 22: 360-371.

Xing L., Tjarnlund K., Lindqvist B., Kaplan G.G., Feigelstock D., Cheng R.H. & Casasnovas J.M. 2000. Distinct cellular receptor interactions in poliovirus and rhinoviruses. *EMBO J* 19: 1207-1216.

Xing L., Huhtala M., Pietiainen V., Kapyla J., Vuorinen K., Marjomaki V., Heino J., Johnson M.S., Hyypia T. & Cheng R.H. 2004. Structural and functional analysis of integrin alpha2I domain interaction with echovirus 1. *J Biol Chem* 279: 11632-11638.

Yalamanchili P., Datta U. & Dasgupta A. 1997. Inhibition of host cell transcription by poliovirus: cleavage of transcription factor CREB by poliovirus-encoded protease 3Cpro. *J Virol* 71: 1220-1226.

Yamaguchi-Koll U., Wiegers K.J. & Drzeniek R. 1975. Isolation and characterization of 'dense particles' from poliovirus-infected HeLa cells. *J Gen Virol* 26: 307-319.

Yamayoshi S., Fujii K. & Koike S. 2014. Receptors for enterovirus 71. *Emerg Microbes Infect* 3: e53.

Yamayoshi S., Ohka S., Fujii K. & Koike S. 2013. Functional comparison of SCARB2 and PSGL1 as receptors for enterovirus 71. *J Virol* 87: 3335-3347.

Yamayoshi S., Yamashita Y., Li J., Hanagata N., Minowa T., Takemura T. & Koike S. 2009. Scavenger receptor B2 is a cellular receptor for enterovirus 71. *Nat Med* 15: 798-801.

Yamayoshi S., Iizuka S., Yamashita T., Minagawa H., Mizuta K., Okamoto M., Nishimura H., Sanjoh K., Katsushima N., Itagaki T., Nagai Y., Fujii K. & Koike S. 2012. Human SCARB2-dependent infection by coxsackievirus A7, A14, and A16 and enterovirus 71. *J Virol* 86: 5686-5696.

Yarar D., Waterman-Storer C.M. & Schmid S.L. 2005. A dynamic actin cytoskeleton functions at multiple stages of clathrin-mediated endocytosis. *Mol Biol Cell* 16: 964-975.

Yoon M., Moir R.D., Prahlad V. & Goldman R.D. 1998. Motile properties of vimentin intermediate filament networks in living cells. *J Cell Biol* 143: 147-157.

Yoon S.Y., Ha Y.E., Choi J.E., Ahn J., Lee H., Kweon H.S., Lee J.Y. & Kim D.H. 2008. Coxsackievirus B4 uses autophagy for replication after calpain activation in rat primary neurons. *J Virol* 82: 11976-11978.

Yoshizawa T., Sorimachi H., Tomioka S., Ishiura S. & Suzuki K. 1995. A catalytic subunit of calpain possesses full proteolytic activity. *FEBS Lett* 358: 101-103.

Ypma-Wong M.F. & Semler B.L. 1987. In vitro molecular genetics as a tool for determining the differential cleavage specificities of the poliovirus 3C proteinase. *Nucleic Acids Res* 15: 2069-2088.

Ypma-Wong M.F., Dewalt P.G., Johnson V.H., Lamb J.G. & Semler B.L. 1988. Protein 3CD is the major poliovirus proteinase responsible for cleavage of the P1 capsid precursor. *Virology* 166: 265-270.

Zelenko Z., Gallagher E.J., Tobin-Hess A., Belardi V., Rostoker R., Blank J., Dina Y. & LeRoith D. 2017. Silencing vimentin expression decreases pulmonary metastases in a pre-diabetic mouse model of mammary tumor progression. *Oncogene* 36: 1394-1403.

Zhao X., Zhang G., Liu S., Chen X., Peng R., Dai L., Qu X., Li S., Song H., Gao Z., Yuan P., Liu Z., Li C., Shang Z., Li Y., Zhang M., Qi J., Wang H., Du N., Wu Y., Bi Y., Gao S., Shi Y., Yan J., Zhang Y., Xie Z., Wei W. & Gao G.F. 2019. Human Neonatal Fc Receptor Is the Cellular Uncoating Receptor for Enterovirus B. *Cell* 177: 155-1565.e16.

Zheng K., Xiang Y., Wang Q., Jin F., Chen M., Ma K., Ren Z. & Wang Y. 2014. Calcium-signal facilitates herpes simplex virus type 1 nuclear transport through slingshot 1 and calpain-1 activation. *Virus Res* 188: 32-37.

ORIGINAL PAPERS

I

A NOVEL OPEN AND INFECTIOUS FORM OF ECHOVIRUS 1

by

Mira Myllynen, Artur Kazmertsuk & Varpu Marjomäki
2016

Journal of Virology 90: 6759-6770.
(Chosen for spotlight in the Journal of Virology 23.5.2016)

AMERICAN SOCIETY FOR MICROBIOLOGY | Journal of Virology

A Novel Open and Infectious Form of Echovirus 1

Mira Myllynen, Artur Kazmertsuk, Varpu Marjomäki

Department of Biological and Environmental Science, Nanoscience Center, University of Jyväskylä, Jyväskylä, Finland

ABSTRACT

One of the hallmarks of enterovirus genome delivery is the formation of an uncoating intermediate particle. Based on previous studies of mostly heated picornavirus particles, intermediate particles were shown to have externalized the innermost capsid protein (VP4) and exposed the N terminus of VP1 and to have reduced infectivity. Here, in addition to the native and intact particle type, we have identified another type of infectious echovirus 1 (E1) particle population during infection. Our results show that E1 is slightly altered during entry, which leads to the broadening of the major virion peak in the sucrose gradient. In contrast, CsCl gradient separation revealed that in addition to the light intact and empty particles, a dense particle peak appeared during infection in cells. When the broad peak from the sucrose gradient was subjected to a CsCl gradient, it revealed light and dense particles, further suggesting that the shoulder represents the dense particle. The dense particle was permeable to SYBR green II, it still contained most of its VP4, and it was able to bind to its receptor $\alpha_2\beta_1$ integrin and showed high infectivity. A thermal assay further showed that the $\alpha_2\beta_1$ integrin binding domain (I-domain) stabilized the virus particle. Finally, heating E1 particles to superphysiological temperatures produced more fragile particles with aberrant ultrastructural appearances, suggesting that they are distinct from the dense E1 particles. These results describe a more open and highly infectious E1 particle that is naturally produced during infection and may represent a novel form of an uncoating intermediate.

IMPORTANCE

In this paper, we have characterized a possible uncoating intermediate particle of E1 that is produced in cells during infection. Before releasing their genome into the host cytosol, enteroviruses go through structural changes in their capsid, forming an uncoating intermediate particle. It was shown previously that structural changes can be induced by receptor interactions and, in addition, by heating the native virion to superphysiological temperatures. Here, we demonstrate that an altered, still infectious E1 particle is found during infection. This particle has a more open structure, and it cannot be formed by heating. It still contains the VP4 protein and is able to bind to its receptor and cause infection. Moreover, we show that in contrast to some other enteroviruses, the receptor-virion interaction has a stabilizing effect on E1. This paper highlights the differences between enterovirus species and further increases our understanding of various uncoating forms of enteroviruses.

Picornaviruses are a large family of pathogens infecting humans and animals across the globe. The vast disease range caused by these viruses spans from simple rashes to paralysis and meningitis. It has been estimated that approximately half of the seasonal common-cold cases reported are caused by rhinoviruses, members of the family subgroup *Enterovirus* (1). Increased emphasis on enterovirus research is caused by the evidence associating type I diabetes, asthma, and myocarditis with members of the enterovirus genus (2–4).

Echovirus 1 (E1), a member of the enterovirus B group, shares the structural characteristics of all picornaviruses: a positive-sense single-stranded RNA genome of ~7,500 nucleotides with a nonenveloped capsid of roughly 30 nm in size that is comprised of four noncovalently interacting viral proteins (VP1, VP2, VP3, and VP4). During the course of picornavirus entry and uncoating, a common sequence of events has been suggested based on poliovirus and rhinovirus studies: the initial receptor-virion interaction on the cell surface begins the conversion of the native virion to an A-particle (altered particle; also termed a 135S particle due to its sediment coefficient in sucrose) (5, 6). Compared to the native virion, the 135S particle has its VP1 N-terminal segment externalized and has lost its inner capsid protein VP4. Both of these changes are thought to be linked with the membrane-virion interaction and possible pore formation by myristylated VP4 (7–9). The altered particles still hold the genome inside the capsid shell, but recent evidence regarding rhinovirus and coxsackievirus B3 (CVB3) indicates that the RNA-capsid interaction is altered (10, 11). Additionally, an opening forms at the 2-fold axis of the 135S particle, which facilitates the genome's egress from the capsid (12–17). The generation of genome-free, empty (80S) particles occurs only after internalization to an endosome compartment, where the final step(s) of picornavirus uncoating is supposed to take place.

In addition to the native (160S), altered (135S), and empty (80S) particle types described above, poliovirus, coxsackievirus B5, swine vesicular disease virus, and bovine enterovirus were shown to band as two separate particle populations in CsCl. In general, the reported buoyant density profiles vary between 1.34 and 1.47 g cm^{-3}, where the major, intact component is usually found to be less dense than the minor component (18, 19, 20). The reported properties of the dense particles, with respect to the native 160S virion, indicate a similar RNA-to-protein ratio but in-

Received 23 February 2016 **Accepted** 26 April 2016

Accepted manuscript posted online 18 May 2016

Citation Myllynen M, Kazmertsuk A, Marjomäki V. 2016. A novel open and infectious form of echovirus 1. J Virol 90:6759–6770. doi:10.1128/JVI.00342-16.

Editor: S. López, Instituto de Biotecnologia/UNAM

Address correspondence to Varpu Marjomäki, varpu.s.marjomaki@jyu.fi.

creased permeability, often reduced infectivity, and increased RNase and protease sensitivity (19, 21, 22). The origin of dense picornavirus particles has been attributed to increased RNA-cesium interactions due to increased permeability to Cs^+ ions (19). While there are clear structural differences between the native particles and A-particles, the relationship between dense particles and A-particles is rarely discussed.

We have shown that E1 induces a macropinocytic entry pathway that has no connections to the conventional acidic clathrin pathway (23–26). E1 accumulates, together with its receptor $\alpha_2\beta_1$ integrin, in nonacidic multivesicular structures that do not label for endosomal proteins found in classical endosomes (25, 27). Interestingly, members of the same enterovirus group B viruses, such as coxsackievirus A9 (CVA9) (28, 29), CVB3, and coxsackievirus B1 (M. Martikainen, A. S. Khojine, H. Hyöty, and V. Marjomäki, unpublished data), show remarkably similar entry characteristics (30). The present data concerning E1 and CVA9 suggest that, in contrast to poliovirus and rhinovirus, binding to their cell surface receptors, $\alpha_2\beta_1$ and $\alpha_v\beta_3$ integrins, respectively, stabilizes the viruses and that uncoating starts only later, gradually after 30 min postinfection (p.i.) in endosomes (15, 23, 28, 31, 32). It therefore seems that the enterovirus group B viruses have similarities in terms of uncoating and genome release from the endosomes and that these aspects may differ from those of poliovirus and rhinovirus.

In this study, we show that E1 does not show a typical transition into a 135S particle during infection but instead goes through smaller structural alterations that cause only small changes in the sedimentation profile in the sucrose gradient. Additionally, we report the densities of E1 particles in the CsCl gradient and identify a previously undescribed dense E1 particle. This dense particle is formed during infection, and it corresponds to the appearance of a shoulder next to intact E1 particles in the sucrose gradient and thus may represent an uncoating intermediate. The dense particle is highly infectious, permeable to small molecules like SYBR green II (SGII), VP4 positive, and capable of receptor interaction. Finally, we show that heating E1 to superphysiological temperatures causes the formation of more fragile, structurally aberrant particles that are distinct from the naturally formed dense particles that are produced in cells during infection.

MATERIALS AND METHODS

Cells, antibodies, and reagents. Cell experiments were carried out with green monkey kidney (GMK) cells, which were obtained from the American Type Culture Collection (ATCC). The following antibodies were used in the experiments: rabbit polyclonal antibody against E1 (23) and secondary goat anti-rabbit antibody conjugated with Alexa Fluor 555 (Molecular Probes, Invitrogen USA).

The glutathione *S*-transferase (GST)–I-domain fusion was a kind gift from Jyrki Heino (University of Turku). Polyethylene glycol 6000, sodium deoxycholate, and a Nonidet P-40 substitute were obtained from Sigma-Aldrich. Eagle's minimum essential medium (MEM), fetal bovine serum (FBS), GlutaMAX, and penicillin-streptomycin antibiotics were obtained from Gibco, Life Technologies.

Virus preparations. Monolayers of GMK cells were infected with E1 (Farouk strain; ATCC) (multiplicity of infection [MOI] of 0.1) for 24 h in 5-layer bottles, after which the cells were collected and lysed via three freeze-thaw cycles. Cell debris was pelleted by centrifugation with a JA-10 rotor (6,080 rpm for 30 min), after which the protein obtained from the supernatant was precipitated by adding polyethylene glycol 6000 (final concentration, 8% [wt/vol]) and NaCl (2.2% [wt/vol]). After overnight precipitation at +4°C, the precipitated material was centrifuged with a JA-10 rotor (8,000 rpm for 45 min), and the pellet was dissolved into R buffer (10 mM Tris-HCl [pH 7.5], 200 mM NaCl, 50 mM $MgCl_2$, 10% [wt/vol] glycerol). To disrupt membranous structures, 0.3% (wt/vol) sodium deoxycholate and 0.6% (vol/vol) Nonidet P-40 substitute were added to the suspension, and the mixture was incubated for 30 min on ice. Membrane debris was pelleted via centrifugation with a TX-200 rotor (4,000 × *g* for 15 min), and the supernatant was divided on top of two 10-ml linear 10 to 40% (wt/vol) sucrose gradients made in R buffer. The gradients were ultracentrifuged with an SW-41 rotor (30,000 rpm for 3 h) and fractioned into 500-μl aliquots from the top. The optical density at 260 nm was measured with a NanoDrop 1000 spectrophotometer (Thermo Scientific) to identify virus-containing fractions, and subsequently, three fractions from each gradient were collected for isopycnic centrifugation in 24% CsCl gradients (10 ml) made in TNE buffer (50 mM Tris [pH 7.5], 100 mM NaCl, 1 mM EDTA). The gradients were ultracentrifuged with an SW-41 rotor (30,000 rpm for 24 h) and fractioned into 500-μl aliquots from the top, and the optical density at 260 nm was measured with a NanoDrop 1000 spectrophotometer (Thermo Scientific) to identify virus-containing fractions.

Before further studies, the virus-containing light and dense fractions were dialyzed separately with a Spectra/Por Micro Float-A-Lyzer instrument with Biotech cellulose ester membranes (Spectrum Laboratories Inc., USA). A dialysis column with a 300-kDa-molecular-mass cutoff was prepared according to the instructions provided by the manufacturer, after which the viruses were dialyzed against 2 mM $MgCl_2$–phosphate-buffered saline (PBS). The buffer was changed after 2 and 4 h, after which the sample was dialyzed overnight. Viruses were concentrated via ultracentrifugation with a 70Ti rotor (35,000 rpm for 2 h), and the pellets were dissolved into 2 mM $MgCl_2$–PBS.

In the case of double-CsCl-gradient purification (Fig. 1Aii), the first purification steps were carried out as described above, and the first round of CsCl purification was carried out after pelleting the membranous debris. Before the second CsCl gradient centrifugation, the collected virus fractions were dialyzed with a Spectra/Por Micro Float-A-Lyzer with Biotech cellulose ester membranes (Spectrum Laboratories Inc., USA). The protein content was estimated from the optical density at 260 nm, as described above.

The radioactive virus was produced in monolayers of GMK cells, which were washed with PBS for 15 min at +37°C and infected with E1 (Farouk strain; ATCC) diluted in low-methionine-cysteine medium supplemented with 1% FBS. After 3 h of infection, 50 μCi ml^{-1} of [^{35}S]methionine-cysteine diluted in low-methionine-cysteine medium supplemented with 1% FBS was added. Infection was allowed to proceed for 24 h at +37°C, after which the cells were collected and lysed via freeze-thaw cycles. The cell debris was pelleted via centrifugation with a TX-200 rotor (3,000 × *g* for 15 min), and the supernatant was collected and incubated with 0.3% (wt/vol) sodium deoxycholate and 0.6% (vol/vol) Nonidet P-40 substitute for 30 min on ice. The membrane structures were pelleted via centrifugation with a TX-200 rotor (4,000 × *g* for 15 min), after which the supernatant was added on top of 40% sucrose cushions (2 ml). The cushions were ultracentrifuged with an SW-41 rotor at 30,000 rpm for 2.5 h, after which the liquid above the cushion and one 500-μl fraction were discarded, while the next three 500-μl fractions were collected. The virus-containing fractions were then ultracentrifuged with an SW-41 rotor (30,000 rpm for 24 h) in 24% CsCl gradients (10 ml) made in TNE buffer. The gradients were fractioned into 500-μl aliquots from the top, and the virus-containing fractions were identified via liquid scintillation counting (PerkinElmer).

Light radioactive E1 was added to cells and bound on ice for 1 h. Infection was allowed to proceed at +37°C for the indicated amount of time (0, 30, 120, or 180 min). The cells were lysed by adding 100 mM octyl-β-D-glucopyranoside (Amresco) on ice, and after 30 min of incubation, the virus-containing cell lysate was collected, added either on top of a 10-ml linear 5 to 20% sucrose gradient in R buffer (35,000 rpm for 2 h) or in a 10-ml gradient of 24% CsCl in TNE buffer (30,000 rpm for 24 h),

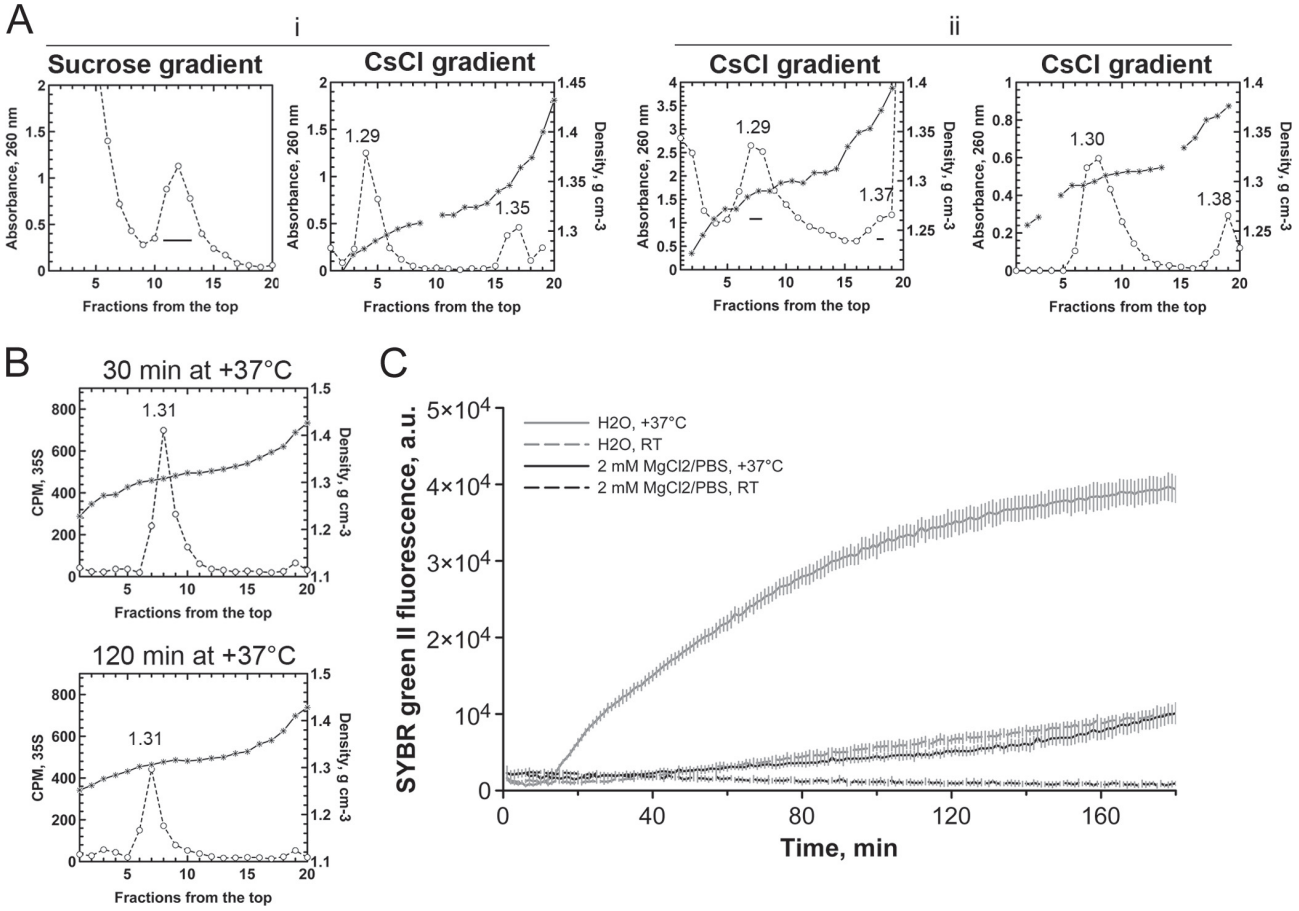

FIG 1 Detection of dense particles in CsCl gradients. (A) Gradient profiles of E1 purified with either a 10 to 40% sucrose-to-CsCl or CsCl-to-CsCl combination. (i) Fractions 11, 12, and 13 (indicated by a line) were collected from the sucrose gradient, mixed, and subjected to the CsCl gradient. (ii) Fractions 7, 8, and 18 (indicated by lines) were collected from the CsCl gradient, mixed, and subjected to a second CsCl gradient. (B) CsCl gradient profile of the *in vitro* conversion of native, light E1 into dense particles after 30 min or 120 min of incubation at +37°C. (C) Real-time measurement of SYBR green II fluorescence at +37°C or RT over 180 min in the presence of light E1 in water or storage buffer (2 mM $MgCl_2$–PBS). The fluorescence of the dye is enhanced when bound to RNA, which enables the determination of virus stability upon heating. The results are averages from three replicates (± standard errors of the means). a.u., arbitrary units.

and ultracentrifuged with an SW-41 rotor. The gradients were fractioned into 500-μl aliquots from the top, and the virus-containing fractions were identified via liquid scintillation counting (PerkinElmer).

For heat treatment of the radioactive virus at +50°C, radioactively labeled E1 was produced as described above and purified via a 40% sucrose cushion, followed by concentration with a 70Ti rotor, as described above. E1 was heated at +50°C for 0 min or 5 min and ultracentrifuged with an SW-41 rotor in either a 10-ml linear 5 to 20% sucrose gradient (35,000 rpm for 2 h) or a 24% CsCl gradient (30,000 rpm for 24 h). The gradients were fractioned into 500 aliquots from the top, and the counts per minute of each fraction were measured via liquid scintillation counting (PerkinElmer).

Cytopathic effect assay. The cytopathic effect (CPE) assay was carried out as previously described (33). The CPE assay was carried out in confluent monolayers of GMK cells. Cells were cultivated in MEM supplemented with 10% FBS, 1% GlutaMAX, and 1% penicillin-streptomycin antibiotics on a 96-well microtiter plate for 1 day, after which the cells were infected with light or dense viruses, which were diluted into MEM supplemented with 1% FBS and 1% GlutaMAX. Three protein amounts were used to infect the cells, 10 ng, 1 ng, and 0.1 ng, and additionally, a control cell, without virus, was included. Each sample included four replicates. After 24 h of infection at +37°C, the infected cells were washed extensively with PBS, and the noninfected cell monolayers were stained with a solution containing crystal violet. Excess stain was washed extensively with sterile water, after which the cell monolayers were treated with 100 μl of lysis buffer to elute the crystal violet. Finally, the absorbance of the crystal violet stain was measured at 570 nm with a Victor X4 2030 multilabel reader (PerkinElmer).

In the I-domain inhibition experiment, 10 ng of virus (light or dense) was incubated with different amounts of I-domain (10 ng, 100 ng, 500 ng, or 1,000 ng) for 1 h at +37°C. Confluent monolayers of the GMK cells were infected with a virus–I-domain mix by binding the virus on ice first for 1 h. The excess virus was washed extensively with PBS containing 0.5% bovine serum albumin, after which infection was allowed to proceed in 1% MEM for 24 h at +37°C. Crystal violet staining and absorbance measurements were carried out as described above.

Endpoint dilution assay. The endpoint dilution assay was carried out in monolayers of GMK cells cultured in 96-well microtiter plates for 1 day in MEM supplemented with 10% FBS, 1% GlutaMAX, and 1% penicillin-streptomycin antibiotics. Infection was carried out in cell monolayers with 30% confluence. Cell monolayers were infected with light or dense virus by preparing a dilution series in MEM supplemented with 1% FBS and 1% GlutaMAX, and infection was monitored daily. After 3 days of infection at +37°C, the medium was removed, and the cell monolayers

were stained with 50 μl of crystal violet stain (8.3 mM crystal violet, 45 mM $CaCl_2$, 10% ethanol, 18.5% formalin, and 35 mM Tris base) for 10 min. The excess crystal violet stain was washed extensively with water, after which the infectivity was determined by calculating the number of dyed (noninfected) and nondyed (infected) wells. The 50% tissue culture infective dose ($TCID_{50}$) was calculated by comparing the numbers of infected and uninfected wells for eight replicates of the same virus concentration. The concentration at which half of the wells would be infected was extrapolated ($TCID_{50}$). Finally, the $TCID_{50}$ values of the light and dense viruses were normalized to the respective protein amounts, as determined by measurement of the A_{260}.

Immunolabeling and microscopy. An immunolabeling experiment was carried out in subconfluent monolayers of GMK cells, which were plated onto coverslips 1 day previously. Monolayers of cells were infected with light or dense virus, and a negative control, without any virus, was also included to remove the antibody-induced background signal during imaging.

Cells were infected with three protein amounts, 250 ng, 75 ng, and 23 ng, by diluting the viruses into MEM supplemented with 1% FBS and 1% GlutaMAX. The viruses were bound on cells for 1 h on ice, after which the excess virus was washed extensively with PBS containing 0.5% bovine serum albumin. The cells were incubated in MEM supplemented with 10% FBS, 1% GlutaMAX, and 1% penicillin-streptomycin antibiotics at +37°C for 6 h, after which the cells were fixed with 4% paraformaldehyde for 30 min at room temperature (RT). Before labeling, the cells were permeabilized with 0.2% Triton X-100 for 5 min. Primary rabbit antibody against E1 was added to cells, and the mixture was incubated at RT for 45 min, after which the cells were washed extensively with PBS. Secondary goat anti-rabbit antibody conjugated with Alexa Fluor 555 (Molecular Probes, Invitrogen USA) was added to cells at RT and incubated for 30 min. Finally, the cells were extensively washed with PBS and mounted with Prolong gold antifade reagent supplemented with 4′,6-diamidino-2-phenylindole (DAPI) (Molecular Probes, Life Technologies).

Immunolabeled samples were imaged with an Olympus IX81 microscope with a FluoView-1000 confocal setup. In total, ~300 cells per sample were checked for infection. The nuclei were counted with a segmentation tool embedded in Bioimage XD software, after which infected cells were counted by hand. The number of infected cells was then compared to the total number of cells to obtain the infection percentage.

Electron microscopy. Butwar-coated copper grids were made hydrophilic via glow discharging with an EMS/SC7620 Mini sputter coater according to the instructions provided by the manufacturer. The virus sample was added to the grid and incubated for 15 s, after which the excess virus was blotted with Whatman 3-mm paper. The viruses were negatively stained by adding 1% phosphotungstic acid (in water) (pH 7.4) to the grid for 1 min, after which the excess stain was blotted with Whatman 3-mm paper. Heat-treated E1 was incubated at 50°C for 5 min before it was added to the grid.

For the I-domain experiment, 1 μg of light or dense virus was incubated with or without 1 μg of I-domain at 37°C for 1 h before it was added to the grid. The samples were dried overnight and imaged with a JEM-1400 (JEOL) transmission electron microscope.

Gel electrophoresis. The protein compositions of the ^{35}S-labeled light and dense viruses were analyzed by using a 4 to 12% NuPAGE Bis-Tris gel (Novex, Life Technologies). The proteins were denatured with the gel sample buffer provided by the manufacturer (NuPAGE; Life Technologies) at 100°C before they were loaded onto the gel. The gel was fixed with 40% methanol and 10% acetic acid for 15 min. The fixative was washed with water, after which the gel was treated with an autoradiography enhancer (Enlightning; PerkinElmer) for 15 min. Excess enhancer was washed with water, and the gel was dried at +70°C for 2 h (Gel dryer 583; Bio-Rad), after which the gel was subjected to autoradiography. The quantification of the band intensities was performed with the Image J gel analysis tool.

Thermal stability assays. The thermal stabilities of the light and dense viruses were assayed by using methods described previously by Walter et al. (34). The fluorescence signal was recorded by using a Bio-Rad C1000 thermal cycler, and the final sample mixture contained 1 μg of light or dense E1 and a 10× concentration of SYBR green II (Invitrogen). All samples were equilibrated at 20°C for 10 min before the thermal stability measurements were begun. For the full temperature range scan, the fluorescence signal was recorded at 10-s intervals and 0.5°C increments. Finally, the sample was cooled back to 20°C, at which point the fluorescence reading was recorded again.

In the I-domain assay, the sample mixture contained 100, 500, or 1,000 ng of I-domain; 1 μg of light E1; and a 10× concentration of SYBR green II (Invitrogen). The measurement was carried out as described above.

The real-time measurement of E1 stability at +37°C was carried out by using a Victor X4 2030 multilabel reader (PerkinElmer) with 485-nm and 535-nm excitation and emission filters, respectively. The sample mixture contained a 10× concentration of SYBR green II (Invitrogen) and 1 μg of light E1 in either deionized water or 2 mM $MgCl_2$–PBS. The fluorescence signal was recorded at 1-min intervals, for 180 min in total.

RNase protection assay. Light or dense E1 was incubated with RNase A (final concentration, 25 μg ml^{-1}) for 30 min at RT before the addition of the virus to cells. Infectivity was determined with an endpoint dilution assay, and the $TCID_{50}$ per milliliter was calculated based on eight replicates, as described above. Finally, the $TCID_{50}$ per milliliter was normalized to the A_{260} values of the viruses.

RESULTS

Detection of a dense particle in a CsCl gradient. In order to produce highly purified echovirus 1 for detailed spectroscopic and biochemical studies, we set out to use a combination approach, using both sucrose and CsCl gradients (Fig. 1A). A 10 to 40% sucrose gradient produced a concentrated sample of E1, which was then subjected to a CsCl gradient (Fig. 1Ai). To our surprise, the CsCl gradient repeatedly showed two bands, a light-density fraction on the top part of the gradient and a well-separated dense fraction in the bottom of the gradient. In CsCl, the light E1 population had an apparent buoyant density of 1.29 g cm^{-3}, while the dense particle banded at 1.35 to 1.38 g cm^{-3} (Fig. 1Ai and ii). The purification of the virus in the CsCl gradient, without the previous sucrose gradient step, also produced the same light and dense fractions (Fig. 1Aii). If the light and dense fractions were collected from the gradient, mixed again, and subjected to a second CsCl gradient separation, this reproduced the same separation of the light and dense fractions (now without very light impurities). These results thus suggest that these two density fractions are found in the CsCl gradient independent of whether the first separation was performed on a sucrose or CsCl gradient. It also further showed that CsCl separation does not progressively produce more of the dense fraction during separation, because the two consecutive gradients produced roughly similar ratios of light and dense fractions. In order to rule out the possibility of a contaminating picornavirus in our stock, we also performed similar CsCl banding experiments using the infectious cDNA clone of E1 and observed that both the top and the bottom components were similar to our stock virus (data not shown).

To rule out the effect of temperature on dense-particle formation, the light fraction was incubated at +37°C for 30 min or 120 min before CsCl gradient fractionation (Fig. 1B). The results showed a remarkable stability of the light particles and clearly showed that the physiological temperature did not alone induce dense-particle formation. In addition, a real-time measurement of

particle opening at +37°C based on the fluorescence of RNA binding SYBR green II dye showed that the virus capsid was stable at +37°C in storage buffer (2 mM $MgCl_2$–PBS), in contrast to the virus incubated in water, which showed opening of the virus for SYBR green II binding already after 15 min at +37°C (Fig. 1C). The virus incubated for 180 min at +37°C in buffer was also shown to be infectious (data not shown).

Formation of the E1 dense particle during infection. In order to understand when the dense E1 particle appears during virus infection in cells, a radioactive virus was produced, and cell homogenates were fractioned by CsCl ultracentrifugation at various time points postinfection (Fig. 2A). First, the light top fractions were collected from the CsCl gradient in order to use only the intact form of the virus as an input for the cell experiments. This light fraction was added to cells, and the distribution of the virus was monitored after fractionation (Fig. 2D). CsCl gradient separation showed that the dense particle had already appeared at 30 min p.i., and the population was apparent at later time points as well (Fig. 2A). After 180 min, the proportional amount of the dense fraction had already decreased, probably due to some particle disruption already at this time point. In order to compare more quantitatively the virus particles found inside and outside cells, quantification of the different particles (empty, light, and dense) in a CsCl gradient was performed for the virus gained after incubating the light fraction on cells for 2 h or adding the light fraction straight into the gradient (Fig. 2B). This measurement showed that inside the cells, more than half of the virus particles were of the dense form, while outside cells, over 80% of the virus particles stayed intact. Even if some dense particles may develop spontaneously, these result support the idea that dense-particle formation is not an artifact caused by centrifugation but, instead, is induced in cells.

Since different forms of enteroviruses are often separated by using a sucrose gradient, we also carried out the same infection time series using a 5 to 20% sucrose gradient for separation (Fig. 2C). The light input fraction from the CsCl purification showed a typical peak in fractions 14 to 17 from the top of the sucrose gradient. At 30 min p.i., the peak generated a shoulder or a widened peak, which still became more evident after 120 and 180 min (Fig. 2C). Thus, in the case of E1, a typical transition of the native peak (160S) to the 135S position was not detected in the sucrose gradient over time, but instead, the native peak became broader, as was observed in our previous studies (23). The time course generation of the denser particle in CsCl correlated with the broadening of the native peak in the sucrose gradient, suggesting that the dense virion was inside this broad peak (Fig. 2A and C). When the broad peak (fractions 12 to 16) was collected from the sucrose gradient and subjected to a CsCl gradient (Fig. 2E), both intact (light) particles and dense particles were detected, further confirming that the shoulder in the sucrose gradient corresponded to the dense particle in the CsCl gradient. In repetitions of this approach, the amount of the left-hand shoulder in the sucrose gradient was positively correlated with the amount of the dense peak of the CsCl gradient produced in relation to the light peak. Based on all these data, E1 is marginally altered from the intact virion upon entry, which can be observed by the appearance of a shoulder in the 5 to 20% sucrose gradient and a distinct high-density particle in the CsCl gradient. This may represent the formation of an E1 uncoating intermediate, which is different from many other enteroviruses.

The dense particle is porous and still contains VP4. To further investigate the structural properties of the dense E1 particle, we performed a thermal stability assay using SYBR green II (SGII) as a reporter (34). The sensitivity of SGII for detecting RNA can be attributed to several factors, including superior fluorescence quantum yield, binding affinity, and fluorescence enhancement when bound to RNA. In a thermal assay, SGII is typically added to the virus sample at room temperature. By increasing the temperature by 0.5°C at 10-s intervals, this assay produces a curve from which the melting temperature (T_m) can be deduced (34). The native light virion showed a T_m of 53°C, while the dense particle was already permeable to SGII at room temperature, leading to high starting values. Thus, measurements of the melting temperature of the dense E1 particle were impossible to perform due to the apparent initial permeability of the capsid to SGII (Fig. 3A). The initial versus final fluorescence measurements (Fig. 3A) confirmed that the genomic material was already fully accessible to SGII in the case of the dense E1 particle, while the native virion denied SGII entry initially. This also explained the density of the dense virion and confirmed previous suggestions regarding the formation of dense particles (19): if the dense particle penetrates SGII, it is permeable to Cs ions as well, leading to the density increase seen in the CsCl gradient.

Because the dense particle of E1 was observed to be porous and previous studies suggested that the dense particles were sensitive to RNase A, we also carried out an assay to evaluate the sensitivity of dense and light particles to RNase A (Fig. 3B). The particles were incubated with the enzyme for 30 min at RT before the addition of the virus to the cells. Infectivities were determined with an endpoint dilution assay, which showed that neither the light nor the dense particles were prone to RNase A-mediated digestions. The RNase A-treated fractions were as infectious as the untreated fractions (Fig. 3B).

We next performed an SDS-PAGE analysis on the protein compositions of both the native and the dense E1 particles in order to determine whether VP4 was present in the virus capsids. Radioactive labeling (^{35}S) indeed showed a significant VP4 signal for the dense E1 particle (Fig. 3C). The amount of VP4 was also quantified by measuring the intensities of the bands via Image J. Quantification revealed that the shares of VP4, based on the intensities of all the capsid proteins VP1 to VP4, were 4.5% and 4.3% for the light and dense virions, respectively. The results corresponded well to the theoretical values calculated based on the sequence of E1. Theoretically, the share of methionines and cysteines in VP4 was 4.3% of the total amount of methionines and cysteines in the sequences of the capsid proteins.

Heat-treated virus particles are distinct from the dense particles detected in cells. The uncoating intermediates of picornaviruses for structural studies are commonly produced by heating the native virion at elevated temperatures for several minutes (12, 13, 16, 35, 36). In the case of poliovirus, the cell-derived uncoating intermediates and heat-converted uncoating intermediates were suggested to be indistinguishable from one another (37). E1 virions heated to 50°C for 5 min (in PBS supplemented with 2 mM $MgCl_2$) produced a wide peak in the sucrose gradient compared to the nonheated virions (Fig. 4Ai). However, the shift in the heated virions was different from what was observed when the native virion was incubated on cells (Fig. 2C and E). In addition, when the heat-treated virions were separated by using CsCl, the native virion band at 1.31 g cm^{-3} almost totally disappeared (Fig. 4Aii),

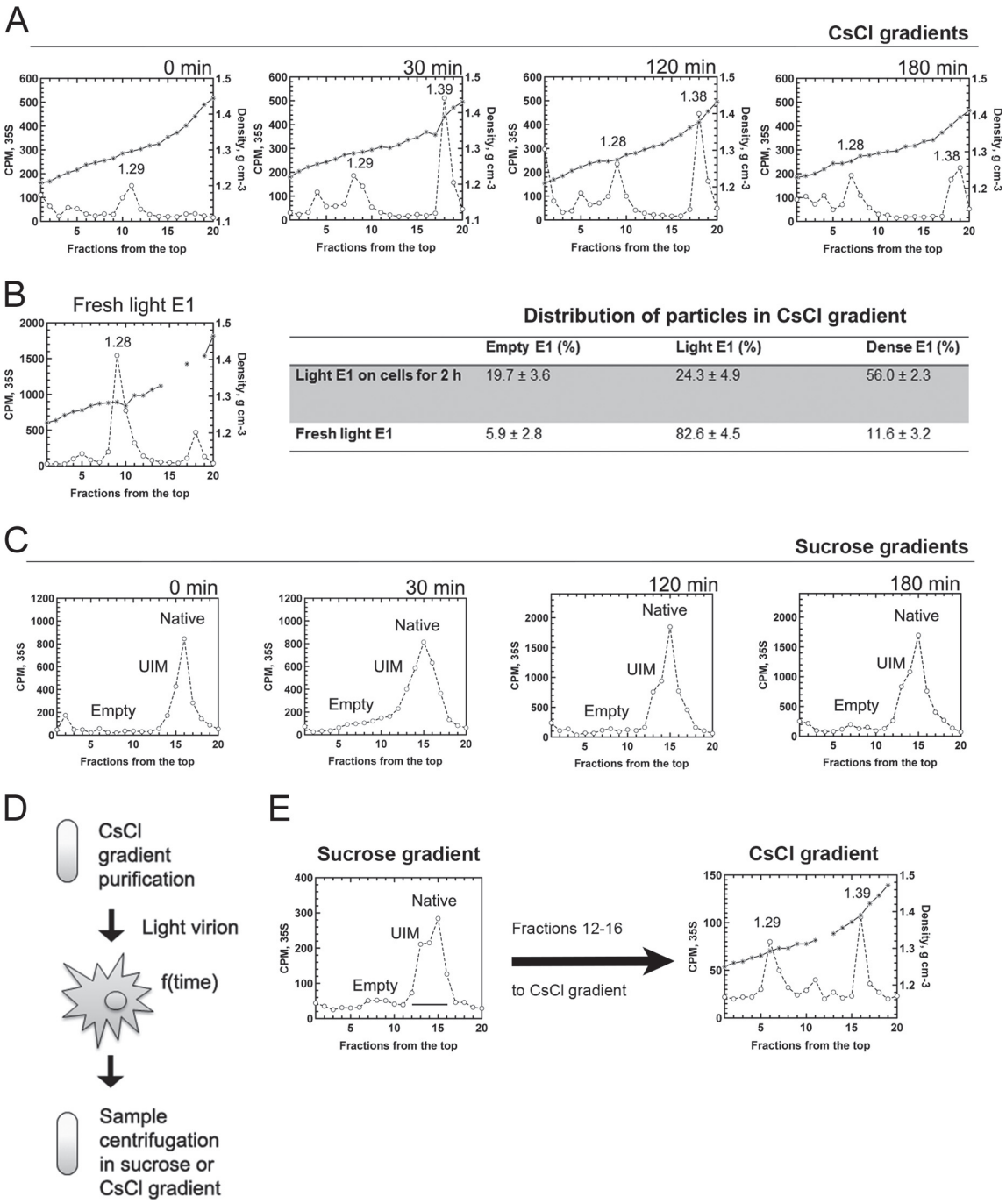

FIG 2 Dense-particle formation in cells during infection. (A) Gradient profiles of the *in vivo* conversion of native E1 (light particle, 1.28 to 1.29 g cm^{-3}) into dense particles (1.38 to 1.39 g cm^{-3}) in CsCl after 0, 30, 120, or 180 min postinfection. (B) Distribution of empty, light, and dense particles in CsCl gradients after incubation of light E1 on cells for 2 h or the addition of light E1 straight into the gradient. The results are averages from four replicates (± standard errors of the means). (C) Gradient profiles of the *in vivo* conversion of native E1 into uncoating intermediate particles (UIM) in a 5 to 20% sucrose gradient after 0, 30, 120, or 180 min postinfection. (D) Schematic image of the *in vivo* experiment in which the light fraction of CsCl-purified [^{35}S]methionine-cysteine-labeled E1 was collected and incubated on cells for the indicated amounts of time. Next, the collected cell homogenate was centrifuged in either a sucrose or a CsCl gradient. (E) After incubation on cells for 120 min, the cell homogenate was collected and centrifuged in a 5 to 20% sucrose gradient. Fractions 12 to 16 (indicated by a line) were collected from the sucrose gradient and subjected to a CsCl gradient.

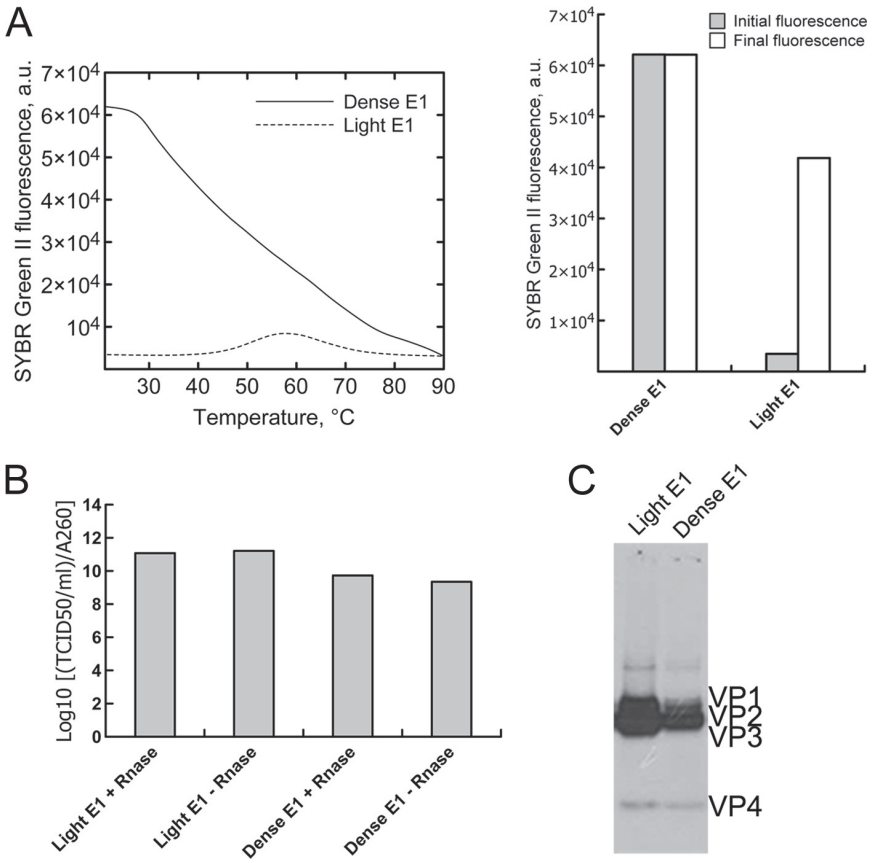

FIG 3 Capsid permeabilization and protein contents of light and dense E1 particles. (A) Thermal stability assay of dense E1 and light E1. The bar chart represents the initial and final absolute fluorescence values from thermal assay measurements. The final fluorescence value was measured after recooling of the sample back to 20°C. (B) Infectivity of light and dense E1 particles with or without RNase A treatment was determined with an endpoint dilution assay. The results are based on data from eight replicates for each sample. (C) ^{35}S-tagged dense and light E1 particles isolated from a CsCl gradient, separated via SDS-PAGE, and detected via autoradiography.

while the dense-particle band at 1.38 to 1.41 g cm^{-3} did not show any apparent increase in signal, indicating that heat conversion did not convert the native virions to the dense E1 particle. Additionally, a small band appeared at 1.22 g cm^{-3}, probably representing the empty virus particles. The absence of the main virion band signal can be explained by the repeated observation of a transparent "smudge" on the tube walls after the gradients had been fractioned, probably representing broken and aggregated virus particles (data not shown). Transmission electron microscopy (TEM) imaging showed that the native virion and the dense particles that naturally occur during E1 infection (Fig. 4B) share the morphology of an intact enterovirus. However, the heat-converted virions often showed an additional protrusion in the vicinity of the capsid (Fig. 4B), unlike the native and the dense E1 particles, further indicating structural differences between the heat-converted and dense E1 particles. It seems probable that the protrusion-showing particles were more open and more easily attracted to aggregations in the subsequent CsCl gradient. The quantification of the presence of protrusions in the heated particles showed that ~50% of the calculated 104 virus particles showed protrusions. Together, these results suggest that the naturally occurring dense particle cannot be formed by heating the virus to superphysiological temperatures, which also indicates that this type of heat treatment cannot be used to reliably monitor the uncoating of E1.

The dense particle is still highly infectious. The infectivity of the poliovirus 135S particle, as well as the altered particle of CVB3, was reported to be greatly reduced in cell cultures compared to the native virion (11, 37). Here, we investigated the dense particle in terms of its capacity to infect GMK cells within (i) a short time scale (Fig. 5A), (ii) an intermediate time scale (Fig. 5B), and (iii) a long time scale (Fig. 5C). All of the infectivity measurements were correlated by using comparable amounts of protein. In Fig. 5A, an antibody-based measurement of E1 infectivity (see Materials and Methods) was used to calculate the number of virus proteins produced in cells at 6 h postinfection. The titration of both the light and dense E1 particles showed a clear response to the decrease in the virus load used, indicating good sensitivity for this method. To evaluate infectivity over a long period of time (3 to 4 days), we determined the $TCID_{50}$ per milliliter for both light and dense E1 particles. Similarly to the antibody method, both light and dense E1 particles were capable of producing comparable levels of infection. Finally, we used a crystal violet-based method (see Materials and Methods) to determine infectivity at 24 h postinfection. We observed that all of the acquired data show high infection rates for

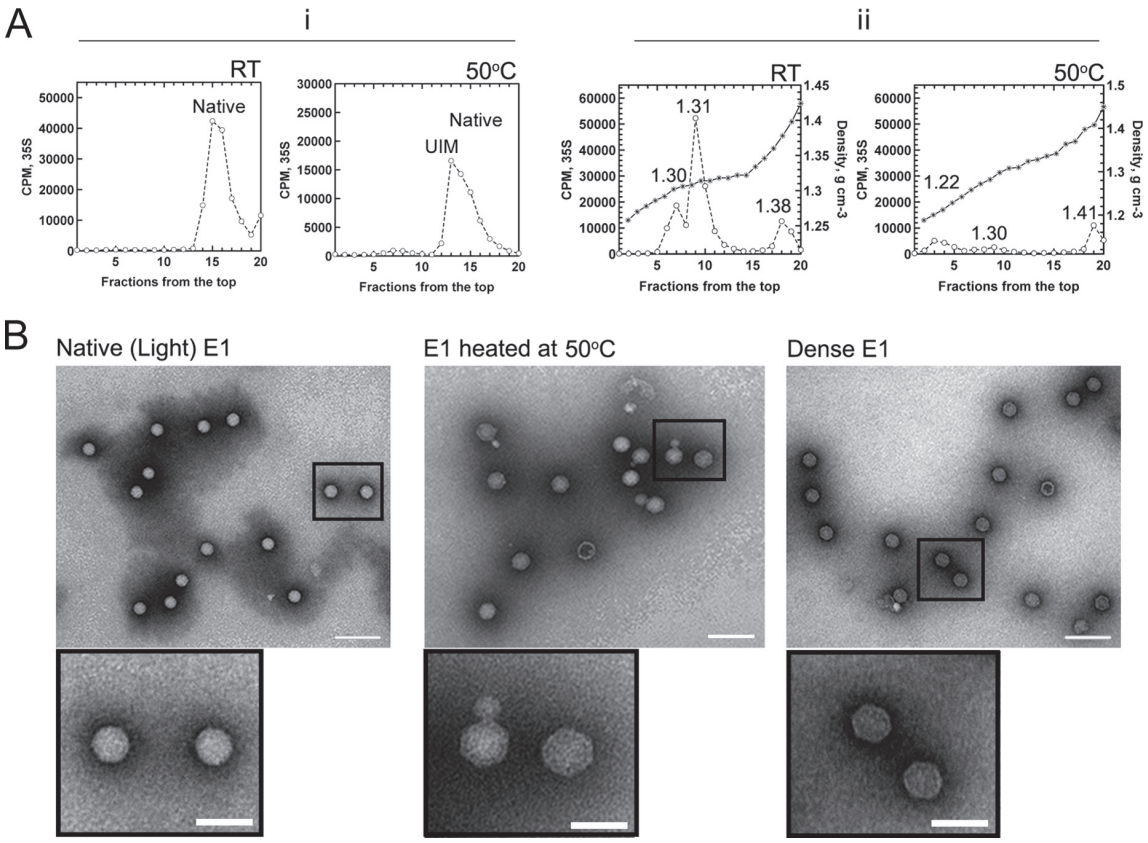

FIG 4 Heat conversion of [^{35}S]methionine-cysteine-labeled E1. (A) The virus was incubated at RT or 50°C for 5 min before loading either onto 5 to 20% sucrose (i) or into a CsCl gradient (ii). (B) Morphological evaluation of virus particles via transmission electron microscopy. The native virion (light), the E1 virion heated at 50°C, and dense E1 were negatively stained with 1% phosphotungstic acid before imaging. Bars, 100 nm and 25 nm for large images and blowups, respectively.

the dense E1 particle, although they were always slightly lower than those of the native virion.

The dense E1 particle is able to bind its receptor. The cell-induced conversion from the native to the altered 135S picornavirus particle is generally triggered by receptor-virion interactions. This type of particle conversion has been shown for at least poliovirus and rhinovirus (5), with both enteroviruses being considered model viruses in uncoating studies. Previous competition studies utilizing the E1 binding domain for its receptor $\alpha_2\beta_1$ integrin, the I-domain, showed that the I-domain is able to prevent the receptor-mediated cell attachment of E1 and that the I-domain alone is not able to initiate the uncoating process of E1 (32, 38). Here, we observed that the I-domain can push native E1 to higher melting temperatures in the presence of low I-domain-to-virion ratios (Fig. 6A), suggesting that the I-domain indeed can stabilize the E1 virion. The observed apparent T_m for E1 was ~53°C in the absence of any I-domain (Fig. 6A), whereas in the presence of the I-domain, the T_m increased by 3°C. We titrated the I-domain against 1 μg of E1 (Fig. 6A), starting from the first observable effective concentration, which corresponded to an I-domain-to-virion ratio of 10 (mole per mole), i.e., 100 ng of the I-domain. In our hands, the saturation point (maximum thermal stability induction by the I-domain) occurred at an I-domain-to-virion ratio of ~60 (mole/mole), that is, 500 ng of the I-domain. Previous studies using a similar I-domain–GST fusion protein suggested that up to five I-domain copies can occupy a single pentamer without any steric hindrance, resulting in a maximum of 60 I-domain copies per virion (32). Similarly to the previous report, the I-domain was able to block E1 infectivity (32). Here, we first incubated E1 with an I-domain–GST fusion protein for 1 h at 37°C prior to the addition of the virus to the cells. The infectivity of the light E1 particle was substantially blocked at an I-domain-to-virion ratio of ~50 (mole/mole) (Fig. 6B). This result was also reproducible with the dense E1 particle, although the I-domain seemed to be a more potent inhibitor at a lower I-domain concentration (Fig. 6B). Interestingly, previous studies on receptor-virion interactions using poliovirus and CVB3 indicated that the altered particle is likely to detach from its receptor (39, 40). By using TEM imaging, we studied whether the I-domain was able to bind both light and dense E1 fractions. After 1 h of incubation with the I-domain at 37°C, both the light and dense virions were clearly bound by several I-domain molecules, qualitatively supporting the observation that the dense E1 particle can bind to its receptor (Fig. 6C). This result also verified that the observed infection-blocking effect of the I-domain was due to capsid binding and not to virion disruption (Fig. 6C).

DISCUSSION

One of the hallmarks of the enterovirus genome delivery process is the generation of metastable uncoating intermediates. Upon ap-

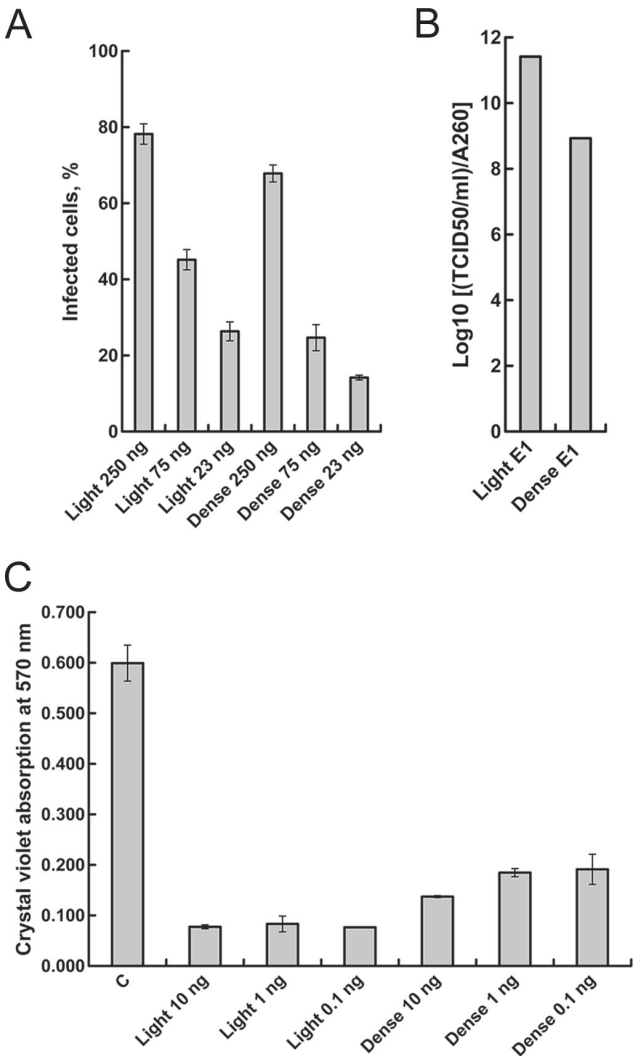

FIG 5 Infectivity of light and dense E1 particles. (A) The number of infected cells after 6 h postinfection was determined by immunolabeling the virus capsid and quantifying the number of infected cells based on confocal imaging. (B) The infectivity of E1 was determined with an endpoint titration assay, in which a dilution series of light or dense E1 with eight parallel dilutions was created. Infection was monitored for 3 days, after which infected cells were washed, and noninfected cells were stained to obtain the $TCID_{50}$ per milliliter (for more details, see Materials and Methods). (C) A CPE assay was used to determine infectivity at 24 h p.i. Three virus loads were used to infect cells: 10, 1, and 0.1 ng. After 24 h of infection, infected cells were washed, and noninfected cells were stained with crystal violet. The absorbance of crystal violet was measured with a microplate reader to evaluate the number of live cells. The results are averages of data from four replicates for each sample (± standard errors of the means).

propriate cues, the native virion is suggested to undergo a series of structural modifications, resulting in the loss of VP4, the externalization of the N-terminal sequence of VP1, and higher porosity, leading to the formation of an uncoating intermediate particle (6, 7). Depending on the enterovirus species, the native-to-altered-particle transition may be powered by a low pH (41) or receptor-virion interactions (42). In some cases, the receptor can serve as a capsid-stabilizing factor utilized only for cell surface attachment, as has been suggested by us and others previously regarding E1 and CVA9 (15, 23, 32, 43).

Here, we demonstrate the characteristics of another infectious, more open form of E1, which we identify as a possible uncoating intermediate particle of E1. This particle is found in cells during early infection and can be isolated by using CsCl gradient separation. In an effort to produce highly purified virus stocks, we found this dense particle when we ran the concentrated virus from a sucrose gradient in a CsCl gradient to further separate any possible impurities. The CsCl gradient separated two particle populations having markedly different buoyant densities (a light component, ~1.29 g cm^{-3}, and a dense component, ~1.37 g cm^{-3}). The commonly reported buoyant densities of the dense picornavirus preparations in CsCl were somewhat heavier, being around 1.44 g cm^{-3} for poliovirus and 1.44 to 1.47 g cm^{-3} for CVB5 and swine enterovirus (18–20). Similar to our findings for E1, the relative proportions of the dense and lighter intact populations for CVB5, poliovirus, or bovine enterovirus were not produced by the CsCl gradient itself, suggesting that the distributions of the two populations were faithful representations of their presence in virus preparations (18). In addition, we were able to show quantitatively that outside the cells, the native E1 virion is rather stable, whereas inside the cells, the dense particle is produced in large amounts after uptake.

Previous studies did not directly correlate the dense-particle populations in the CsCl gradient with the uncoating intermediate particles found after receptor-virion interactions. Here, in our study, we showed that the change in sucrose gradient sedimentation of the virus was correlated with the appearance of the dense-particle population in a CsCl gradient. The change was not evident on the cell surface but occurred after internalization at around 30 min p.i., which is in agreement with the uncoating time frame for poliovirus and for E1 (31, 44), suggesting that the observed dense E1 particle might be an uncoating intermediate. Additionally, when the broadened peak was collected from the sucrose gradient and subjected to CsCl gradient separation, both native particles and dense particles were observed. The minor change in the sucrose gradient was also explained via SDS-PAGE results, which showed that the VP4 protein was still mostly present in the dense particles. In our previous studies, we named the shoulder peak the 135S virion, as it was a dogma in the field that the 135S form is the intermediate form between the intact and empty forms (23, 45). However, in the light of the present data, it appears likely that the uncoating intermediate of E1 differs from those of some other enteroviruses and cannot be termed a true 135S particle, which has been shown to lack the VP4 protein (5). Therefore, we decided not to use this term but to use "uncoating intermediate particle" instead. Interestingly, previous studies on the dense poliovirus isolated from HeLa cells during infection showed the presence of VP4 using radioactive labeling, while silver staining could not detect VP4 for CVB5 or swine enterovirus (19, 20). This may reflect real differences in the presence of VP4 in the dense particle or differences in the sensitivities of the detection methods used (19, 20).

The large difference in the buoyant densities between the top and bottom components has been explained by a more open capsid structure that permits interactions between RNA and cesium. Data from our thermal assay experiments also suggest that the increased density is due to the capsid porosity in the case of the dense E1 particle. Previous reports using thermal assays with pi-

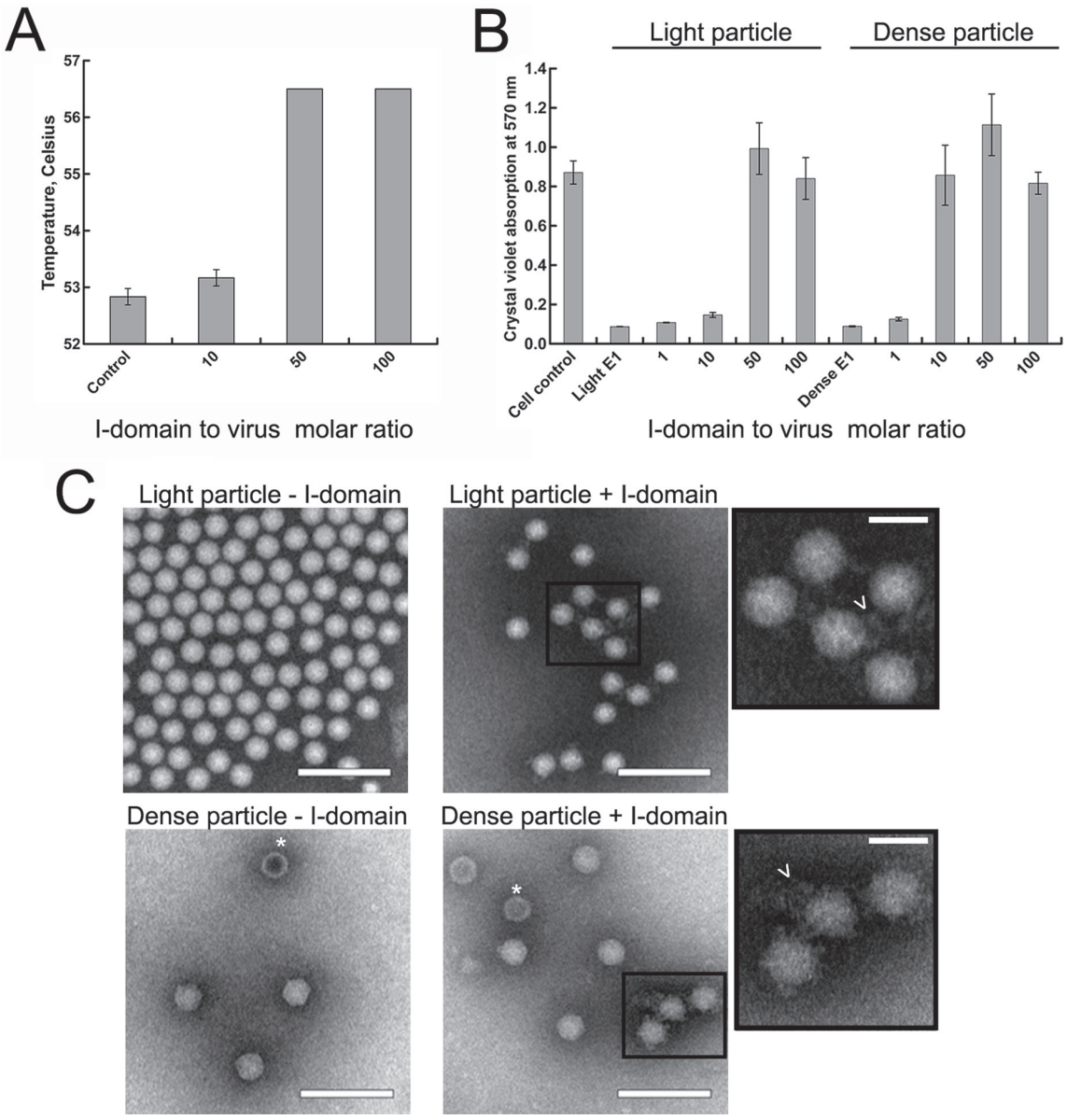

FIG 6 Receptor binding of light and dense E1 particles. (A) The melting temperature of E1 only (control) or with the I-domain was determined with a thermal assay in which SYBR green II was used as a reporter. (B) A competition assay was carried out to evaluate whether dense E1 could bind to the I-domain. Light or dense E1 was first incubated with four amounts of the I-domain for 1 h at 37°C, after which the virus was bound on cells for 1 h on ice. After washing the unbound virus, infection was allowed to proceed for 24 h at 37°C, after which infected cells were washed and noninfected cells were stained with crystal violet. The absorbance of crystal violet was measured with a microplate reader to evaluate the number of live cells. The results are averages of data from four replicates for each sample (± standard errors of the means). (C) The binding of the I-domain to E1 was also visualized via transmission electron microscopy. Light or dense E1 was incubated with or without the I-domain for 1 h at 37°C before addition to the grid and negative staining using phosphotungstic acid. The I-domain can be seen as hairy structures around the particles (arrowheads), and empty particles were also detected (asterisks). Bars, 100 nm and 25 nm for large images and blowups, respectively.

cornaviruses and SYBR green as a reporter molecule further showed that the 135S particles are permeable to small dye molecules (13). Additionally, it has been shown that native rhinovirus particles can permit dye access when incubated at 37°C, indicating that at a physiological temperature, the virus capsid may transition into a more dynamic state (46, 47). Here, we observed that the native E1 virion does not permit SYBR green II to penetrate the capsid structure at RT or 37°C, suggesting a tighter capsid structure than that of rhinovirus.

Heating of the native particles to superphysiological temperatures has been suggested to accurately mimic uncoating (37). However, the resulting profiles of such heat-converted enteroviruses in sucrose gradients have been shown to differ from one another, suggesting differences in their responses to heating and

difficulties in fully controlling the uncoating process by heating (48). Structural studies of A-particles have been performed mainly by heating native particles (12, 13, 16, 49) or by inducing particle alteration with a soluble receptor (11). In contrast to results for other enteroviruses, the heat conversion of native E1 virions differed from that of the E1 virions found in cells during infection. This was demonstrated by the fact that heating produced morphologically distinct particles with aberrant breakages, leading to a more extensive disruption in the subsequent CsCl gradients. The protrusions attached to the heated particles certainly suggest that the instability of the heated particles is linked to a different opening strategy than that of the particles derived from infected cells.

Previous reports suggest that upon conversion from the native virion to the altered 135S particles, there is a major loss in infectivity when the altered particles are used to infect cells *de novo* (37). This is not surprising given the fact that VP4 has been consistently shown to play a crucial role in the final genome delivery step, at least for poliovirus (8, 50). However, here, we demonstrate that dense E1 is not devoid of VP4, as was confirmed by radioactive detection. In addition, the slight shift in the virion peak in the sucrose gradient also suggests that only small changes in the virion structure occur during uncoating. Furthermore, we showed that dense E1 did not lose its ability to infect susceptible cells; rather, based on three well-established approaches to evaluate the infectivity of the particles, we confirmed the high infectivity of the dense particle.

In the cases of poliovirus and CVB3, receptor-induced 160S-to-135S conversion has been accompanied by the detachment of the virion-receptor complex (39, 40). Here, our biochemical and morphological experiments with the binding domain of the $\alpha_2\beta_1$ integrin receptor, the I-domain, did not apparently show lower levels of binding to the dense particle. The interaction between the receptor and dense E1 was also supported by infection experiments, where infection was determined after the dense virus was bound on ice and unbound virus was washed away. However, since the dense particle was shown to be a more open structure and slightly less infectious than the native virion, currently, it is possible that the change in the capsid structure might also have a small effect on receptor binding. Our previous studies on E1 suggested that the binding of the virus to its receptor $\alpha_2\beta_1$ integrin does not lead to extensive structural alterations in the E1 capsid, which is very similar to what was suggested previously for its close relative CVA9 (15, 32). Rather, these viruses are first transported to the endosomes, where, after some lag time, uncoating commences, leading to successful infection (27, 31). Importantly, we were able to confirm the previous assumption and directly show, using thermal assays, that receptor binding indeed stabilizes the native virus particle.

Conclusion. In conclusion, we have demonstrated that in addition to the native virus, another infectious E1 particle is found during infection. This particle has a more open structure and, hence, a higher buoyant density in CsCl gradients than the native virus. The dense particle still contains VP4 and is capable of binding to its receptor, and this binding leads to the stabilization of the virus particle and, later, to successful infection. Additionally, we show that this dense particle is distinct from the more fragile particle produced upon heat conversion.

ACKNOWLEDGMENTS

We thank Visa Ruokolainen for participating in the control experiments. We also thank Jyrki Heino for the GST–I-domain fusion and James Hogle for engaging in important discussions during this project.

FUNDING INFORMATION

This work, including the efforts of Mira Myllynen, Artur Kazmertsuk, and Varpu Marjomäki, was funded by Suomen Akatemia (Academy of Finland) (257125).

REFERENCES

1. **Monto AS.** 2002. Epidemiology of viral respiratory infections. Am J Med **112**(Suppl 6A):4S–12S.
2. **Hober D, Sauter P.** 2010. Pathogenesis of type 1 diabetes mellitus: interplay between enterovirus and host. Nat Rev Endocrinol **6:**279–289. http://dx.doi.org/10.1038/nrendo.2010.27.
3. **Roivainen M, Alfthan G, Jousilahti P, Kimpimäki M, Hovi T, Tuomilehto J.** 1998. Enterovirus infections as a possible risk factor for myocardial infarction. Circulation **98:**2534–2537. http://dx.doi.org/10.1161/01.CIR.98.23.2534.
4. **Laitinen OH, Honkanen H, Pakkanen O, Oikarinen S, Hankaniemi MM, Huhtala H, Ruokoranta T, Lecouturier V, Andre P, Harju R, Virtanen SM, Lehtonen J, Almond JW, Simell T, Simell O, Ilonen J, Veijola R, Knip M, Hyöty H.** 2014. Coxsackievirus B1 is associated with induction of beta-cell autoimmunity that portends type 1 diabetes. Diabetes **63:**446–455. http://dx.doi.org/10.2337/db13-0619.
5. **Tuthill TJ, Groppelli E, Hogle JM, Rowlands DJ.** 2010. Picornaviruses. Curr Top Microbiol Immunol **343:**43–89. http://dx.doi.org/10.1007/82_2010_37.
6. **Bergelson JM, Coyne CB.** 2013. Picornavirus entry. Adv Exp Med Biol **790:**24–41. http://dx.doi.org/10.1007/978-1-4614-7651-1_2.
7. **Paul AV, Schultz A, Pincus SE, Oroszlan S, Wimmer E.** 1987. Capsid protein VP4 of poliovirus is N-myristoylated. Proc Natl Acad Sci U S A **84:**7827–7831. http://dx.doi.org/10.1073/pnas.84.22.7827.
8. **Danthi P, Tosteson M, Li QH, Chow M.** 2003. Genome delivery and ion channel properties are altered in VP4 mutants of poliovirus. J Virol **77:**5266–5274. http://dx.doi.org/10.1128/JVI.77.9.5266-5274.2003.
9. **Brabec M, Schober D, Wagner E, Bayer N, Murphy RF, Blaas D, Fuchs R.** 2005. Opening of size-selective pores in endosomes during human rhinovirus serotype 2 in vivo uncoating monitored by single-organelle flow analysis. J Virol **79:**1008–1016. http://dx.doi.org/10.1128/JVI.79.2.1008-1016.2005.
10. **Pickl-Herk A, Luque D, Vives-Adrian L, Querol-Audi J, Garriga D, Trus BL, Verdaguer N, Blaas D, Caston JR.** 2013. Uncoating of common cold virus is preceded by RNA switching as determined by X-ray and cryo-EM analyses of the subviral A-particle. Proc Natl Acad Sci U S A **110:**20063–20068. http://dx.doi.org/10.1073/pnas.1312128110.
11. **Organtini LJ, Makhov AM, Conway JF, Hafenstein S, Carson SD.** 2014. Kinetic and structural analysis of coxsackievirus B3 receptor interactions and formation of the A-particle. J Virol **88:**5755–5765. http://dx.doi.org/10.1128/JVI.00299-14.
12. **Butan C, Filman DJ, Hogle JM.** 2014. Cryo-electron microscopy reconstruction shows poliovirus 135S particles poised for membrane interaction and RNA release. J Virol **88:**1758–1770. http://dx.doi.org/10.1128/JVI.01949-13.
13. **Ren J, Wang X, Hu Z, Gao Q, Sun Y, Li X, Porta C, Walter TS, Gilbert RS, Zhao Y, Axford D, Williams M, McAuley K, Rowlands DJ, Yin W, Wang J, Stuart DI, Rao Z, Fry EE.** 2013. Picornavirus uncoating intermediate captured in atomic detail. Nat Commun **4:**1929. http://dx.doi.org/10.1038/ncomms2889.
14. **Seitsonen JJ, Shakeel S, Susi P, Pandurangan AP, Sinkovits RS, Hyvönen H, Laurinmäki P, Yla-Pelto J, Topf M, Hyypiä T, Butcher SJ.** 2012. Structural analysis of coxsackievirus A7 reveals conformational changes associated with uncoating. J Virol **86:**7207–7215. http://dx.doi.org/10.1128/JVI.06425-11.
15. **Shakeel S, Seitsonen JJ, Kajander T, Laurinmäki P, Hyypiä T, Susi P, Butcher SJ.** 2013. Structural and functional analysis of coxsackievirus A9 integrin alphavbeta6 binding and uncoating. J Virol **87:**3943–3951. http://dx.doi.org/10.1128/JVI.02989-12.
16. **Shingler KL, Yoder JL, Carnegie MS, Ashley RE, Makhov AM, Conway JF, Hafenstein S.** 2013. The enterovirus 71 A-particle forms a gateway to

allow genome release: a cryoEM study of picornavirus uncoating. PLoS Pathog **9:**e1003240. http://dx.doi.org/10.1371/journal.ppat.1003240.
17. **Levy HC, Bostina M, Filman DJ, Hogle JM.** 2010. Catching a virus in the act of RNA release: a novel poliovirus uncoating intermediate characterized by cryo-electron microscopy. J Virol **84:**4426–4441. http://dx.doi.org/10.1128/JVI.02393-09.
18. **Rowlands DJ, Shirley MW, Sangar DV, Brown F.** 1975. A high density component in several vertebrate enteroviruses. J Gen Virol **29:**223–234. http://dx.doi.org/10.1099/0022-1317-29-2-223.
19. **Yamaguchi-Koll U, Wiegers KJ, Drzeniek R.** 1975. Isolation and characterization of 'dense particles' from poliovirus-infected HeLa cells. J Gen Virol **26:**307–319. http://dx.doi.org/10.1099/0022-1317-26-3-307.
20. **Urakawa T, Hamada N, Shingu M.** 1987. Isolation and antigenic characterization of dense particles of swine enteroviruses. Kurume Med J **34:**65–73. http://dx.doi.org/10.2739/kurumemedj.34.65.
21. **Cova-Baczko L, Aymard M.** 1982. Echovirus 11 dense particles: isolation and preliminary characterization. J Gen Virol **60:**159–163. http://dx.doi.org/10.1099/0022-1317-60-1-159.
22. **Wiegers KJ, Yamaguchi-Koll U, Drzeniek R.** 1977. Differences in the physical properties of dense and standard poliovirus particles. J Gen Virol **34:**465–473. http://dx.doi.org/10.1099/0022-1317-34-3-465.
23. **Marjomäki V, Pietiäinen V, Matilainen H, Upla P, Ivaska J, Nissinen L, Reunanen H, Huttunen P, Hyypiä T, Heino J.** 2002. Internalization of echovirus 1 in caveolae. J Virol **76:**1856–1865. http://dx.doi.org/10.1128/JVI.76.4.1856-1865.2002.
24. **Karjalainen M, Kakkonen E, Upla P, Paloranta H, Kankaanpää P, Liberali P, Renkema GH, Hyypiä T, Heino J, Marjomäki V.** 2008. A raft-derived, Pak1-regulated entry participates in alpha2beta1 integrin-dependent sorting to caveosomes. Mol Biol Cell **19:**2857–2869. http://dx.doi.org/10.1091/mbc.E07-10-1094.
25. **Karjalainen M, Rintanen N, Lehkonen M, Kallio K, Mäki A, Hellstrom K, Siljamäki V, Upla P, Marjomäki V.** 2011. Echovirus 1 infection depends on biogenesis of novel multivesicular bodies. Cell Microbiol **13:**1975–1995. http://dx.doi.org/10.1111/j.1462-5822.2011.01685.x.
26. **Liberali P, Kakkonen E, Turacchio G, Valente C, Spaar A, Perinetti G, Bockmann RA, Corda D, Colanzi A, Marjomäki V, Luini A.** 2008. The closure of Pak1-dependent macropinosomes requires the phosphorylation of CtBP1/BARS. EMBO J **27:**970–981. http://dx.doi.org/10.1038/emboj.2008.59.
27. **Soonsawad P, Paavolainen L, Upla P, Weerachatyanukul W, Rintanen N, Espinoza J, McNerney G, Marjomäki V, Cheng RH.** 2014. Permeability changes of integrin-containing multivesicular structures triggered by picornavirus entry. PLoS One **9:**e108948. http://dx.doi.org/10.1371/journal.pone.0108948.
28. **Huttunen M, Waris M, Kajander R, Hyypiä T, Marjomäki V.** 2014. Coxsackievirus A9 infects cells via nonacidic multivesicular bodies. J Virol **88:**5138–5151. http://dx.doi.org/10.1128/JVI.03275-13.
29. **Heikkilä O, Susi P, Tevaluoto T, Härmä H, Marjomäki V, Hyypiä T, Kiljunen S.** 2010. Internalization of coxsackievirus A9 is mediated by beta-2-microglobulin, dynamin, and Arf6 but not by caveolin-1 or clathrin. J Virol **84:**3666–3681. http://dx.doi.org/10.1128/JVI.01340-09.
30. **Marjomäki V, Turkki P, Huttunen M.** 2015. Infectious entry pathway of enterovirus B species. Viruses **7:**6387–6399. http://dx.doi.org/10.3390/v7122945.
31. **Siljamäki E, Rintanen N, Kirsi M, Upla P, Wang W, Karjalainen M, Ikonen E, Marjomäki V.** 2013. Cholesterol dependence of collagen and echovirus 1 trafficking along the novel alpha2beta1 integrin internalization pathway. PLoS One **8:**e55465. http://dx.doi.org/10.1371/journal.pone.0055465.
32. **Xing L, Huhtala M, Pietiäinen V, Käpylä J, Vuorinen K, Marjomäki V, Heino J, Johnson MS, Hyypiä T, Cheng RH.** 2004. Structural and functional analysis of integrin alpha2I domain interaction with echovirus 1. J Biol Chem **279:**11632–11638. http://dx.doi.org/10.1074/jbc.M312441200.
33. **Schmidtke M, Schnittler U, Jahn B, Dahse H, Stelzner A.** 2001. A rapid assay for evaluation of antiviral activity against coxsackie virus B3, influenza virus A, and herpes simplex virus type 1. J Virol Methods **95:**133–143. http://dx.doi.org/10.1016/S0166-0934(01)00305-6.
34. **Walter TS, Ren J, Tuthill TJ, Rowlands DJ, Stuart DI, Fry EE.** 2012. A plate-based high-throughput assay for virus stability and vaccine formulation. J Virol Methods **185:**166–170. http://dx.doi.org/10.1016/j.jviromet.2012.06.014.
35. **Garriga D, Pickl-Herk A, Luque D, Wruss J, Caston JR, Blaas D, Verdaguer N.** 2012. Insights into minor group rhinovirus uncoating: the X-ray structure of the HRV2 empty capsid. PLoS Pathog **8:**e1002473. http://dx.doi.org/10.1371/journal.ppat.1002473.
36. **Harutyunyan S, Kumar M, Sedivy A, Subirats X, Kowalski H, Kohler G, Blaas D.** 2013. Viral uncoating is directional: exit of the genomic RNA in a common cold virus starts with the poly-(A) tail at the 3′-end. PLoS Pathog **9:**e1003270. http://dx.doi.org/10.1371/journal.ppat.1003270.
37. **Curry S, Chow M, Hogle JM.** 1996. The poliovirus 135S particle is infectious. J Virol **70:**7125–7131.
38. **King SL, Cunningham JA, Finberg RW, Bergelson JM.** 1995. Echovirus 1 interaction with the isolated VLA-2 I domain. J Virol **69:**3237–3239.
39. **Lonberg-Holm K, Gosser LB, Kauer JC.** 1975. Early alteration of poliovirus in infected cells and its specific inhibition. J Gen Virol **27:**329–342. http://dx.doi.org/10.1099/0022-1317-27-3-329.
40. **Goodfellow IG, Evans DJ, Blom AM, Kerrigan D, Miners JS, Morgan BP, Spiller OB.** 2005. Inhibition of coxsackie B virus infection by soluble forms of its receptors: binding affinities, altered particle formation, and competition with cellular receptors. J Virol **79:**12016–12024. http://dx.doi.org/10.1128/JVI.79.18.12016-12024.2005.
41. **Prchla E, Kuechler E, Blaas D, Fuchs R.** 1994. Uncoating of human rhinovirus serotype 2 from late endosomes. J Virol **68:**3713–3723.
42. **Joklik WK, Darnell JE, Jr.** 1961. The adsorption and early fate of purified poliovirus in HeLa cells. Virology **13:**439–447. http://dx.doi.org/10.1016/0042-6822(61)90275-6.
43. **Rossmann MG, He Y, Kuhn RJ.** 2002. Picornavirus-receptor interactions. Trends Microbiol **10:**324–331. http://dx.doi.org/10.1016/S0966-842X(02)02383-1.
44. **Brandenburg B, Lee LY, Lakadamyali M, Rust MJ, Zhuang X, Hogle JM.** 2007. Imaging poliovirus entry in live cells. PLoS Biol **5:**e183. http://dx.doi.org/10.1371/journal.pbio.0050183.
45. **Pietiäinen V, Marjomäki V, Upla P, Pelkmans L, Helenius A, Hyypiä T.** 2004. Echovirus 1 endocytosis into caveosomes requires lipid rafts, dynamin II, and signaling events. Mol Biol Cell **15:**4911–4925. http://dx.doi.org/10.1091/mbc.E04-01-0070.
46. **Kremser L, Konecsni T, Blaas D, Kenndler E.** 2004. Fluorescence labeling of human rhinovirus capsid and analysis by capillary electrophoresis. Anal Chem **76:**4175–4181. http://dx.doi.org/10.1021/ac049842x.
47. **Kremser L, Petsch M, Blaas D, Kenndler E.** 2004. Labeling of capsid proteins and genomic RNA of human rhinovirus with two different fluorescent dyes for selective detection by capillary electrophoresis. Anal Chem **76:**7360–7365. http://dx.doi.org/10.1021/ac048999m.
48. **Airaksinen A, Somerharju P, Hovi T.** 2001. Variation in liposome binding among enteroviruses. Virology **279:**539–545. http://dx.doi.org/10.1006/viro.2000.0722.
49. **Bubeck D, Filman DJ, Cheng N, Steven AC, Hogle JM, Belnap DM.** 2005. The structure of the poliovirus 135S cell entry intermediate at 10-angstrom resolution reveals the location of an externalized polypeptide that binds to membranes. J Virol **79:**7745–7755. http://dx.doi.org/10.1128/JVI.79.12.7745-7755.2005.
50. **Panjwani A, Strauss M, Gold S, Wenham H, Jackson T, Chou JJ, Rowlands DJ, Stonehouse NJ, Hogle JM, Tuthill TJ.** 2014. Capsid protein VP4 of human rhinovirus induces membrane permeability by the formation of a size-selective multimeric pore. PLoS Pathog **10:**e1004294. http://dx.doi.org/10.1371/journal.ppat.1004294.

II

HOST CELL CALPAINS CAN CLEAVE STRUCTURAL PROTEINS FROM THE ENTEROVIRUS POLYPROTEIN

by

Mira Laajala, Minna M. Hankaniemi, Juha Määttä, Vesa P. Hytönen, Olli H. Laitinen & Varpu Marjomäki
2019

Submitted manuscript

III

HUMAN ENTEROVIRUS GROUP B VIRUSES RELY ON VIMENTIN DYNAMICS FOR EFFICIENT PROCESSING OF VIRAL NON-STRUCTURAL PROTEINS

by

Paula Turkki, Mira Laajala, Malin Flodström-Tullberg & Varpu Marjomäki
2019

Journal of Virology, in press